

1986

Lateral variability in a coastal plain estuary (fronts, density, lateral circulation)

Linda Mary Huzzey

College of William and Mary - Virginia Institute of Marine Science

Follow this and additional works at: <https://scholarworks.wm.edu/etd>



Part of the [Oceanography Commons](#)

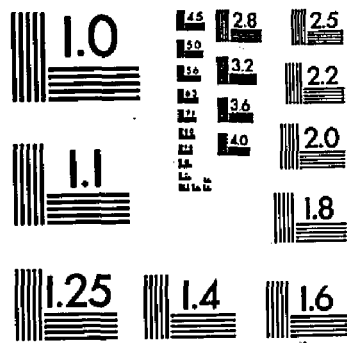
Recommended Citation

Huzzey, Linda Mary, "Lateral variability in a coastal plain estuary (fronts, density, lateral circulation)" (1986). *Dissertations, Theses, and Masters Projects*. Paper 1539616706.

<https://dx.doi.org/doi:10.25773/v5-57t3-s072>

This Dissertation is brought to you for free and open access by the Theses, Dissertations, & Master Projects at W&M ScholarWorks. It has been accepted for inclusion in Dissertations, Theses, and Masters Projects by an authorized administrator of W&M ScholarWorks. For more information, please contact scholarworks@wm.edu.

U·M·I



MICROCOPY RESOLUTION TEST CHART
NATIONAL BUREAU OF STANDARDS
STANDARD REFERENCE MATERIAL 1010a
(ANSI and ISO TEST CHART No. 2)

University Microfilms International
A Bell & Howell Information Company
300 N. Zeeb Road, Ann Arbor, Michigan 48106

INFORMATION TO USERS

While the most advanced technology has been used to photograph and reproduce this manuscript, the quality of the reproduction is heavily dependent upon the quality of the material submitted. For example:

- Manuscript pages may have indistinct print. In such cases, the best available copy has been filmed.
- Manuscripts may not always be complete. In such cases, a note will indicate that it is not possible to obtain missing pages.
- Copyrighted material may have been removed from the manuscript. In such cases, a note will indicate the deletion.

Oversize materials (e.g., maps, drawings, and charts) are photographed by sectioning the original, beginning at the upper left-hand corner and continuing from left to right in equal sections with small overlaps. Each oversize page is also filmed as one exposure and is available, for an additional charge, as a standard 35mm slide or as a 17"x 23" black and white photographic print.

Most photographs reproduce acceptably on positive microfilm or microfiche but lack the clarity on xerographic copies made from the microfilm. For an additional charge, 35mm slides of 6"x 9" black and white photographic prints are available for any photographs or illustrations that cannot be reproduced satisfactorily by xerography.

8702423

Huzzey, Linda Mary

LATERAL VARIABILITY IN A COASTAL PLAIN ESTUARY

The College of William and Mary in Virginia

PH.D. 1986

University
Microfilms
International 300 N. Zeeb Road, Ann Arbor, MI 48106

Copyright 1987

by

Huzzey, Linda Mary

All Rights Reserved

PLEASE NOTE:

In all cases this material has been filmed in the best possible way from the available copy. Problems encountered with this document have been identified here with a check mark .

1. Glossy photographs or pages
2. Colored illustrations, paper or print _____
3. Photographs with dark background
4. Illustrations are poor copy _____
5. Pages with black marks, not original copy _____
6. Print shows through as there is text on both sides of page _____
7. Indistinct, broken or small print on several pages _____
8. Print exceeds margin requirements _____
9. Tightly bound copy with print lost in spine _____
10. Computer printout pages with indistinct print _____
11. Page(s) _____ lacking when material received, and not available from school or author.
12. Page(s) _____ seem to be missing in numbering only as text follows.
13. Two pages numbered _____. Text follows.
14. Curling and wrinkled pages _____
15. Dissertation contains pages with print at a slant, filmed as received _____
16. Other _____

University
Microfilms
International

LATERAL VARIABILITY IN A COASTAL PLAIN ESTUARY

A Dissertation

Presented to

The Faculty of the School of Marine Science

The College of William and Mary in Virginia

In Partial Fulfillment

Of the Requirements for the Degree of

Doctor of Philosophy

by

Linda M. Huzzey

1986

APPROVAL SHEET

This dissertation is submitted in partial fulfillment of
the requirements for the degree of

Doctor of Philosophy

Linda M. Huzzey
Linda M. Huzzey

Approved, October 1986

John M. Brubaker
John M. Brubaker, Ph.D.
Committee Chairman

Albert Y. Kuo
Albert Y. Kuo, Ph.D.

Evon P. Ruzicki
Evon P. Ruzicki, Ph.D.

Richard L. Wetzel
Richard L. Wetzel, Ph.D.

William C. Boicourt
William C. Boicourt, Ph.D.
Horn Point Environmental Laboratories
University of Maryland

©1987

LINDA MARY HUZZEY

All Rights Reserved

TABLE OF CONTENTS

	Page
ACKNOWLEDGEMENTS.	iv
LIST OF TABLES.	v
LIST OF FIGURES	vi
ABSTRACT.	vii
I. INTRODUCTION	2
II. LITERATURE REVIEW	
PART I: Lateral Circulation in Estuaries	8
PART II: Small Scale Fronts	20
1. Estuarine Fronts.	21
2. Plume Fronts.	23
3. Shelf-Sea Fronts.	25
4. Models of Small Scale Fronts.	27
III. LATERAL DENSITY DISTRIBUTION	
A. Methods.	34
B. Results	
1. Density Distribution	
a. Spring Tides	38
b. Mean Tides	47
c. Neap Tides	53
2. Pressure Gradients	56
3. Lateral Circulation.	65
IV. CURRENTS	
1. Experimental Methods and General Results.	72
2. Tidal Analysis.	91
3. Lateral Variability in Current Magnitude and Phase.	94
(i) Lateral Phase Difference.	96
(ii) Velocity Shear.	103
V. FRONTS IN THE YORK RIVER	108
VI. DISCUSSION	118
VII. SUMMARY AND CONCLUSIONS.	135
LITERATURE CITED.	137
VITA.	144

ACKNOWLEDGEMENTS

I would like to thank Dr. John M. Brubaker for his patience and support throughout this project. Thanks are also extended to the committee members for their assistance and advice.

This study entailed many hours of field data collection and would not have been possible without the help of many people. In particular I would like to thank Sharon Miller and George Pongonis for their encouragement and trust in my seamanship; the staff of the Vessel Operations Department for the deployment and retrieval of current meter moorings; Buddy Matthews, Steve Snyder and Scott Fenstamacher of the Department of Physical Oceanography for assistance in the preparation and maintenance of field instruments; and the many people who assisted with the actual field work, namely: Pat Barthle, Brett Burdick, Kevin Curling, Paul de Fur, Karl Dydak, Tracy Eanes, Ken Finkelstein, Bob Gammisch, Mal Green, Mary Sue Jablonsky, Beth Lester, Mohamed Moustafa, Bill Rizzo, Bryan Salley, Kay Strobel and Anne Wilber.

I would also like to thank Sam White, the pilot extraordinaire, for his patience and cheerfulness, throughout many long hours of aerial surveys.

I would also like to acknowledge Dr. D. Johnson of NORDA for the loan of his current meters; and Dr. Chris S. Welch for valuable discussions and criticisms of this manuscript.

And last, but not least, I would like to sincerely thank Anne C. Wilber for sharing not only an office, but also her good humor and friendship.

LIST OF TABLES

Table		Page
IV.1	Current meter station locations.	72
IV.2	Directions of principal axes	82
IV.3	Times and locations of drogue experiments.	82
IV.4	Amplitude of harmonic constituents	92
IV.5	Results of cross-spectral analysis	98
IV.6	Duration of flood and ebb cycles	102

LIST OF FIGURES

FIGURE		PAGE
1.1	Location of the study area	6
3.1	Location of CTD sampling stations	35
3.2	Density distribution, 12 May 1983	39
3.3	Density distribution, Spring tides	42
3.4	Density profiles, Spring tides	45
3.5	Density distribution, Mean tides	48
3.6	Density profiles, Mean tides	50
3.7	Density distribution, Neap tides	54
3.8	Density profiles, Neap tides	55
3.9	Horizontal pressure gradients - mean tides	59
3.10	Horizontal pressure gradients - spring tides	61
3.11	Horizontal pressure gradients - neap tides	63
3.12	Patterns of lateral circulation - mean tides	67
3.13	Patterns of lateral circulation - spring tides	70
3.14	Patterns of lateral circulation - neap tides	71
4.1	Location of current meter stations	73
4.2	Time series of observed currents	75
4.3	Scatter plots of observed currents	80
4.4	Principal axes and mean currents	83
4.5	Schematic diagram of a drogue	84
4.6	Drogue tracklines	86
4.7	Non-tidal residual currents	95

4.8	Power spectra, April/May 1985	97
4.9	'Along-channel' current velocities	100
4.10	Velocity difference between channel and shoals	105
4.11	Velocity shear indicated by drogue tracks	106
5.1	Aerial photographs	110
5.2	Fronts noted from aerial surveys	114
5.3	Fronts observed during CTD transects	115
5.4	Fronts observed during spring tides	117
6.1	Model values - no phase case	121
6.2	Model values - varying phase	122
6.3	Observed density differences between channel and shoals	125
6.4	Lateral circulation patterns	130
6.5	Isopycnals, 7 June 1984	132
6.6	a) Schematic diagram of a tidal mixing front	
	b) Streamlines of cross-frontal flow	133

ABSTRACT

A series of observations of the density distribution across the York River estuary documents distinct lateral differences in density and degree of vertical mixing. The magnitude of the density differences varies throughout the tidal cycle; maximum lateral gradients occur at times of minimum current. When the density distribution is sufficiently inhomogenous, longitudinal estuarine fronts are generated. These fronts are axially aligned, up to several miles in length, and are apparent for less than 2 hours at any given location. Although the density difference across the frontal boundary is often small, horizontal pressure gradients acting over a broad frontal region generate the convergent circulations necessary to maintain these fronts. Measurements of the longitudinal velocities across the same section reveals negligible phase difference but a significant amplitude difference between the currents in the channel and those over the shoals. Differential advection across the estuary due to this velocity shear is the process by which the observed density distribution is generated.

LATERAL VARIABILITY IN A COASTAL PLAIN ESTUARY

I. INTRODUCTION

The classical picture of estuarine circulation emerged from early studies by, amongst others, Stommel (1953) and Pritchard (1952,1954,1956). From this viewpoint partially-mixed estuaries are regarded as two layered systems, with the depth-averaged salinity decreasing from the mouth to the head of the estuary, and a longitudinal non-tidal circulation pattern which is directed down-estuary near the surface and up-estuary near the bed. Wind stress at the surface may act to produce circulations but this is not a requirement. Generally it is assumed that these circulations are evenly distributed across the estuary. There are indications however that this may not be correct, and that lateral variability may play an important role in the dynamics of partially-mixed estuaries (Dyer, 1977). Lateral components to the circulation may arise as a result of depth variations across the estuary, longitudinal irregularities in the cross-sectional form, channel bends, or the inflowing of waters from tributary rivers. Such secondary circulations have been documented by, for example, Dyer (1973), Doyle and Wilson (1978), and Boicourt (1982). Despite this, field observations are frequently made only along the axis of the estuary and conditions are assumed constant across the width for a given depth. Furthermore the difficulty of three dimensional modelling has caused many investigators to assume that the vertical circulation effects may be more important than the lateral, and thus treat estuaries

as laterally homogenous. Due to the large width-to-depth ratio of many coastal plain estuaries, plus the great changes in depth across a given section, it is unlikely that these estuaries are, in fact, laterally homogenous. Klemas and Polis (1977) noted regions of strong lateral density gradients in the Delaware Bay. These regions are termed 'fronts'.

Fronts are a very widespread phenomena occurring on many spatial and temporal scales, and in many different estuarine and oceanic systems. As was noted by Denman and Powell (1984), there are almost as many definitions of fronts as there are scientists studying fronts! Garvine and Monk (1974) in their study of the Connecticut River plume followed Cromwell and Reid (1955) in defining fronts as 'a narrow band on the sea surface across which the density changes abruptly'. A more precise definition used by Fearnhead (1975) considered a front to be 'a boundary surface formed by the horizontal juxtaposition of two distinct water masses and the intersection of that surface with the air-sea boundary'. Klemas and Polis (1977) on the other hand simply considered fronts to be regions, within the estuary, of extremely strong gradients in velocity and density. In this way the term 'front' has also been used to describe the leading edge of the salt wedge intrusion into estuaries.

The definition used by Denman and Powell (1984) will be used in this study, namely a 'front is a discontinuity in the horizontal distribution of water mass properties on the scale of observation'. In estuaries, the most significant water mass property is salinity, and

thus fronts can be taken to illustrate boundaries between water masses of differing densities. Fronts are usually of greater length than width by several orders of magnitude, and are usually considered to be zones of convergent circulation. By continuity, convergence usually requires compensatory vertical circulation. Frequently fronts are also regions of high current shear and enhanced mixing and diffusion. Fronts found within estuaries vary widely in their relation to the tidal dynamics and bathymetry. Within coastal plain estuaries, such as the York River, the fronts seen are commonly aligned parallel to the axis of the estuary and/or the main channel, and exist for only a few hours. Similar features have been documented in the Delaware Bay (Klemas and Polis, 1977). These fronts may be termed 'longitudinal fronts'. Their short time scale suggests that they are linked to the intra-tidal dynamics, rather than the residual circulation. Their positioning suggests that they are a result of the lateral dynamic balance.

The objectives of this study were to examine the lateral variation in velocity and density, throughout the tidal cycle, across a partially-mixed coastal plain estuary with a view towards developing an understanding of the possible mechanism for genesis of these frontal features. The field data were collected in two discrete series of experiments: the first examined the lateral density distribution, and the second the variation in tidal currents across the estuary. The method and results pertaining to each of these data sets have been combined and are presented separately in Chapters 3 and 4. Chapter 5 outlines the observations of fronts in the study area. The discussion

of these results and ideas pertaining to frontogenesis in coastal plain estuaries is presented in Chapter 6.

DESCRIPTION OF THE STUDY AREA

The York River is a partially-mixed coastal plain estuary situated on the western shore of the Chesapeake Bay (Fig.1). It is approximately 52 km in length from Tue Marsh Light at the mouth, to West Point at the confluence of the Mattaponi and Pamunkey Rivers. The constriction of the channel between Gloucester Point and Yorktown provides a natural division of the river into two segments. The lower part is 3 to 4 km wide, has channel depths of 20m and is orientated east-west. The upper York River is narrower with widths of 2 to 2.5 km and channel depths of 10m. It is orientated southeast-northwest and is quite straight for much of it's length. There are no significant tributary rivers.

The estuary is tidal throughout, the mean tidal range increasing from 0.7m at the mouth to 1.1m at West Point. The tidal wave is purely progressive at Tue Marsh but tends toward a standing wave further upriver. At Clay Bank, a short distance down-estuary from the study transect, the phase difference is on the order of 1.5-2 hours. The average freshwater discharge into the York River is $56.4 \text{ m}^3/\text{sec}$ (Hyer et al., 1978). This inflow tends to be greater than average in the period between January and April. Surface salinities vary seasonally and are typically 15 - 21 at the mouth and 2 - 7 at West Point (Brooks, 1983).

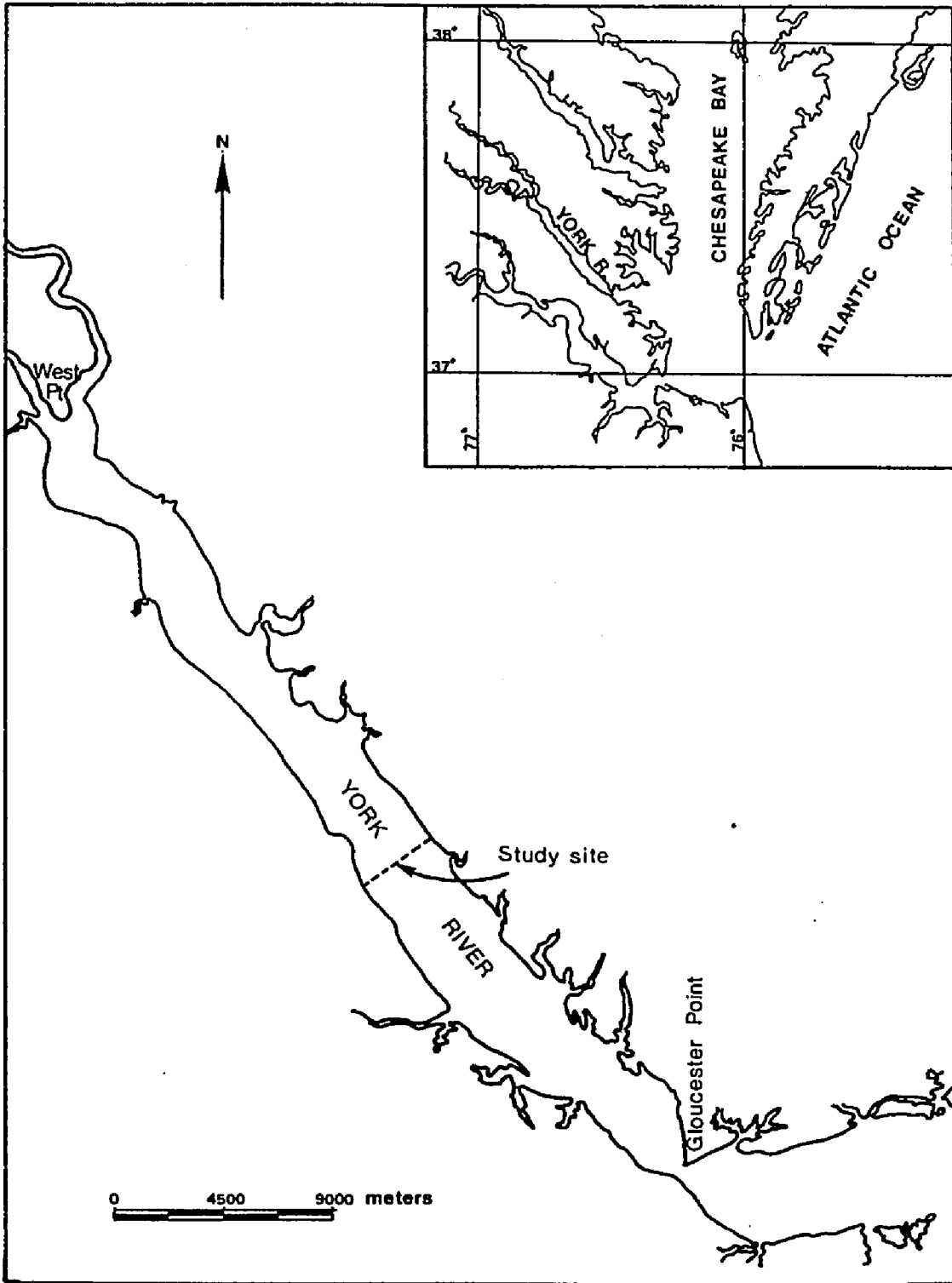


FIG.1 Location of the study area

The study transect was deliberately located in one of the more uniform reaches in order to minimize the possibility that any observed lateral variability in density or currents might be attributed to the influence of bends in the channel. The river is 3,000 meters wide at this point. For almost 50% of this distance the water depth is less than 2 meters. The main channel is 10.5m deep and is located asymmetrically in the section. Sampling stations were located at positions on and between the inner edge of the bordering shoals.

II. LITERATURE REVIEW

PART I: LATERAL CIRCULATION IN ESTUARIES

One of the earliest investigations of the lateral dynamic balance in estuaries was that of Pritchard (1956). Utilizing temperature, salinity and current velocity data from two sections of the James River he evaluated the magnitude of each of the terms in the lateral momentum equation. For mean steady-state conditions (and using a left-handed coordinate system with x positive down-estuary) this equation becomes

$$0 = -\langle \alpha \frac{\partial p}{\partial y} \rangle_0 + b_0' + fu - \frac{\partial}{\partial x} \langle u' v' \rangle - \frac{\partial}{\partial z} \langle w' v' \rangle - \frac{\partial}{\partial y} \langle v' v' \rangle \quad (2.1)$$

1 2 3 4 5 6

To obtain this equation Pritchard assumed that (a) the mean lateral velocity is zero and hence all mean field acceleration terms vanish and (b) that the mean pressure force may be expressed as the pressure force relative to that at the surface (Term 1), which can be computed knowing the salinity and temperature distribution, plus a constant (Term 2) representing the component of the pressure force at the surface. Furthermore terms 4 and 6, the horizontal components of the turbulent flux of momentum, were considered negligible. Evaluation of the remaining terms led Pritchard to conclude that, in the lateral direction, the primary force balance is between the Coriolis force (Term 3) and the lateral pressure force (Term 1). The difference between the

two terms was attributed to the turbulent eddy term (Term 5). Stewart (1957) questioned the existence of a finite value for such a term and also the assumption that the mean lateral velocity is zero. Instead he proposed that the pressure gradient and Coriolis force are balanced by a centrifugal force due to flow curvature. Using velocity values taken from Pritchard (1956), a radius of curvature was calculated which was found to be in accordance with the channel curvature in the James River.

Dyer (1973) similarly examined the magnitude of the terms in the lateral momentum equation which he formulated (in a steady-state, tidally-averaged condition) as:

$$u \frac{\partial v}{\partial x} + v \frac{\partial v}{\partial y} + w \frac{\partial v}{\partial z} = -\rho^{-1} \frac{\partial p}{\partial y} + C - f\bar{u} + \rho^{-1} \frac{\partial \tau}{\partial z} \quad (2.2)$$

where C is a constant representing the sea surface slope. Dyer considered that in a meandering estuary the curvature of streamlines of the flow along the estuary is likely to be significant and give rise to centripetal accelerations. These should be numerically equal to the field accelerations on the left-hand side of equation (2.2). In addition he eliminated the terms involving the sea surface slope and the gradient in Reynolds stress, both of which can be assumed to be constant with depth, by taking the difference between each term calculated at two separate depths. Thus equation (2.2) becomes:

$$\Delta(u \frac{\partial v}{\partial x}) + \Delta(v \frac{\partial v}{\partial y}) + \Delta(w \frac{\partial v}{\partial z}) = -\Delta \rho^{-1} (\frac{\partial p}{\partial y}) - \Delta(f\bar{u}) \quad (2.3)$$

where Δ is the operator $\partial/\partial z$. Using data collected in the Veller estuary and Southampton Water the magnitude of each of the terms in (2.3) was obtained and used to estimate the radius of curvature of the flow. Widely varying results were obtained, many of which did not match the physical dimensions of the particular estuaries, illustrating the difficulty of making sufficiently accurate measurements of velocities to calculate the field acceleration terms.

The lateral dynamic balance across the lower Hudson estuary, between Sandy Hook and Rockaway Point, was investigated by Doyle and Wilson (1978). Utilizing the 'difference technique' of Dyer and similarly assuming that the field acceleration terms are equivalent to the tidally-averaged centripetal accelerations, the terms in the lateral momentum equation were calculated from field data. In this instance the field acceleration terms themselves were not estimated, instead the tidally averaged values of speed and radius of curvature were determined from current meter data. These authors concluded that across this transect the centripetal and Coriolis accelerations are balanced by the lateral pressure gradient. Although the numbers they cite contain some irregularities it would seem that the primary dynamic balance at this location could be described by such a simple relationship.

A quite different approach to the formulation of lateral dynamic balance was adopted by Nunes and Simpson (1985). As part of a study of axial convergence in a small and well-mixed estuary they assume that the lateral pressure gradient is balanced by internal frictional stresses. That is:

$$\frac{\partial p}{\partial y} = \bar{\rho} N_z \frac{\partial^2 v}{\partial z^2} \quad (2.4)$$

where N_z is the vertical eddy viscosity and assumed constant and $\bar{\rho}$ is the mean density. Thus no consideration is given to the role of Coriolis and /or inertial accelerations. The lateral velocities are considered to be maintained solely by horizontal density gradients. Solving equation (2.4) results in an expression for v in terms of the lateral horizontal pressure gradient and water depth. Such a result was found to fit with their observations. However this approach may not be as applicable in larger and more stratified estuaries.

Prych (1970) conducted a laboratory study of the lateral mixing of tracer fluids in turbulent open-channel flow. In the experiments in which there was a difference in density between the tracer and the ambient fluid it was observed that density-induced secondary currents enhanced the lateral mixing of the two fluids. An expression for the lateral momentum balance was formulated by equating the pressure gradient with eddy viscosity.

Many investigators have recognised the possible importance of lateral gradients in density and velocity to the longitudinal dispersive characteristics of estuaries. The flux of salt through a channel cross-section is given by

$$F_s(t) = \iint u s \, dA \quad (2.5)$$

Hansen (1965) decomposed this expression into the flux due to the sectional mean current and salinity plus a flux due to local deviations of salinity and current. This latter has been termed the 'shear effect' and is due to both density currents and bottom friction. Using data taken across a section near the mouth of the Columbia River estuary, Hansen showed that this effect balanced about 45% of the salt advected seaward with the mean river discharge. In this analysis no distinction was made between the vertical and lateral shear effect.

Fischer (1972) examined the magnitude of various mass transport mechanisms in partially mixed estuaries. In a manner similar to Hansen (1965) he decomposed the instantaneous velocity and salt concentration into temporally and spatially averaged term plus their deviations. Neglecting the contribution of the 'phase effect', the total dispersion was shown to be the sum of four terms representing transverse net circulation, vertical net circulation (more often called gravitational circulation), transverse oscillatory shear and vertical oscillatory shear. Each of these terms he evaluated using previously published theoretical or empirical results. From this he found the dispersion due to the transverse net circulation to be an order of magnitude greater than the vertical net circulation. Whilst the values he calculated are subject to some degree of assumptions and errors this result does illustrate the potential importance in transverse gradients in velocity and salinity.

Dyer (1974) extended Fischer's method of calculating the salt flux by including the tidally-fluctuating cross-sectional area. Using field

measurements from three separate estuaries he calculated the magnitude of each of the most important terms. In Southampton Water and the Mersey estuary, both partially-mixed, it was found that in contrast to Fischer's prediction, the magnitude of the net transverse circulation was equivalent to that of the vertical circulation. In the Veller estuary (salt-wedge) however the net transverse circulation was much less than the vertical circulation. Dyer (1974) concluded that the proportion of the salt balance effected by lateral circulation is greater in partially-mixed estuaries than in salt-wedge estuaries. Indeed, with a further decrease in stratification, and development of a vertically homogeneous estuary, lateral effects should predominate.

This hypothesis was investigated by Murray and Siripong (1978) who examined the salt-flux in a shallow well-mixed estuary. Using analysis of variance techniques the time averaged salt flux was decomposed into 10 terms. Only three of these were considered significant: the advective flux, the vertical gradient flux and the lateral gradient flux. These terms were evaluated from field data and it was found that in this estuary the lateral gradient flux is 1.5 times that of the vertical. Using this same analytical method Uncles et.al. (1984) examined measurements made in the upper reaches of the Tamar estuary, a partially-mixed estuary. They found that the transverse shear dispersion was very small in narrow sections near the head of the estuary but was comparable with the vertical shear dispersion at the widest section. West and Mangat (1986) collected velocity and salinity profiles at five stations across a section of the Conway estuary for parts of an ebb and flood tide. Their data showed that the magnitude of

the vertical and transverse shear dispersion varied both spatially and temporally. It was found that both vertical and transverse shear contribute to the dispersion. The value of the resulting dispersion coefficients were generally larger for the ebb tide than for the flood tide.

The occurrence of non-uniformity in salinity and velocity across partially-mixed estuaries has been documented in many studies. Pritchard (1952) found that the mean salinity in the Chesapeake Bay and James River was consistently higher on the right-hand side of the estuary (looking up-estuary) - a distribution he attributed to the influence of earth's rotation. In a series of experiments in the Mersey estuary Bowden and Sharaf-el-Din (1966) obtained similar results with a salinity difference as much as 1.19 at the surface and 0.69 at the bed over a horizontal distance of 1 km. The tidally-averaged distribution of sigma-t across the Sandy Hook-Rockaway Pt. transect during August 1982 revealed horizontal density gradients as high as $0.6 \text{ kg/m}^3/\text{km}$ at mid-depth in the section, again with the higher density water on the right-hand side of the estuary (Doyle and Wilson, 1978). In the Columbia River estuary at times of high discharge this pattern of salinity distribution was also apparent (Hansen, 1965).

All of these examples pertain to tidally-averaged conditions. Quite different distributions may be seen at times within the tidal cycle. Dyer (1973), using an extensive set of measurements of the Southampton Water, found that there was a significant gradient in surface salinity across the estuary, both at high and low water, but in

this instance the fresher water was on the right-hand side. This is opposite to that expected as a result of the Coriolis force, and Dyer attributed the distribution to topographic effects. He also found that the lateral salinity gradient increased with river discharge and decreasing tidal range. At one location the maximum lateral gradient was found to be about three times the longitudinal salinity gradient.

Observations of the velocity and salinity profiles were made throughout a tidal cycle across a section of the Rio Guayas estuary (Ecuador) by Murray et al. (1975). This study investigated not only lateral variability but the intra-tidal changes in lateral distributions. The section studied was 2280m wide and had an average depth of 6.5m. Hourly measurements were taken at six stations across the estuary over three successive tidal cycles. These were assumed to give a nearly synoptic picture due to the minimal diurnal inequality in temperature, salinity and tidal height at that location. The data were combined and maps of the cross-sectional distribution of speed and salinity were constructed for each lunar hour. Lunar hour zero was chosen as the time of slack before flood. In fact only the mid-section of the water column appeared to be slack at this time, the surface layer was still ebbing whilst the currents at the bottom had started to flood. The salinity throughout the section was at its tidal cycle minimum. The water overlying the central channel was weakly stratified whilst that to the sides was well-mixed. The least dense water was found at the surface on the right-hand side (looking upstream). Two hours later, at approximately maximum flood, current speeds of up to 150 cm/s were observed over the upper and eastern (right-hand) side of the channel,

the vertical stratification over the channel had sharpened and a lens of markedly less dense water was found on the surface left-hand side of the estuary. As the flood current weakened the higher velocities were still found to the right-hand side of the estuary, and the salinities continued to increase. The water column remained weakly vertically stratified and zones of strong lateral salinity gradient developed, particularly at the sides of the channel. At slack before ebb a distinct lateral current shear occurred, with the flood still in progress on the eastern (right-hand) side whilst the other side of the estuary had begun to ebb. The water column over the channel was now well-mixed, that to the sides partially stratified. As the ebb phase progressed the maximum velocities continued to be found in a sub-surface jet over the eastern side of the channel. The salinity distributions showed regions of strong lateral gradients with a well-developed plume of fresher water forming on the surface to the western (left-hand) side of the channel. At lunar hour 10 the edges of this plume showed a change in salinity of 7 over a horizontal distance of only 200m. These observations clearly illustrate the possible magnitude and variation in the lateral salinity gradients which may occur in a partially-mixed estuary. As this estuary is located in the southern hemisphere the distributions cannot be considered due to rotational effects. The authors consider them to be possibly due to channel shape.

Other than the influence of the Coriolis force, lateral circulation effects in estuaries result from topographic or channel irregularities, the influence of tributary rivers and flow around channel bends. Dyer (1977) proposed that, in partially-mixed estuaries, flow around a bend

would produce a secondary current from the outside to the inside of the bend at the surface, looking seaward, and in the opposite direction in the lower layer. The pycnocline would thus be expected to slope downward toward the inside of the bend. To test this hypothesis Boicourt (1982) attempted to obtain direct measurements of the direction and magnitude of lateral velocity components near a bend in the Potomac River. An array of 39 current meters on 19 moorings in an 8 km segment of the river was deployed. Lateral velocity components up to 40 cm/s were measured, and whilst the circulation pattern did not exactly follow Dyer's proposed model, distinct secondary flows were evident in the tidal currents as were topographically generated eddies, both along the side boundaries and over the deep channel. The data collected by West and Mangat (1986) was taken at a section immediately down-estuary of a large bend. Resulting cross-sectional distributions of velocity and salinity show highest velocities and lowest salinities in the deepest part of the channel near to the outside of the bend. The salinity distribution is consistent with a secondary flow toward the inside of the bend at the surface.

In some wide, shallow and well-mixed estuaries a lateral separation of the residual flows has been observed (Dyer, 1977) with the ebb currents dominant in the deeper channel and flood currents dominant in the shallower parts. For partially-mixed estuaries however, Fischer et al. (1979) proposed that the upstream flow is concentrated in the deeper portions of the channel whilst the return current occurs in the shallows. A net transport from deep to shallow areas is required to complete the circulation. It should be noted that it was this pattern

of transverse variation in the residual circulation that Fischer (1972) presumed to be generating the transverse net circulation term in the salt balance. However Dyer (1974) in his examination of the same term considered such lateral circulations to arise from the influence of Coriolis and centrifugal forces.

In the southern part of San Francisco Bay Cheng and Gartner (1985) concluded that the residual tidal currents, which showed a distinct lateral variation in direction and magnitude, are topographically generated when the wind is low and variable. In the summer months however, when the winds are moderate and steady, wind-driven residuals dominate. In the Potomac River Boicourt (1982) found that cross-estuary winds drive a lateral circulation cell, with upwelling on the lee shore and downwelling on the windward shore. The return flow occurred immediately below the pycnocline.

Irregularities in cross-sectional bathymetry were shown experimentally by Sumer and Fischer (1977) to generate transverse currents whose direction reversed with the tide. The channel section used was a nearly triangular trapezoid whose longer sloping side was made undulating in an attempt to introduce large-scale transverse eddies into the flow. They found that the transverse salinity gradient varied throughout the tidal cycle due to the increased vertical mixing along the wavy side, plus a frictionally-induced phase lag between the shallow and deeper parts of the channel. The density distribution generated a transverse flow which was directed onto the shoal areas at the surface during flood tide, with a return flow along the bottom, and in the

opposite direction during ebb tide. The marked difference in depths across many coastal plain estuaries may influence lateral circulations in other ways also. Schijf and Schonfeld (1953) proposed that the shoal areas may act as storage basins and in this way influence the longitudinal mixing. Lateral seiching in Southampton Water measured by Dyer (1982) was considered to be due to internal waves generated by the periodic intrusion of the pycnocline on to the shallow shoals to the sides of the channel. Cannon (1969) measured significant velocity fluctuations in the Patuxent estuary with a period that matched a calculated cross-estuary surface seiche.

In well-mixed estuaries significant lateral gradients in density can be generated by differential advection of the longitudinal density gradient. This was first noted by Imberger (1976) and examined in more detail by Smith (1980). Using this principle Nunes and Simpson (1985) explained the transverse circulations and distinct axial convergence which they observed in the Conway estuary in North Wales. The cross-estuary salinity difference and associated flows occurred only during the flood tide phase, and only in the region of the estuary where the longitudinal gradients are largest. Transverse velocities up to 10 cm/s, or 20% of the axial velocity, and horizontal salinity differences across the 200m wide channel of 1 were measured.

In conclusion therefore, this review of the literature has shown that there have been few studies of the lateral density distribution in estuaries, and especially of the changes in density which occur on an intra-tidal time scale. Lateral variability in density and velocity

may, however, be dynamically important, and characteristic of many estuaries.

PART II: SMALL SCALE FRONTS

Fronts are widespread phenomena of oceanic systems. They occur at all scales, from those which are hundreds of kilometers in length and persist for months at a time, to those of only a few hundred meters, found in estuaries and other shallow coastal areas, whose existence can be very transitory.

For the purposes of this review only 'small-scale' fronts will be considered. Here 'small-scale' is taken to mean that rotation does not play a major dynamical role in either the formation or maintenance of the fronts. A front is generally defined as a boundary between water masses across which there is an appreciable gradient in density and other physical properties. Small-scale fronts can be broadly divided into:

- (i) estuarine fronts - occurring within estuaries
- (ii) plume fronts - occurring at the boundaries of buoyant outflows issuing from the mouths of rivers and/or estuaries
- (iii) shelf-sea fronts - occurring at location across the continental shelf where there is a transition from a stratified to a well-mixed regime.

This latter type is considered to be quasi-geostrophic. Beyond the shelf and within the ocean are other types of fronts, eg. bordering the

Gulf Stream and in association with areas of upwelling, but these are all of a much larger scale.

1. ESTUARINE FRONTS

Although fronts observed within estuaries appear to be varied, and possibly even site-specific, they are all characterized by:

- a. an intra-tidal time scale
- b. spatial predictability, which is sometimes due to a strong bathymetric influence on their location.

The details of their dynamics are determined by the circulation and mixing of water masses within the particular estuary.

The possible importance of fronts to the circulation of an estuary was first noted by Godfrey and Parslow (1975) who described two kinds of fronts within the Port Hacking (Australia) estuary: one which occurred on the ebbing tide when the bathymetrically modified tidal currents brought dissimilar water masses together, and another which formed on the flooding tide at the boundaries to inner basins. These latter 'rising-tide' fronts were further studied by Huzzey (1982) who confirmed their dynamics as being due to the incoming flood tide entering the more brackish inner basins as a turbulent density current. The position of the front was found to be dependant on the water depth and density difference between the two water masses.

A similar tidally-induced front in the Saint Lawrence estuary was studied by Ingram (1976). There it was found that a sharply defined

boundary, marked by a color change and density difference of up to 5 kg/m^3 , moved laterally across the estuary within the first hour after high tide. This boundary extended 8-10m below the surface and its final position appeared to be limited by bathymetry. Convergent velocities of 45-50 cm/s were recorded. It was concluded that the driving mechanism was the cross channel pressure gradient resulting from tidal height inequality.

In shallower and partially-mixed estuaries fronts are frequently found bordering shoals and other bathymetric features. An extensive network of such fronts, which may be termed 'longitudinal', can be seen in the Delaware Bay. Observations by Klemas and Polis (1977) revealed that some of these fronts may extend for many miles parallel to the axis of the Bay's channels. In the vicinity of the surface front salinity gradients of $4/\text{m}$ and convergent velocities of 10 cm/s were recorded. There appeared to be a change between vertically well-mixed and stratified conditions across the frontal zone, the frontal boundary merging into the normal pycnocline at depth. Sequential mapping, using Landsat images, showed that there are great changes in the positions of these fronts over one hour periods, indicating rapid generation and decay, and that their location appeared to be related to the bathymetry. Aerial photography and satellite imagery were used to delineate frontal zones in the James River and lower Chesapeake Bay (Nichols et al., 1972, Nichols, 1975). Measurements of the water properties in the vicinity of these boundaries revealed no marked discontinuity in temperature and salinity. It was noted however that these features recurred at comparable stages of successive tides and in similar positions.

Within the smaller and frequently well-mixed estuaries around the United Kingdom two other examples of estuarine fronts have been observed, both of which occur during flood tide. Simpson and Nunes (1981) describe a 'tidal intrusion' front which occurs at the mouth of the River Seiont as the incoming tide stems the down-estuary fresh water flow. The surface front is V shaped and extends across the entire width of the estuary. Convergent velocities of 15 cm/s and a change in salinity of up to 30 across the frontal zone were recorded. Upstream of the front the flow is two layered and a simplified two-dimensional model of this front, considering the upper freshwater layer as a buoyancy current, was developed. In contrast to this type of front an 'axial convergence zone' has been found in several well-mixed estuaries (Nunes and Simpson, 1985 Simpson and Turrell, 1985). This forms as a result of transverse density gradients produced by the non-uniform advection of the longitudinal salinity gradient along the estuary. It only occurs in the latter part of the flood cycle, and in regions of the estuary where the longitudinal density gradient is the greatest. A diagnostic model of this lateral circulation was developed and verified using field data obtained from a specially developed boat-mounted sensor system. Convergent velocities of up to 20 cm/s were measured.

2. PLUME FRONTS

As the relatively fresher water discharges from an estuary or river mouth into the adjacent coastal ocean it frequently forms a plume or coastal jet, at the boundaries of which fronts can be found. These boundaries are often strikingly apparent due to the difference in color

and turbidity between the plume and ambient coastal water. Wright and Coleman (1971) noted the apparent convergence associated with the plume boundary of the Mississippi River. Extensive investigations of the frontal zone of the Connecticut River plume (Garvine, 1974, Garvine, 1977, Garvine and Monk, 1974) have revealed convergent velocities up to 50 cm/s and a change in density across the surface front of up to 9 kg/m^3 . The frontal boundary appeared sinuous. Beneath the surface the interface sloped downward over a horizontal distance of the order of 50m until it attained a depth of 1 to 2 metres. Beyond that the isopycnals were approximately level and it was therefore postulated that the cross-frontal circulation is generated by the horizontal pressure gradients within the frontal zone, continuity being maintained by a downward vertical mass flux across the interface. Bowman (1978) observed frontal zones surrounding the Hudson River plume across which there was a change in salinity of 5. Studies of the Great Whale River plume (Ingram, 1981) showed it to be characterized by a thickness of 1-2m and very strong horizontal and vertical salinity gradients in the frontal zone. A more fine scaled set of measurements across a frontal zone associated with the Collie River outflow (Brubaker, 1982) revealed large amplitude undulations in the density field and strong dissipation of kinetic energy generated by wind stirring and interfacial shear. Analogous plume fronts may be found within estuaries following a period of intense rainfall (Godfrey and Parslow, 1975, Wolanski and Collis, 1976). These are usually transitory features with a residence time on the order of days.

3. SHELF-SEA FRONTS

Beyond the vicinity of estuaries and rivers and their brackish effluents, another type of small-scale front can be found within the relatively shallow continental shelf seas. These 'shelf-sea' fronts were first noted by Simpson (1971) who observed that a region of weak tidal currents in the Irish Sea was strongly stratified during the summer months, and bounded by marked temperature fronts. This was further investigated by Simpson and Hunter (1974) who used remote sensing techniques plus ship surveys to map the positions of regions of maximum surface temperature gradient. These regions were found to be similarly located on all surveys and correspond to boundaries between stratified and vertically-mixed water masses. They hypothesised that this transition between stratified and unstratified regimes was controlled by the level of tidal mixing. This idea was expressed mathematically by considering the ratio between the buoyancy input in the form of solar heating and the kinetic energy generated on the bed by tidal motion. When simplified, this model predicted that a critical value of the parameter h/u^3 (where h =water depth and u =amplitude of the tidal velocity) should mark the division between a mixed and stratified water column. Mapping values of this parameter for the Irish Sea they found that a value of 65-100 corresponded to the observed position of fronts.

Investigations of a similar front in the English Channel by Pingree et al. (1974) showed that the water on either side of the front was differentiated by temperature and salinity, and the frontal boundary

itself very turbulent and sinuous, with wavelengths of the order of 100m. Convergent velocities of approximately 25 cm/s were estimated from drogue studies and, due to the lack of strong along front flow, they concluded that the dynamic balance in the frontal region was not simply geostrophic. However subsequent studies by Simpson (1976) and Simpson et al. (1979) revealed the presence of residual along-front velocity components whose magnitude was of the same order as the geostrophic shear inferred from the density gradient. These studies confirmed that the location of such fronts does conform to the h/u^2 model, even though in the instance of the Islay front (Simpson et al., 1979), temperature plays a secondary role in controlling the density. This study additionally showed that the distribution and concentration of phytoplankton in the frontal region was closely related to the physical structure. Shelf-sea fronts have also been found in the Eastern Bering Sea where Schumacher et al. (1979) identified a persistent front parallel to the 50m isobath during the ice-free seasons, separating a well-mixed coastal domain from a two layered central shelf domain.

Remote sensing, particularly by IR imagery, has proved useful in not only mapping the position of these fronts but also identifying large scale (20-40km) cyclonic eddies which are thought to play a role in cross-frontal mixing (Pingree, 1978). Simpson and Bowers (1979) used this technique to investigate the extent to which the mean position of such fronts adjusts to variations in both the rate of tidal mixing and surface heat flux. They found that these fronts move very little, suggesting the existence of a feedback mechanism. In this way, once the

stratification is established the efficiency of mixing is reduced, so that even when increased tidal stirring occurs at spring tides, the stratified condition persists. Schumacher et al. (1979) suggest that such a feedback mechanism is important to the process of frontogenesis in the Eastern Bering Sea. Field investigations of the structure of shelf-sea fronts using an undulating towed CTD (Allen, Simpson and Carson, 1980) have confirmed that although the frontal structure does respond to the semi-diurnal tidal cycle it's mean position remains constant and it is not affected by the neap-spring cycle.

4. MODELS OF SMALL-SCALE FRONTS

Many attempts have been made to characterize the observed small-scale frontal structures by mathematical models. Most such models are concerned with either shelf-sea or plume fronts whose dynamics appear to be more consistent and more easily generalized than those of 'estuarine' fronts.

Following his field investigations of the Connecticut River plume Garvine (1974) developed an integral and steady state two-dimensional model of plume fronts. In this model he prescribes the form of the vertical density and velocity variation and assumes that the driving force for the motion is the horizontal pressure gradient generated in the frontal zone by the sloping free surface and isopycnals. This pressure gradient is balanced by the turbulent dissipative processes of interfacial friction and mass entrainment. This model also showed the strong convergence at the surface front and associated downwelling along

the inclined frontal interface which had been observed in the field. It was found that an overall dynamic balance could be achieved when the frontal system advanced into the ambient fluid at a speed which made the bulk Richardson number of order one.

This integral model was subsequently expanded to incorporate the effects of rotation and wind stress (Garvine, 1979a, 1979b). The predicted circulation then contained a jet of velocity parallel to the front with speeds below geostrophic values, as well as the two-sided convergence and sinking normal to the front. The model was compared to field observations of fronts of various scales ranging from river plume fronts to the Gulf Stream front. Unfortunately these field observations often contained limited data, especially of the vertical velocity profile, so the model was not rigorously tested. This concept was further extended by the inclusion of a thermodynamic or buoyancy equation (Garvine, 1980) which was used to evaluate the various components of the potential and kinetic energy equations for the different scale fronts. This model showed that the direction of turbulent mass entrainment is always downward. It should be noted that all of these models developed by Garvine pertain only to the hydrography of established and persistent fronts. They do not consider the mechanisms of frontogenesis.

A markedly different approach to modelling of plume fronts was taken by Kao et al. (1977) who numerically solved, via an initial boundary value problem, the full two-dimensional Navier-Stokes and diffusion equations. A turbulence model using the Munk-Anderson

parameterization for density stratification was included. The results showed that the plume propagates as a gravity current, with a front at its outer boundary, and attains a constant velocity with magnitude dependant on the densimetric Froude number of the inflow. The structure within the plume showed the features of a headwave with shoaling isopycnals towards the surface front, downwelling circulation and a two-sided surface convergent flow at the front. These results compare favourably with the field observations of Garvine and Monk (1974) and incidentally help justify some of the assumptions made in the steady state model of Garvine (1974). In this model the evaluation of frontal speed utilizes inviscid theory but the other aspects (confluence at the front, upwelling/downwelling etc) depend on friction. In addition to describing the spreading density current, this model contributes to our understanding of the dynamics of establishment of the front itself.

Inclusion of the effects of rotation and ambient stratification (Kao et.al.,1978) showed that the deflection, due to the Coriolis effect, of the forward motion of the buoyancy current decreases the forward speed of the front. When steady state is achieved the front becomes stationary relative to the ambient fluid and exhibits a strong baroclinic along-front jet in addition to surface convergence and downwelling at the front. It was also found that internal waves could be formed during frontal progression when the downwelling jet impinges on the thermocline.

In contrast to his earlier (and mathematically complex) thermodynamic model of upper ocean density fronts Garvine (1981,1982)

proposed that buoyant plumes could be divided into two domains - a frontal domain where dissipative effects are important and an interior region of the flow where the dynamics of inviscid non-linear gravitational spreading dominate. In this way the front itself is treated as moving discontinuity across which the flow properties are related by the appropriate jump conditions. This approach, which neglects rotation, was used to model the steady state flow produced by the supercritical outflow of buoyant water into coastal water with a uniform alongshore current. The results were considered to explain many observed features of the Connecticut River plume. O'Donnell and Garvine (1983) developed a numerical scheme to include time dependence into the governing equations and Garvine (1984) used this model to investigate the mechanism for the formation of multiple rings of fronts which have been observed in some shallow buoyant plumes.

Stigebrandt (1980) considered the problem of the motion of non-rotating plume fronts in terms of hydraulic theory. It was assumed that the velocity of the front and depth of the layer upstream of the front is controlled by a transition section behind the current head where the Richardson number becomes critical. The dynamics of the head, or frontal zone, are not important to the propagation of the density current, although this zone is the site of interfacial mixing which generates the observed convergent circulation near the front. Thus the secondary circulation is viewed as being superimposed on the first order hydraulic motion of the front.

Models of the shelf-sea fronts have largely followed the postulate of Simpson and Hunter (1974) that these fronts occur where the ratio of kinetic and potential energy within the water column attains a critical value. This 'stratification parameter' was contoured over a part of the British continental shelf by Fearnhead (1975) who found a critical value of 2.0 - 2.5, depending on latitude. Pingree and Griffiths (1978) undertook similar contouring on the entire shelf seas surrounding the British Isles and, by comparison with infrared satellite images and observational data obtained a critical value of 1.5. The mixing model was extended by Simpson, Allen and Morris (1978) to include the effect of wind mixing. Thus they consider the overall potential energy balance of the water column to be the sum of the stabilizing force of buoyancy input due to solar heating, plus the destabilizing influences of tidal and wind mixing. This model assumes a constant 'efficiency' or rate of conversion of kinetic energy, from wind or tidal mixing, to potential energy. Such a model predicts that the position of the front will oscillate over the neap-spring tidal cycle. However observations have suggested the occurrence of a feedback mechanism whereby this efficiency is influenced by the existing level of stratification. Accordingly Simpson and Bowers (1981) modified the energy model to allow for variable efficiency. Although these energy models appear to successfully predict the mean positions of shelf-sea fronts, they do not predict the detailed structure of the front, and consider only vertical mixing processes. The circulation in the frontal zone was investigated by James (1978) in a two-dimensional numerical model. By incorporating both friction and Coriolis force he showed that convergent flow and

upwelling can occur at the transition between well-mixed and stratified water masses.

Assuming non-rotating and frictionless flow Nof (1979) proposed that the mutual intrusion (driven by pressure gradients) of water bodies which had been exposed to varying degrees of vertical mixing could generate regions of strong horizontal density gradients. These predictions were tested via a tank experiment and the density structure produced was found to be similar to that observed in shelf seas. It was suggested that this mechanism may also generate estuarine fronts. This concept was elaborated upon by Wang (1984) using a two-dimensional numerical model. The flow adjustment between two initially separated water masses of different density was found to generate a surface and bottom front propagating in opposite directions and strong recirculation in the frontal zone. Including viscosity slowed the frontal propagation and including rotation generated a baroclinic along-front jet. The instance of a sloping bed was also considered. In the non-rotating case it was shown that the flow adjustment will be affected downslope gravitational acceleration. The propagation of the surface plume into the deep water is the same as in the flat bottom case. However the shoreward propagation of the bottom front is retarded by gravity. Thus, because the heavier water cannot intrude into the shallow region, a stationary front is formed at the break in slope. The findings of this model were shown to compare favourably with observations of the frontal structure and mean southward current associated with the New England shelf-slope front.

To date, no numerical models have been developed to specifically examine the dynamics of the type of estuarine fronts considered in this study. There have been many observations of such 'longitudinal fronts', most notably by Klemas and Polis (1977) in the Delaware Bay. However the conditions associated with their formation and maintenance are still uncertain. This study aims to develop an understanding of possible frontogenesis mechanisms, in conjunction with a detailed study of the intra-tidal lateral variation in velocity and density across the York River estuary.

III. LATERAL DENSITY DISTRIBUTION

A. METHODS

A series of experiments was conducted with the aim of documenting the variability of the lateral density structure across the York River throughout a tidal cycle.

Six stations, marked by buoys, were set up across the study transect (see Fig.3.1). A vertical CTD cast, using a continuously recording Neil-Brown CTD, was made at each station once every hour. Only one boat was used, thus the stations were sampled sequentially, always starting at station 1. The transect took approximately 15 minutes to complete. Each days sampling was timed to start at the time of predicted slack tide. With the exception of two tidal cycles, the flood and ebb portions of the tidal cycle were sampled on separate days.

Previous studies (Haas,1977, Ruzecki and Evans,1986) have shown this estuary to undergo a neap-spring variation in stratification. To assess the influence of this destratification cycle on the lateral density structure the experiments were conducted during times of predicted spring, mean and neap tides. For the purposes of this study the tidal range was divided in the following way:

spring - tidal range of greater than or equal to 0.8 meters

mean - tidal range of 0.7 or 0.6 meters

STUDY TRANSECT
(LOOKING UP-ESTUARY)

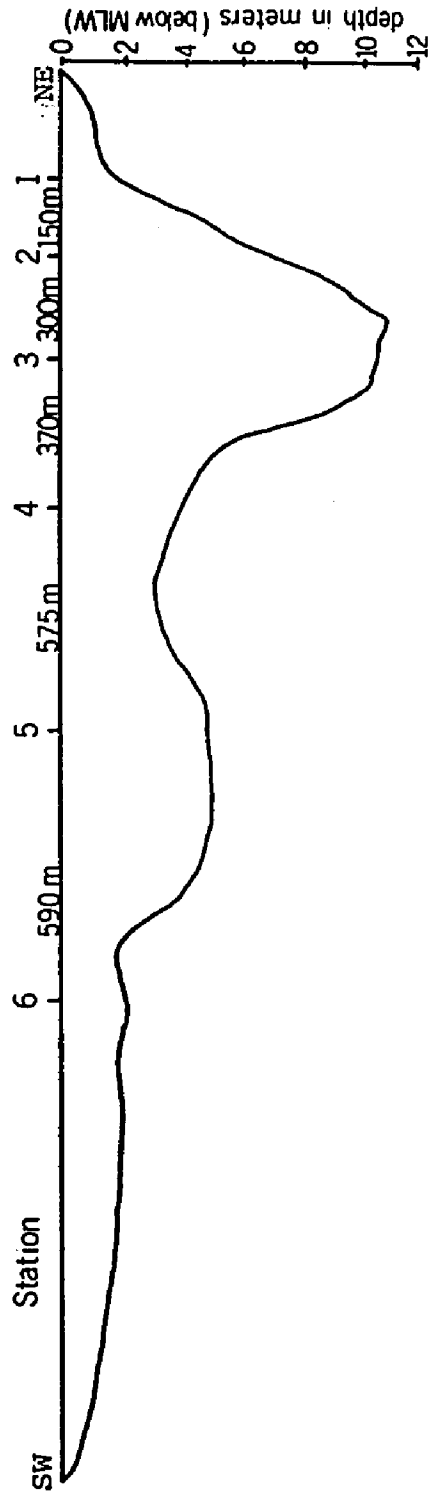


FIG.3.1 Location of the CTD sampling stations across the study transect.

neap - tidal range of less than or equal to 0.5 meters

Sampling was repeated on several occasions for each tidal range condition to enable a more generalized picture of the density structure to be obtained. The dates are listed below.

	SPRING	MEAN	NEAP
	12 May 1983	10 May 1983	
FLOOD	13 May 1983	17 May 1984	**
		18 May 1984	
		15 June 1984	
	12 May 1983	25 May 1984	21 June 1984
EBB	13 May 1983	7 June 1984	22 June 1984
		8 June 1984	

**experiments abandoned due to adverse weather conditions

In order to standardize and compare the results for similar phases of the tidal cycle from different days, the tide was divided into 12 'Tide Hours', HOUR 1 being the time of predicted slack-before-ebb (U.S. Dept. of Commerce, 1983, 1984). Using this scheme maximum ebb falls between Hour 3 and Hour 4, maximum flood between Hour 9 and Hour 10 and Hour 7 is the time of slack-before-flood.

The main disadvantage of this method is that the tidal cycle is not exactly 12 hours in duration. There may also be a difference in tidal

phase across the estuary although it is unlikely that this is as great as one hour. Grouping the data in this way however makes it possible to obtain an understanding of the generalized change, through the tidal cycle, of the lateral density structure, which was the aim of these experiments.

As it is only the relative density difference, in both the lateral and vertical direction, which is of interest here, the data for each transect or section was further standardized by subtracting the section average. Then the data for the same tide hour on all days (of the same tidal range) was then combined and averaged.

Although the 1984 data set for mean and neap tides was collected over a total period of one month the freshwater flow conditions, and thus the average salinity, varied very little during this time. For this reason the data collected on 10 May 1983 was not included in the analysis of mean tide conditions because the salinity was found to be very different on that date. In an effort to eliminate the direct effects of wind on the circulation, data was collected only on days when the winds were 10 mph or less.

B. RESULTS

1. DENSITY DISTRIBUTION

a) SPRING TIDES

The sequence of changes in the lateral density distribution through a spring tide cycle is illustrated by data collected on 12 May 1983 (Fig.3.2), as well as standardized and averaged sections (Fig.3.3). In both instances lateral inhomogeneities in the density distribution occur, particularly in the upper 2 meters of the water column, and there is a persistent tilt to the isopycnals, downwards toward the south-western side of the estuary. As a result the boundary at the inner edge of the south-western shoal is frequently the site of strong lateral density gradients. This is especially so during the ebb cycle (Figs.3.2a, 3.3a), and may be attributed to the influence of the Coriolis force on the longitudinal flow.

The sequence of events through a tidal cycle can best be traced by observing the sequential location of water of a particular density. With reference to the 12 May 1983 data (Fig.3.2), from which the section averages have not been subtracted, and considering, for example, water with a density between $6.5\sigma_t$ and $7.0\sigma_t$ as our 'tracer', it can be seen that at Hour 1 (slack-before-ebb) this water is in a narrow band tilted downward between Stations 5 and 6. One hour later the layer has become slightly thicker and more laterally extensive. By Hour 3 it can be found in a horizontal band about 1 meter thick across most of the estuary, from station 1 to between stations 4 and 5 it is at the

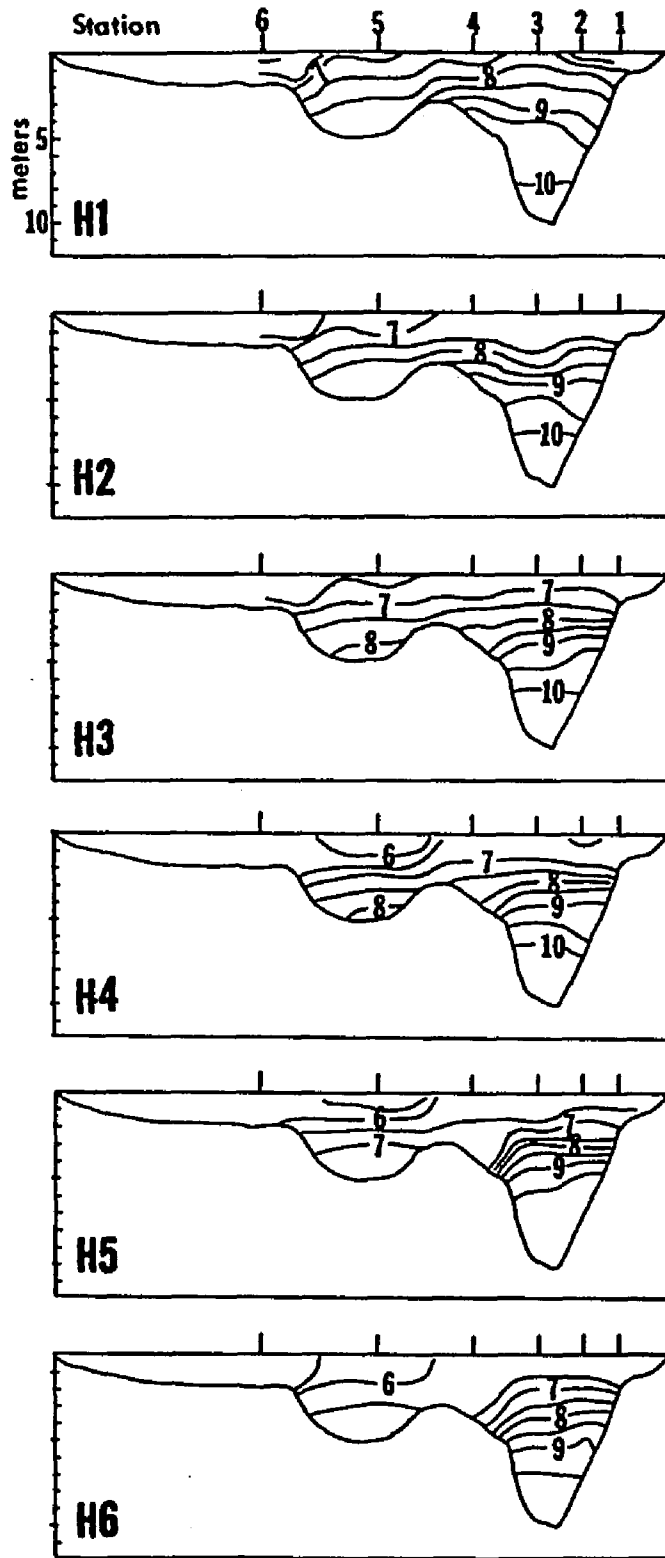


FIG. 3.2a

Cross-sectional density distribution,
12 May 1983. (0.5 sigma-t intervals)

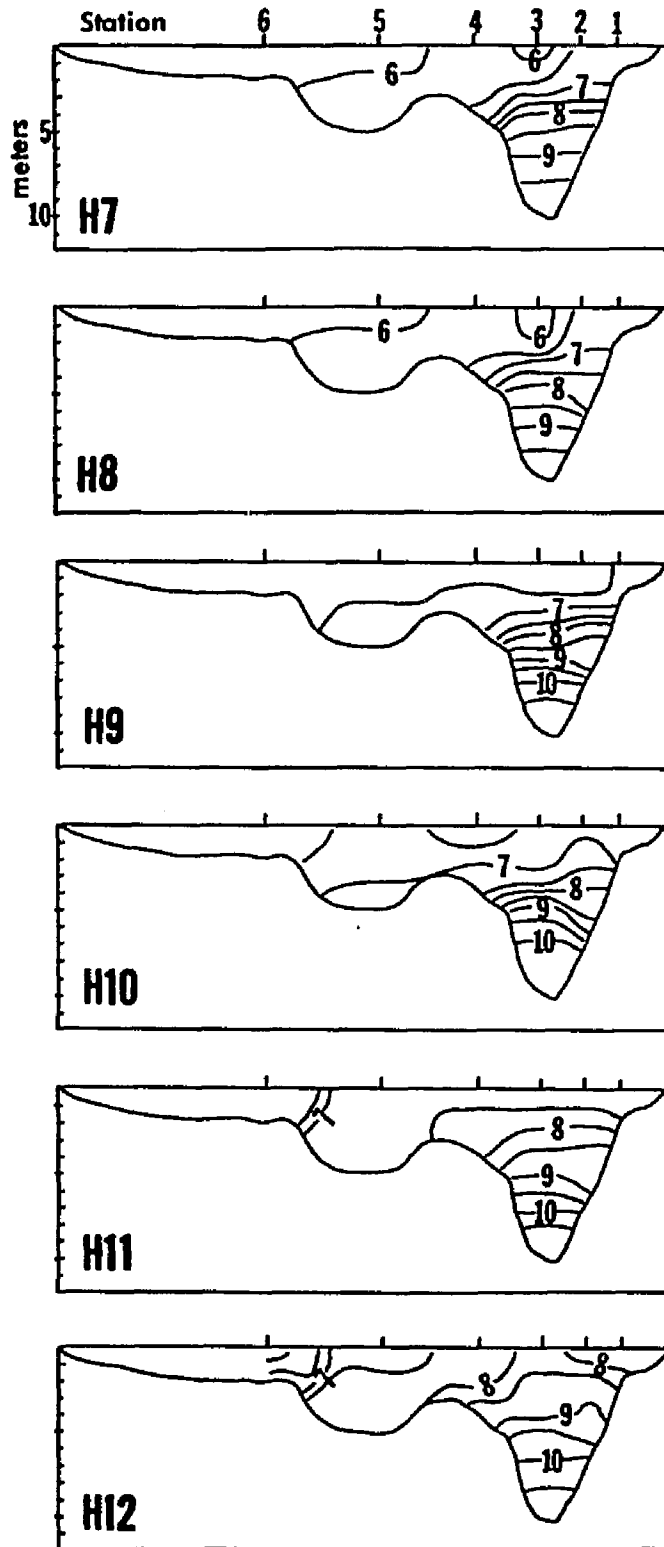


FIG.3.2 b

Cross-sectional density distribution,
12 May 1983. (0.5 sigma-t intervals)

surface, south-west of that it plunges downward. As the ebb phase progresses, bringing in even less dense water at the south-western side, this layer remains intact but gets depressed further down the water column. By Hour 7 (slack-before-flood) the water of this density occupies the entire water column over the north-eastern shoal, extending down in a layer across the main channel. There is little change in the next hour but by Hour 9 the layer has thickened and started to move vertically upwards. Then at Hour 10 it occupies most of the water column from a depth of 3 meters to the surface at all stations except station 6 on the south-western shoal. After Hour 10 there is a significant change, the $6.5-7.0\sigma_t$ water, having been displaced by denser water flooding along the main channel, is once again located at the inner edge of the south-western shoal. The observed distribution at Hour 12 is almost identical to that at Hour 1.

A similar sequence can be seen in the standardized sections illustrated in Fig.3.3. As the sigma-t values contoured are relative to each section mean a particular water mass cannot be followed in the same way. However the change in lateral density structure can be observed.

At the beginning of the ebb cycle (Hour 1) the freshest water is located over both shoals, and a very strong lateral density gradient forms at the inner edge of the south-western shoal where the isopycnals intersect the bed. The stratification in the channel is much less than at mean tide (see Fig.3.5), and remains so throughout the ebb tide. Although this section is within a portion of the York River that has been identified (Ruzecki and Evans, 1986) as experiencing the least

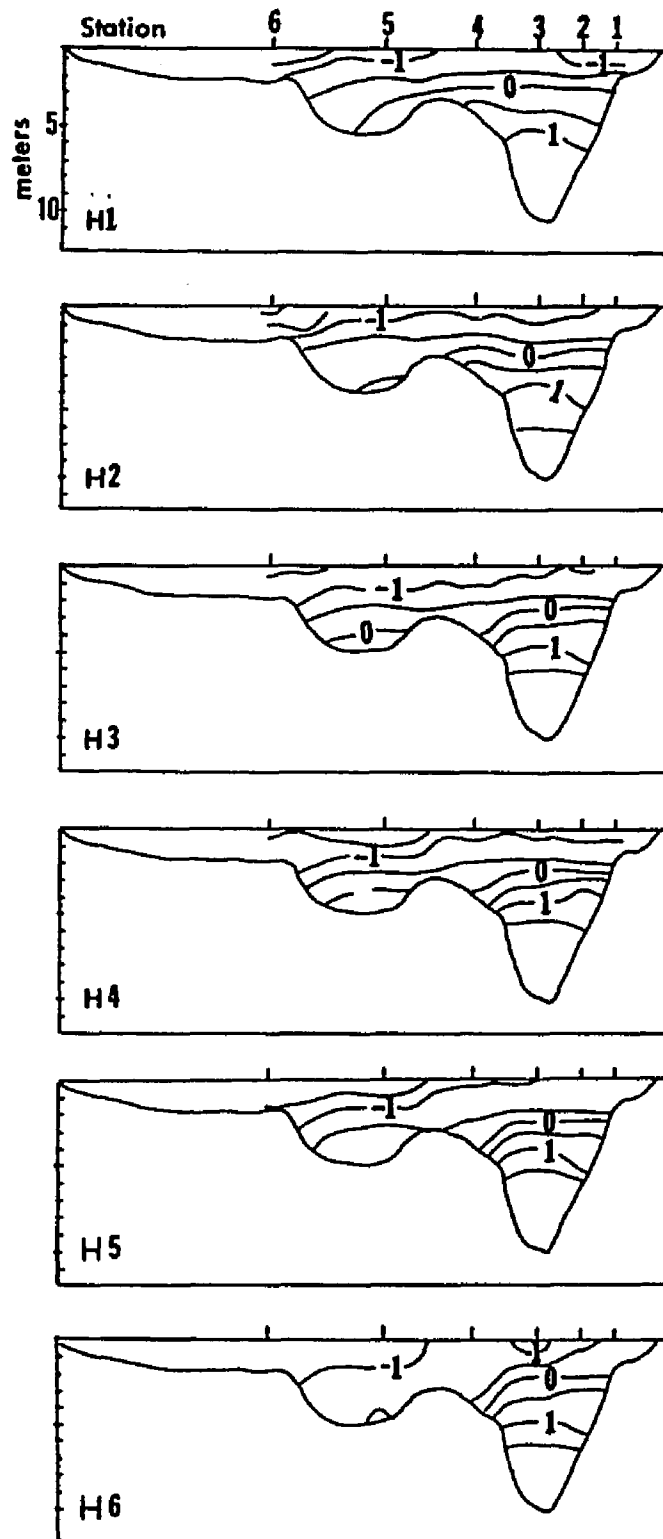


FIG.3.3a

Cross-sectional density distribution,
Spring tides. (0.5 sigma-t intervals)

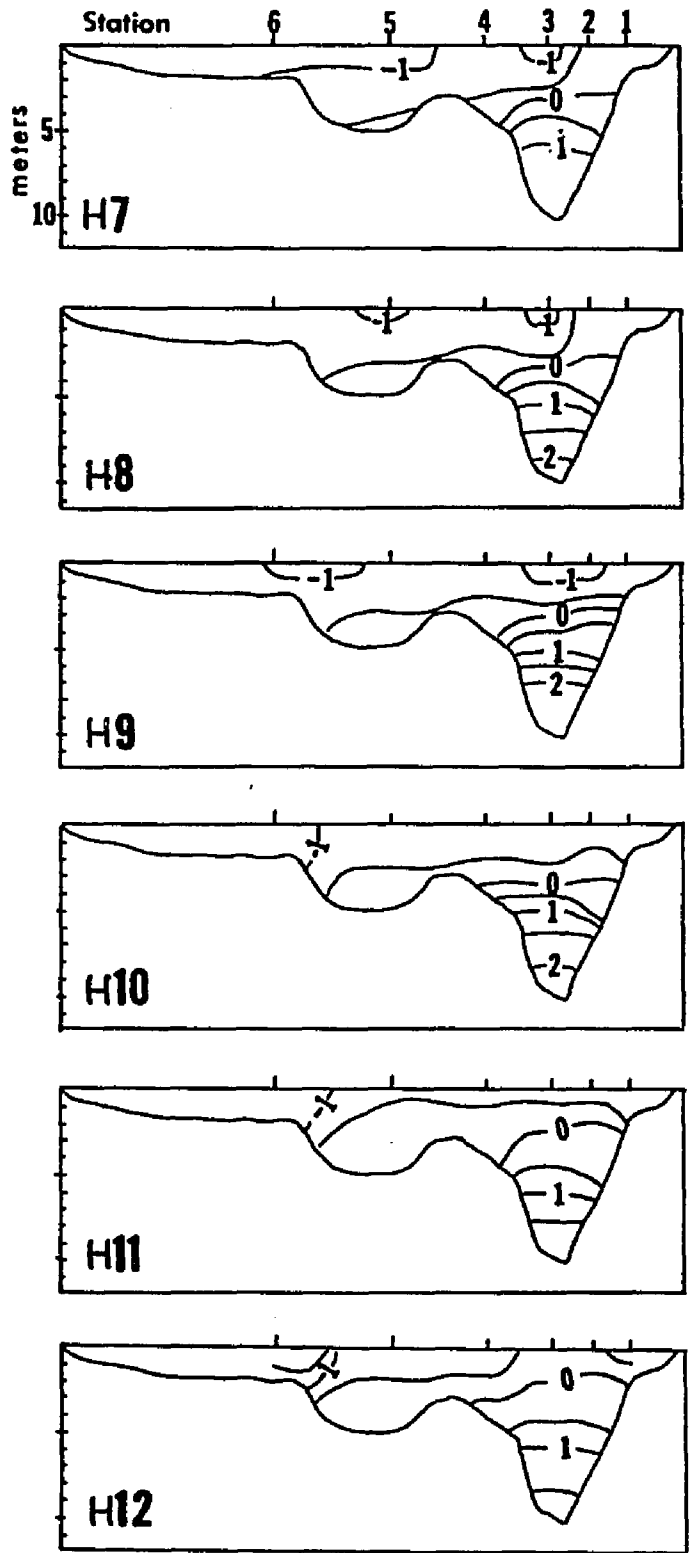


FIG.3.3b

Cross-sectional density distribution,
Spring tides. (0.5 sigma-t intervals)

destratification, it is not surprising to find markedly less stratification at times of spring tides. The isopycnals, except at the inner edge of the south-western shoal, are generally level across the estuary at Hour 2. One hour later however they start to show some tilting, with the freshest water laying in a wedge extending from the south-western side of the estuary across to the main channel. The pycnocline in the main channel becomes more well-defined (see Fig.3.4) and by maximum ebb (Hour 4) the secondary channel also becomes stratified. This is in contrast to mean tides where stratification is almost entirely restricted to the main channel. At Hour 5 a region of marked lateral density gradient is located in the centre of the estuary, and by Hour 6, the pycnocline has broadened and the freshest water is found in a lens at the surface over the main channel and again on the south-west shoal.

This density distribution continues through the early part of the flood cycle (see Hour 7, 8, and 9, Fig.3.3b) the surface fresh layer over the channel becoming broader with time. There is a distinct change however at Hour 10. The least dense water in the section is now once again located over the south-western shoal. The inner boundary to this shoal is marked by steeply tilting isopycnals, although the upper layer over the remainder of the estuary is laterally homogenous. Some lateral density gradients develop by Hour 12 where the density distribution is transitional to that of slack-before-ebb.

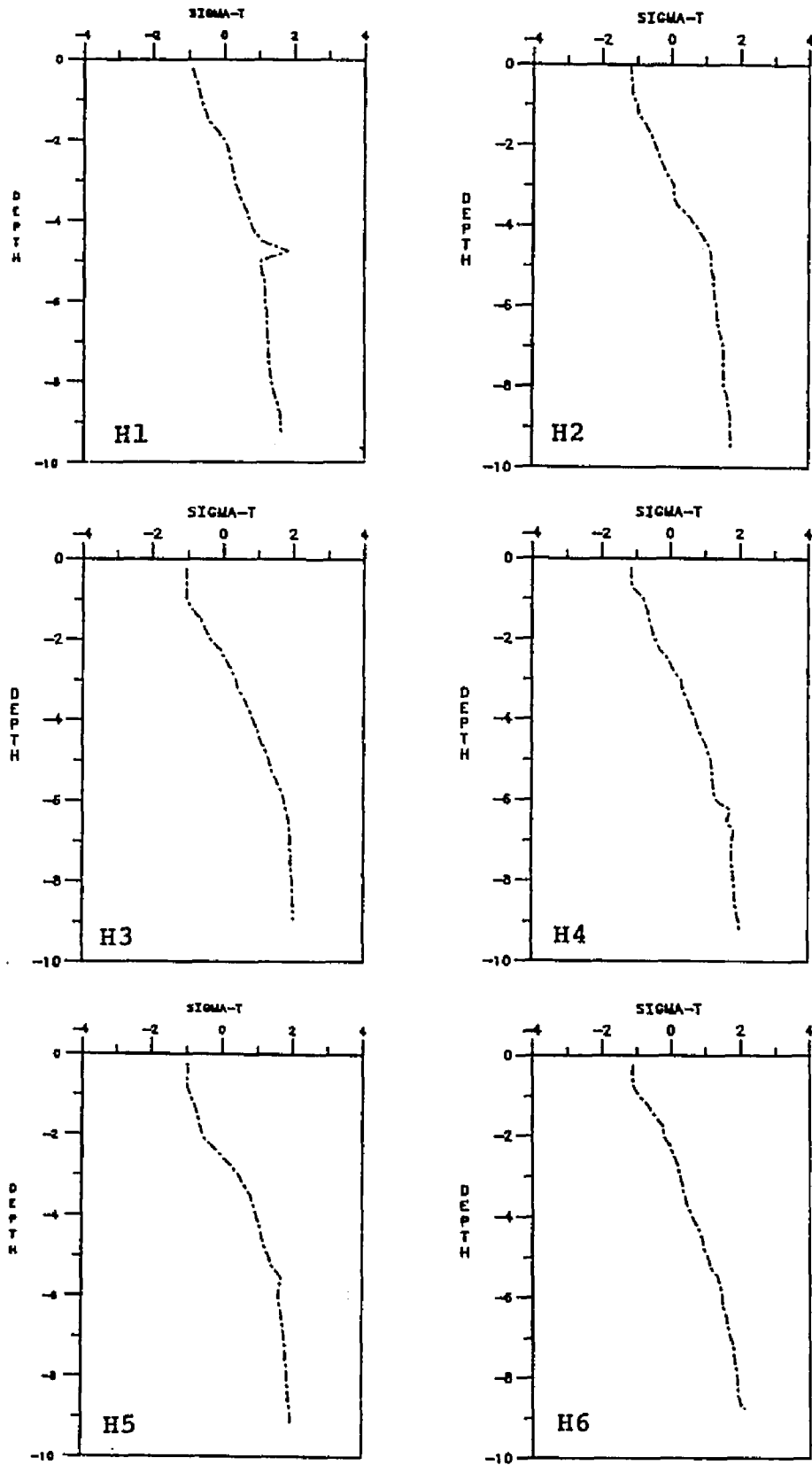


FIG.3.4a Vertical density profiles at Station 3, Spring tides.

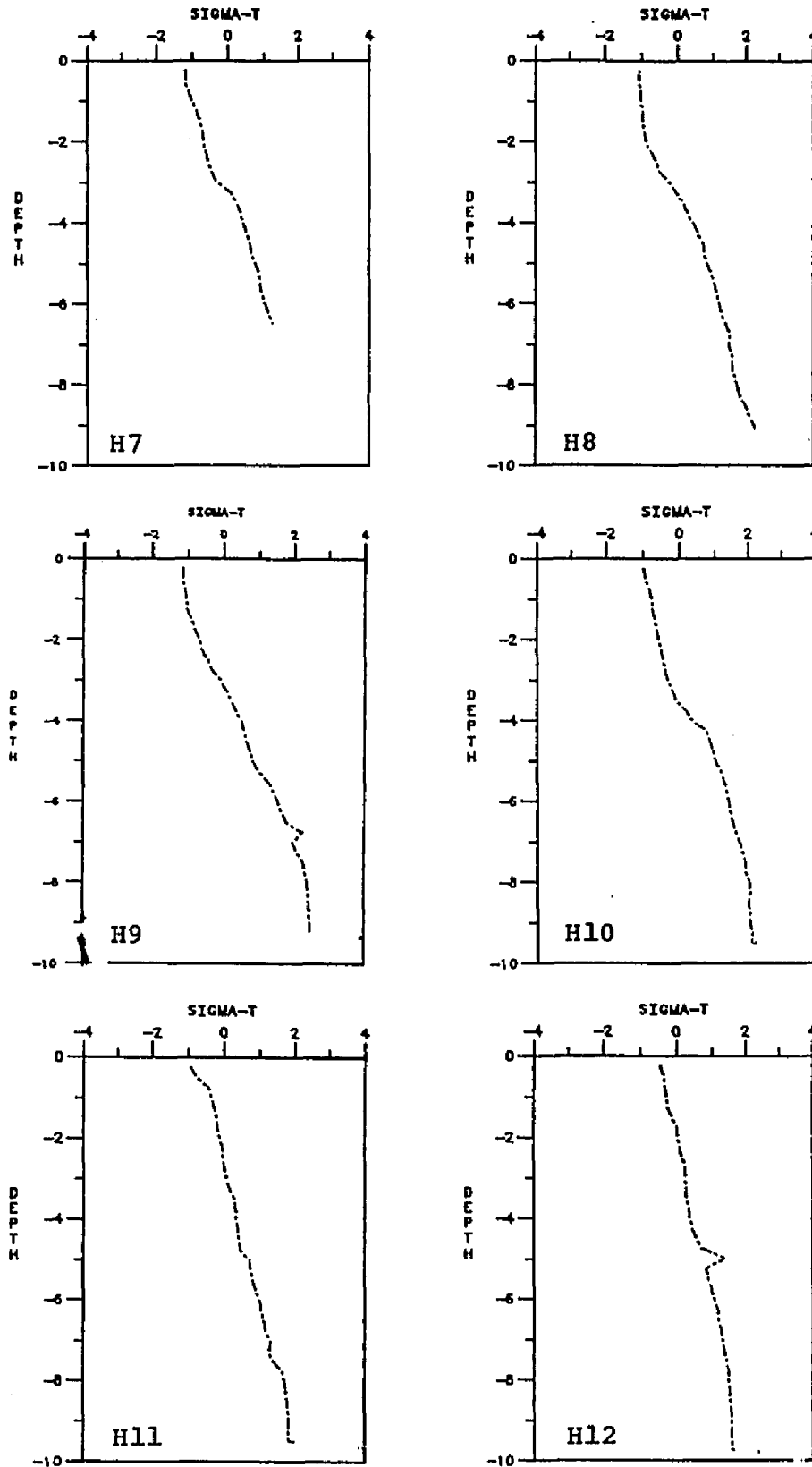


FIG.3.4b Vertical density profiles at Station 3, Spring tides.

b) MEAN TIDES

Looking at the sequence of isopycnal contours illustrated in Fig 3.5 reveals once again a cyclical pattern. In this instance stratification is restricted to the main channel, the more dense water below the pycnocline rarely intruding onto the neighbouring shoals.

With reference to Fig.3.5a, at slack-before-ebb (Hour 1) the least dense water is located over the shoal areas (less than or equal to 2m deep) to the sides of the estuary. A zone of strong horizontal density gradient forms at the inner edge of both of these shoals. One hour later (Hour 2) the ebb tidal phase has begun and lateral gradients in the upper layer are considerably diminished. The freshest water can now be found in a wedge extending from the north-east bank to midway across the estuary, and again on the south-west shoal. A pycnocline has begun to form over the main channel. As the ebb progresses (Hour 3 - Hour 5) this pycnocline becomes increasingly well-defined (see Fig.3.6). Lateral gradients in the upper 1-2m disappear, this layer becoming uniformly fresh over the complete width of the estuary. The isopycnals across the channel show some downward tilting on the south-western side of the channel whilst the secondary channel becomes partially stratified. At the junction between this minor channel and the south-western shoal the isopycnals turn downward and intersect the bed making a distinct boundary between a partially stratified and well-mixed regime. At the end of the ebb cycle (Hour 6) the lateral density structure changes greatly. The pycnocline virtually disappears (see Fig.3.6) and the most dense water is located along the right-hand bank of the channel bed.

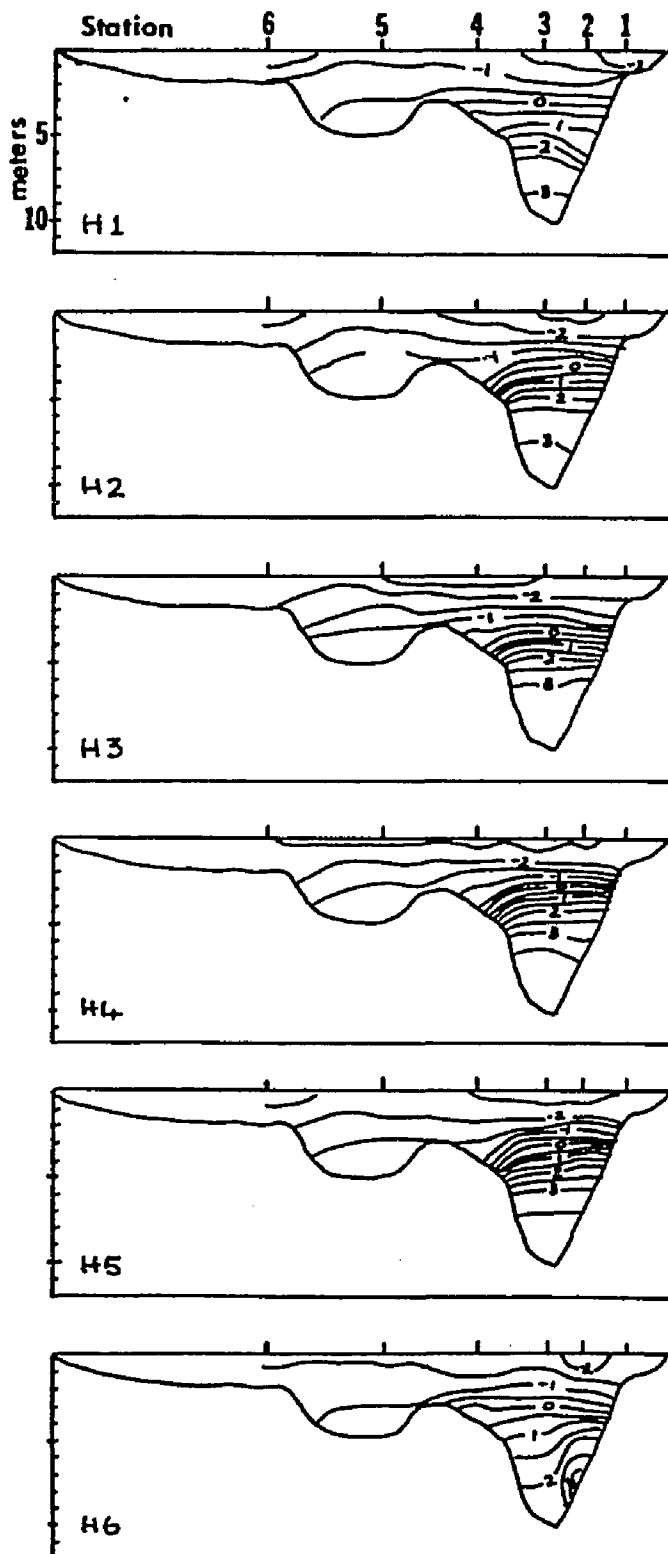


FIG. 3.5a

Cross-sectional density distribution,
 Mean tides. (0.5 sigma-t intervals)

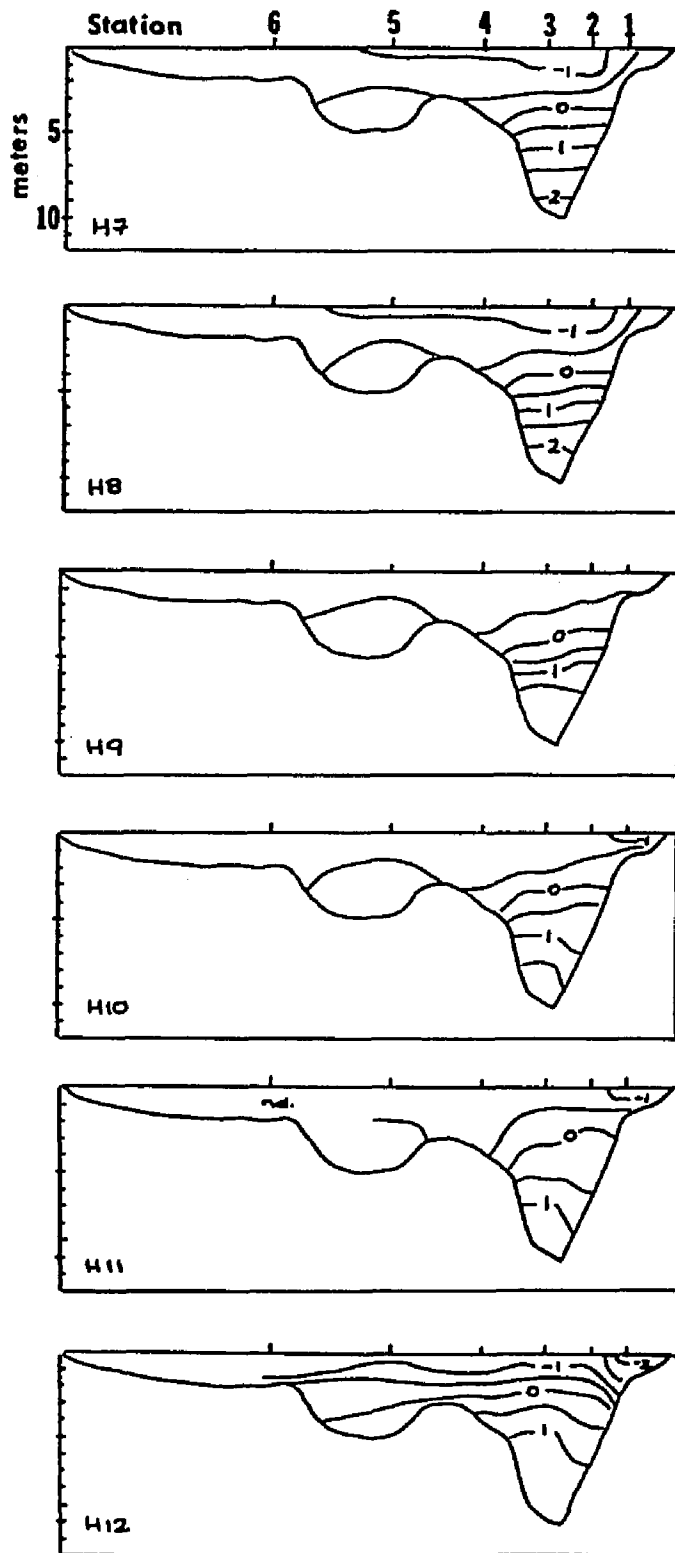


Fig.3.5b

Cross-sectional density distribution,
 Mean tides. (0.5 sigma-t intervals)

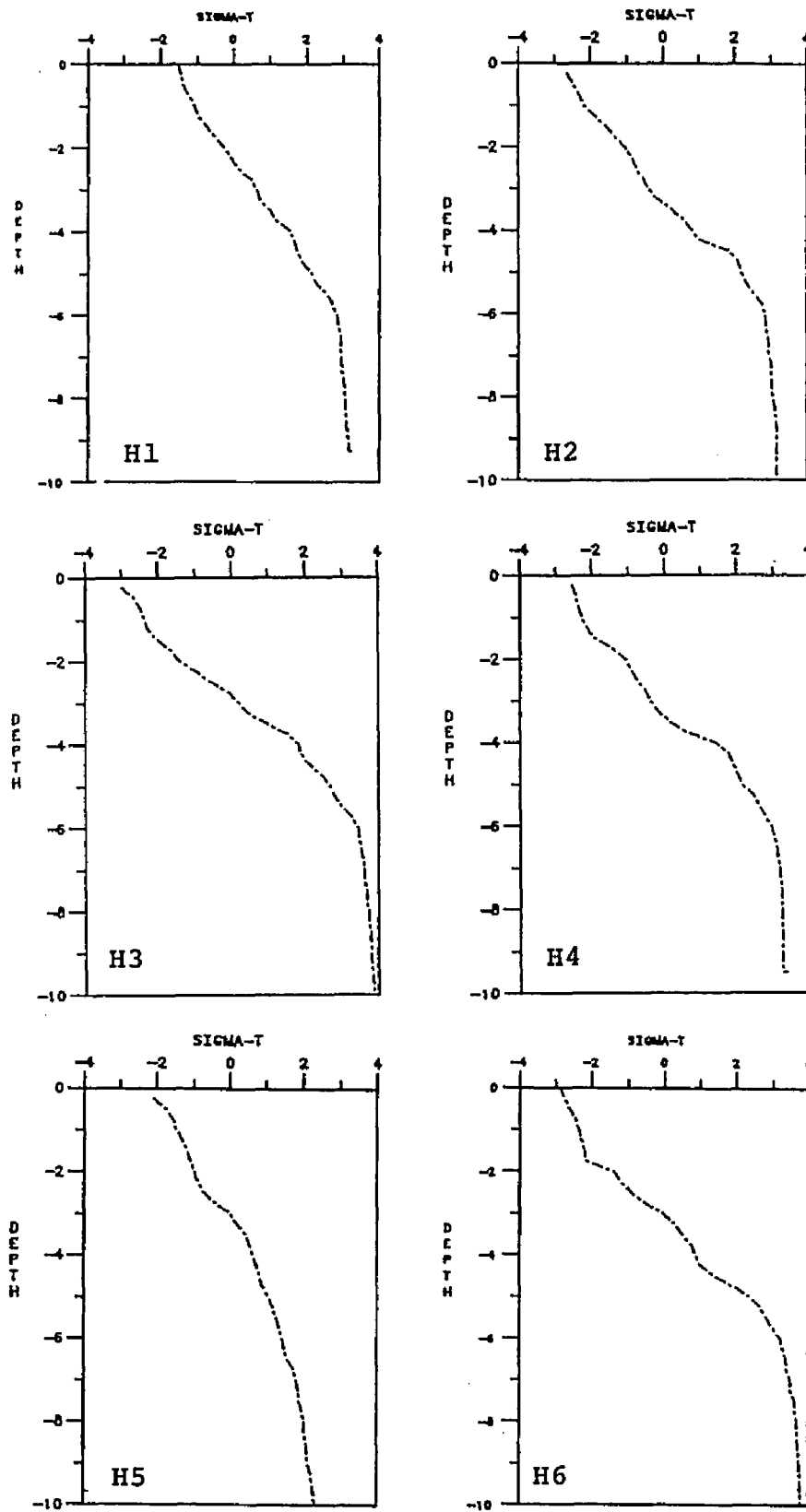


FIG.3.6a Vertical density profiles at Station 3, Mean tides.

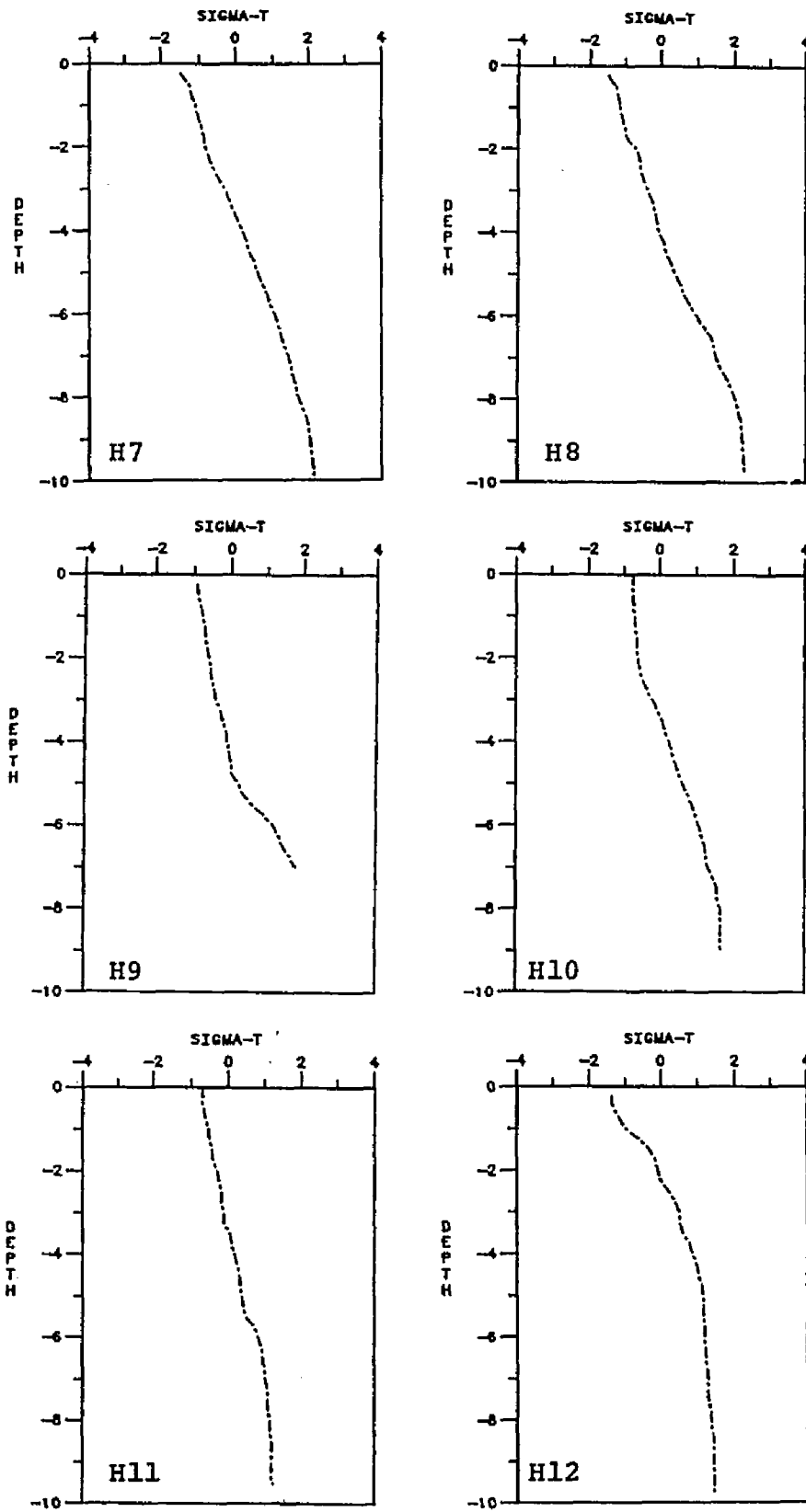


FIG.3.6b Vertical density profiles at Station 3, Mean tides.

The lateral homogeneity of the upper water column is disrupted by a small lens of less dense water isolated over the main channel.

One hour later, at slack-before-flood (Hour 7), this lens of less dense water has become deeper and broader, spreading over the entire width of the channel. As a consequence, the estuary once again shows lateral inhomogeneity at the surface, only now the least dense water is over the main channel. Below this the density is uniform laterally and vertically, below this in the channel the density increases linearly with depth. Hour 9 is the time of maximum flood current and a minimum in density difference both laterally and vertically across the section. Through the subsequent flood tide cycle lateral inhomogeneities develop as the water over the north-eastern shoal area becomes relatively fresher (see Hours 10,11,12, Fig.3.5). Vertically the channel becomes less stratified through the latter part of the flood cycle (see Figs.3.5b, 3.6) until Hour 12 is reached. At this time the density structure shows a transition towards that of Hour 1. The pycnocline is now domed upwards over the main channel and as result abuts the much fresher water located over the adjacent north-eastern shoal. This forms a region of very strong lateral density gradient.

From this generalized picture of the tidally varying density distribution during mean tide conditions it is apparent that the times at which the lateral density differences are greatest are at, or close to, the times of slack tide. Spatially these regions of maximum gradient are found at the inner edges of the shoals where the bathymetry shows a distinct break in slope.

c) NEAP TIDES

The data set for the cross-sectional density distribution during neap tides encompasses only the ebb cycle and the time of slack before flood, thus no assessment can be made as to the change in lateral density throughout a complete tidal cycle. For the sections measured however several features are apparent (Fig.3.7). During the early part of the ebb cycle (H2,H3) sloping isopycnals in the upper layer create lateral density differences, particularly at the inner boundary of the south-western shoal. This region has also been seen to be one of strong lateral density gradients under other tidal range conditions. As the ebb progresses (H4,H5) the upper mixed layer deepens and the pycnocline narrows (see Fig.3.8) resulting in laterally homogenous conditions across much of the upper layer. The end of the ebb brings a sudden change in lateral density distribution, and by H7 lateral and vertical density differences across the section are at a minimum. By comparison with mean and spring tide conditions it seems that, at least during the ebb, much of the estuary is laterally homogenous, that stratification is restricted to the main channel (except during H2 and H3 when the secondary channel is partially stratified) and that the total surface to bottom density difference in the channel is less than under mean tide conditions (see Fig.3.5a).

In summary therefore, it appears that the generalized change in the lateral density distribution through a tidal cycle is independent of the tidal range. With exception of the early part of the flood cycle, the freshest water is located over the shoals, particularly the south-western shoal. The isopycnals across the section are frequently tilted.

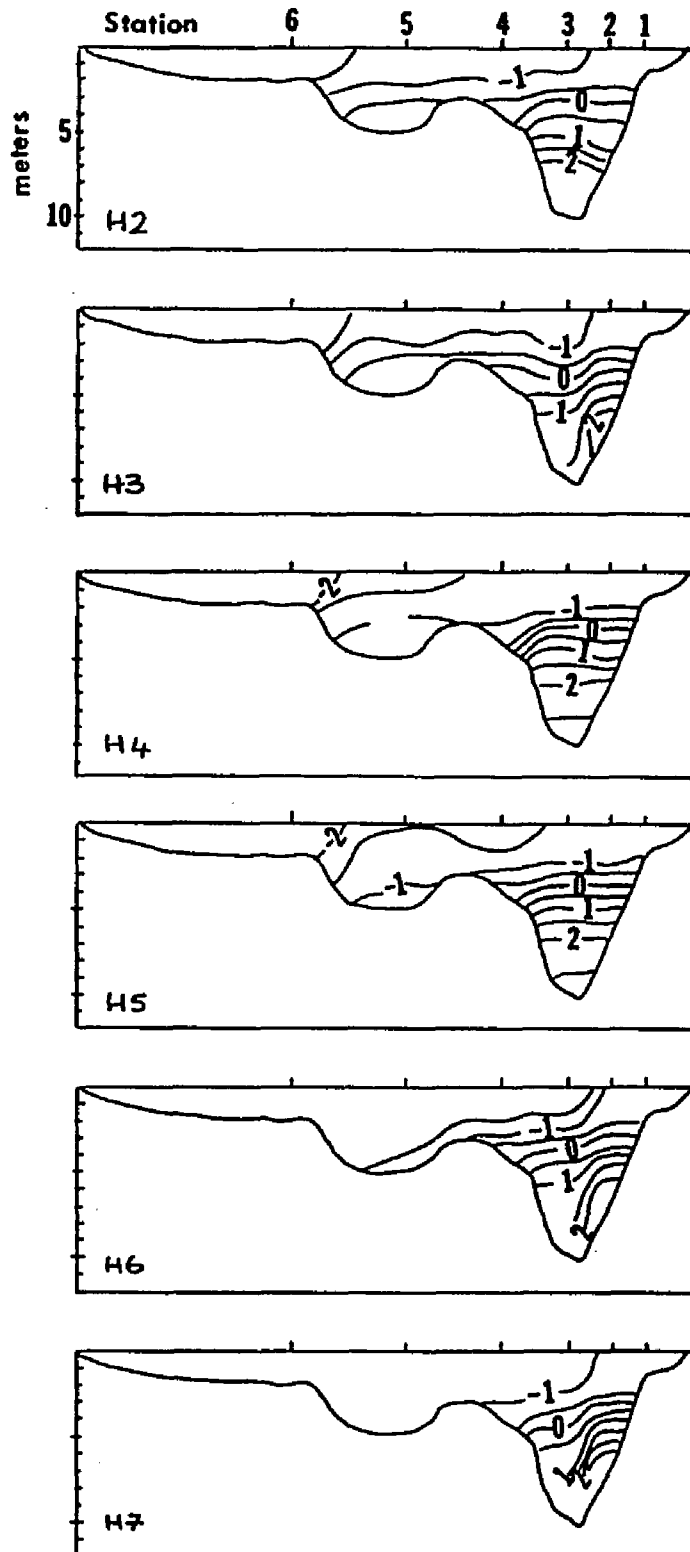


FIG.3.7

Cross-sectional density distribution, Neap tides. (0.5 sigma-t intervals)

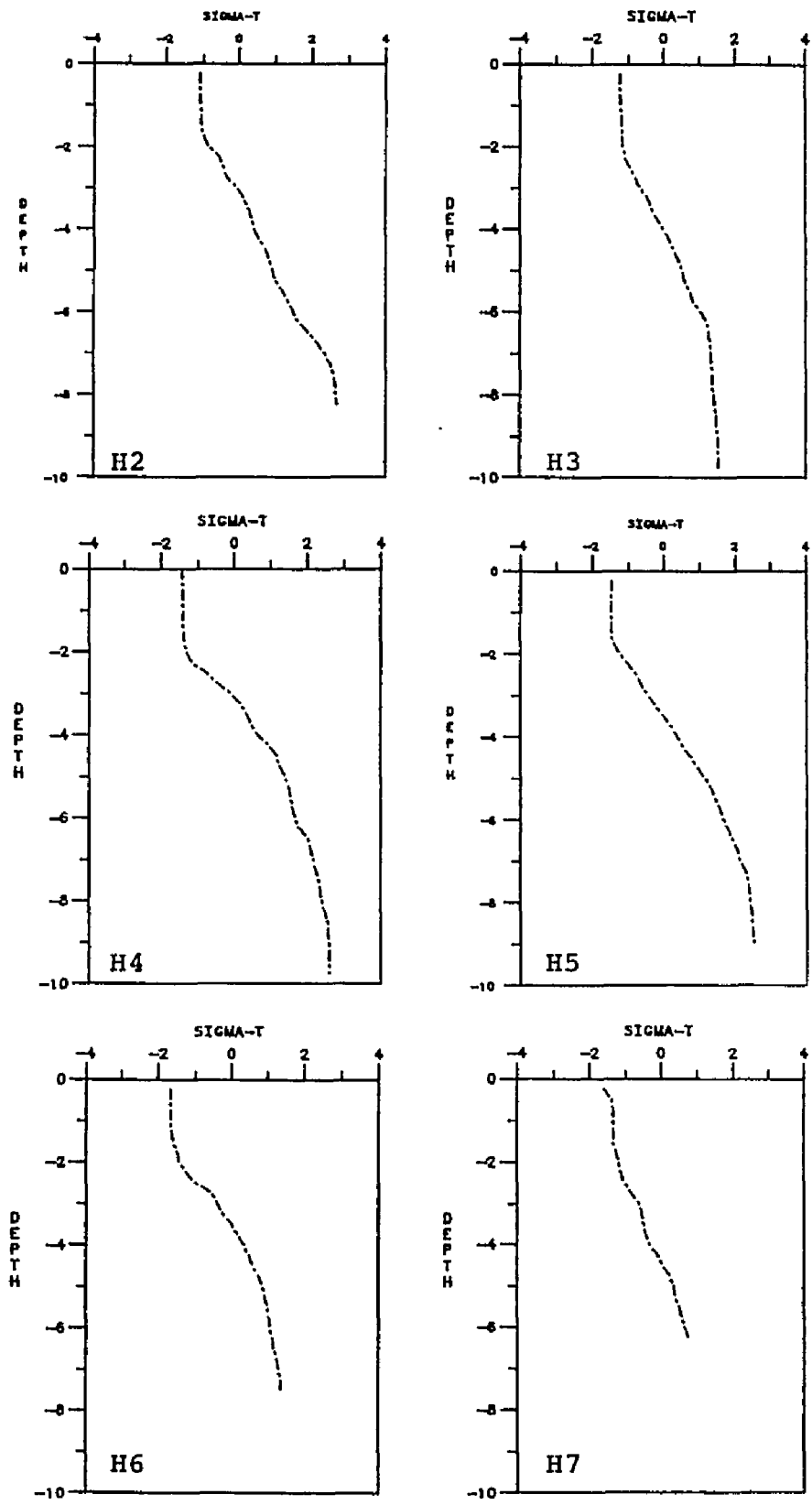


FIG.3.8 Vertical density profiles at Station 3, Neap tides.

The direction of this tilt is in accordance with geostrophic predictions. The magnitude of the slope, estimated from contour plots of the tidally-averaged density for mean tide conditions, is -4.3×10^{-4} . This is slightly greater than predicted using the thermal wind equation. Using representative values of density difference and velocity shear, the slope was estimated to be -2.0×10^{-4} . The difference between these values is not large and thus it can be supposed that the isopycnal slopes observed are largely due to the influence of the Coriolis force. Comparison of these results with the observations of Murray et al. (1975) shows some similarities. The Rio Guayas estuary has a much larger tidal range (3.3m) and a more uniform depth in the cross-section, thus the shoal and channel areas are not so clearly delineated. However they found that, as we have seen in the York River, the shallow areas to the sides of the estuary remained well-mixed throughout the tidal cycle and that the vertical stratification is least during the time of flooding tide.

2. PRESSURE GRADIENTS

The observed lateral differences in density will generate horizontal pressure gradients which play a significant role in estuarine dynamics. Assuming pressure to follow the hydrostatic law :

$$\frac{\partial p}{\partial z} = \rho g$$

or
$$p(z) - p' = \int \rho g dz$$

where p' is a constant. Differentiating this with respect to y gives:

$$\frac{\partial p}{\partial y} = \frac{\partial}{\partial y} \int_z^\eta \rho g dz \quad (3.1)$$

where η is the free surface elevation. Using Leibnitz's rule equation (3.1) can be reduced to:

$$\frac{\partial p}{\partial y} = \rho(\eta) g \frac{\partial \eta}{\partial y} + g \int_z^\eta \frac{\partial \rho}{\partial y} dz \quad (3.2)$$

(1) (2)

Thus the pressure gradient can be considered the sum of two parts - one due to the free surface slope, the barotropic component (Term 1), and the other due to the density distribution, the baroclinic component (Term 2).

The barotropic component cannot be evaluated as η will always be an unknown. This problem has been circumvented by other researchers in various ways. Pritchard (1956) notes this term to be constant but does not evaluate it explicitly nor include when considering the relative magnitude of terms in the lateral momentum equation. When examining the lateral dynamic balance Dyer (1973) eliminated the surface slope by taking the difference between each term in the lateral momentum equation calculated at two separate depths. This approach was also followed by Doyle and Wilson (1978). In the formulation of the lateral momentum equation used by Nunes and Simpson (1985) the barotropic term was removed when solving the equation for v , the lateral velocity, by judicious use of boundary conditions.

For the purposes of this discussion no attempt is made to evaluate the barotropic term, instead it's role in the proposed lateral circulation will be considered qualitatively.

Returning to equation (3.2), and dividing the equation through by $\rho(\eta)$, the baroclinic component becomes:

$$P = \frac{-g}{\rho(\eta)} \int_z^{\eta} \frac{\partial \rho}{\partial y} dz \quad (3.3)$$

Substituting $\rho(\eta)$ by a reference density, in this instance the cross-sectional mean density, and making equation (3.3) applicable to data measured at discrete depths results in the following expression for the lateral horizontal pressure gradient:

$$P = \frac{gz}{\rho_0} \sum \frac{\Delta \sigma_t}{\Delta y} \quad (3.4)$$

where σ_t is a depth-averaged value.

Using this equation the horizontal pressure gradients were calculated as simple linear gradient between adjacent stations at 0.25m depth increments for each of the hourly sections representing mean, spring and neap tides. By way of illustration, the magnitude and direction of these pressure gradients at depths of 0.5m, 1.0m, 2.0m and 3.0m were plotted in Figs.3.9, 3.10, 3.11.

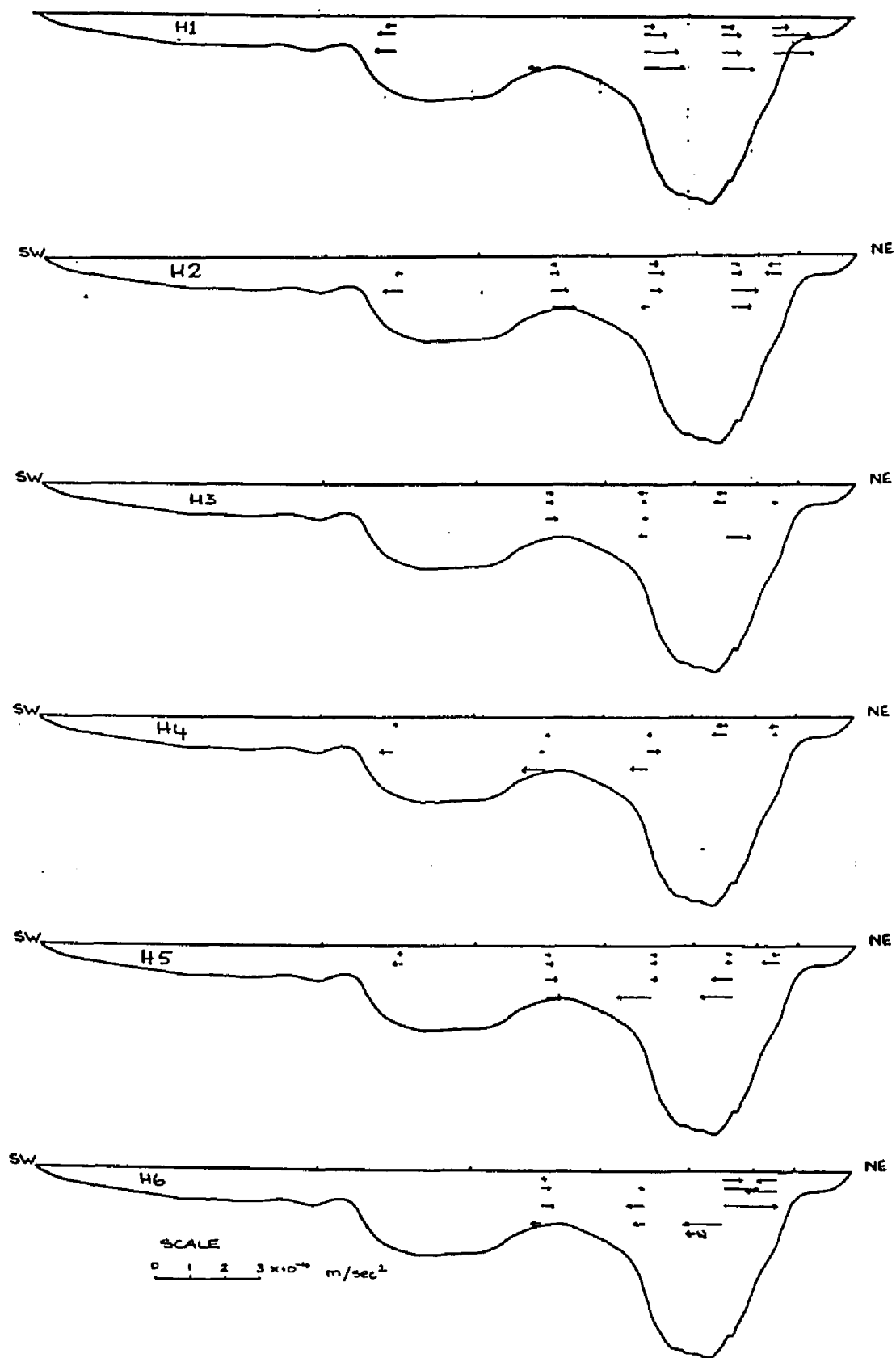


FIG.3.9a Horizontal pressure gradients at Mean tides.

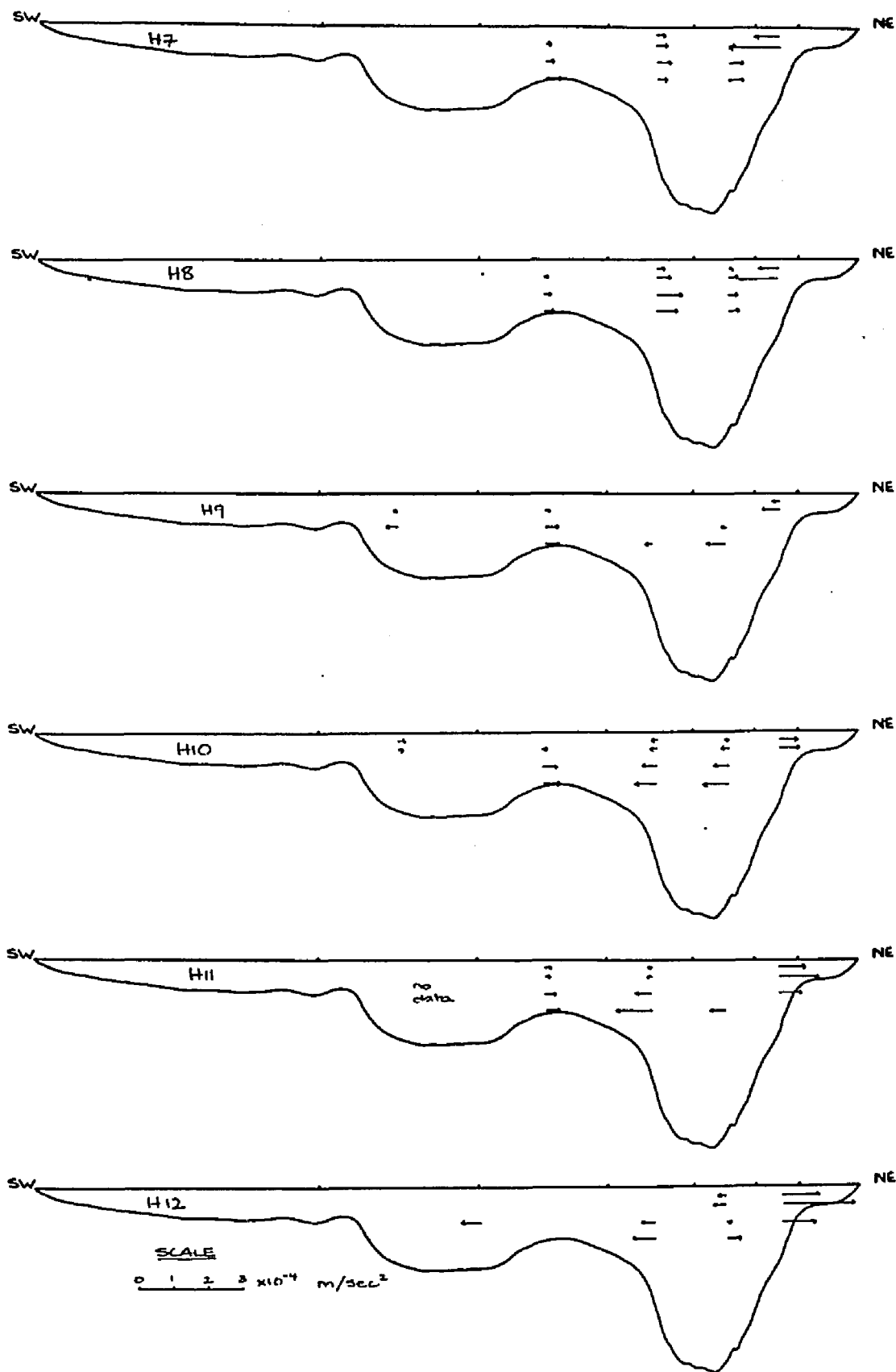


FIG. 3.9b

Horizontal pressure gradients
at Mean tides.

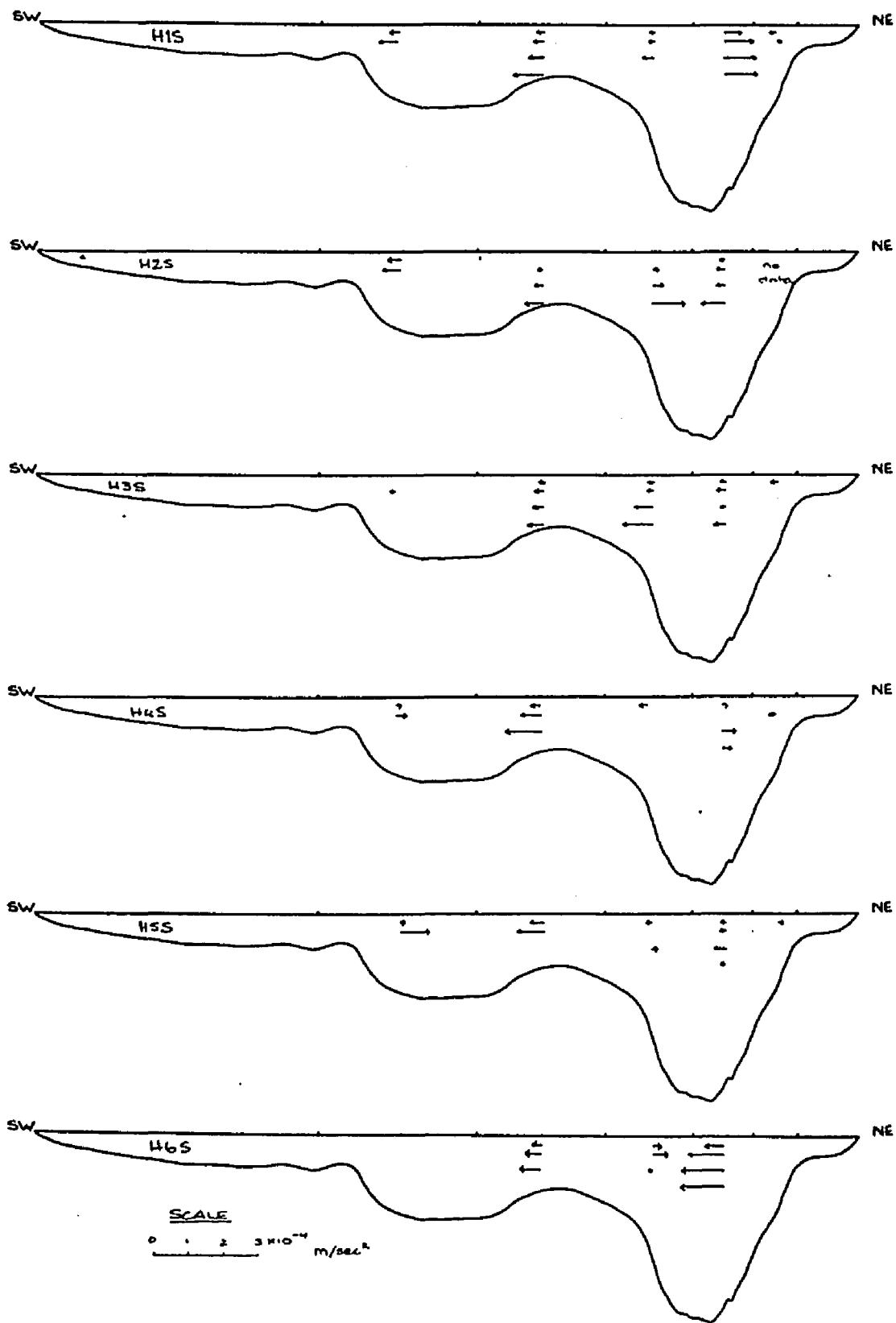


FIG. 3.10a Horizontal pressure gradients at Spring tides.

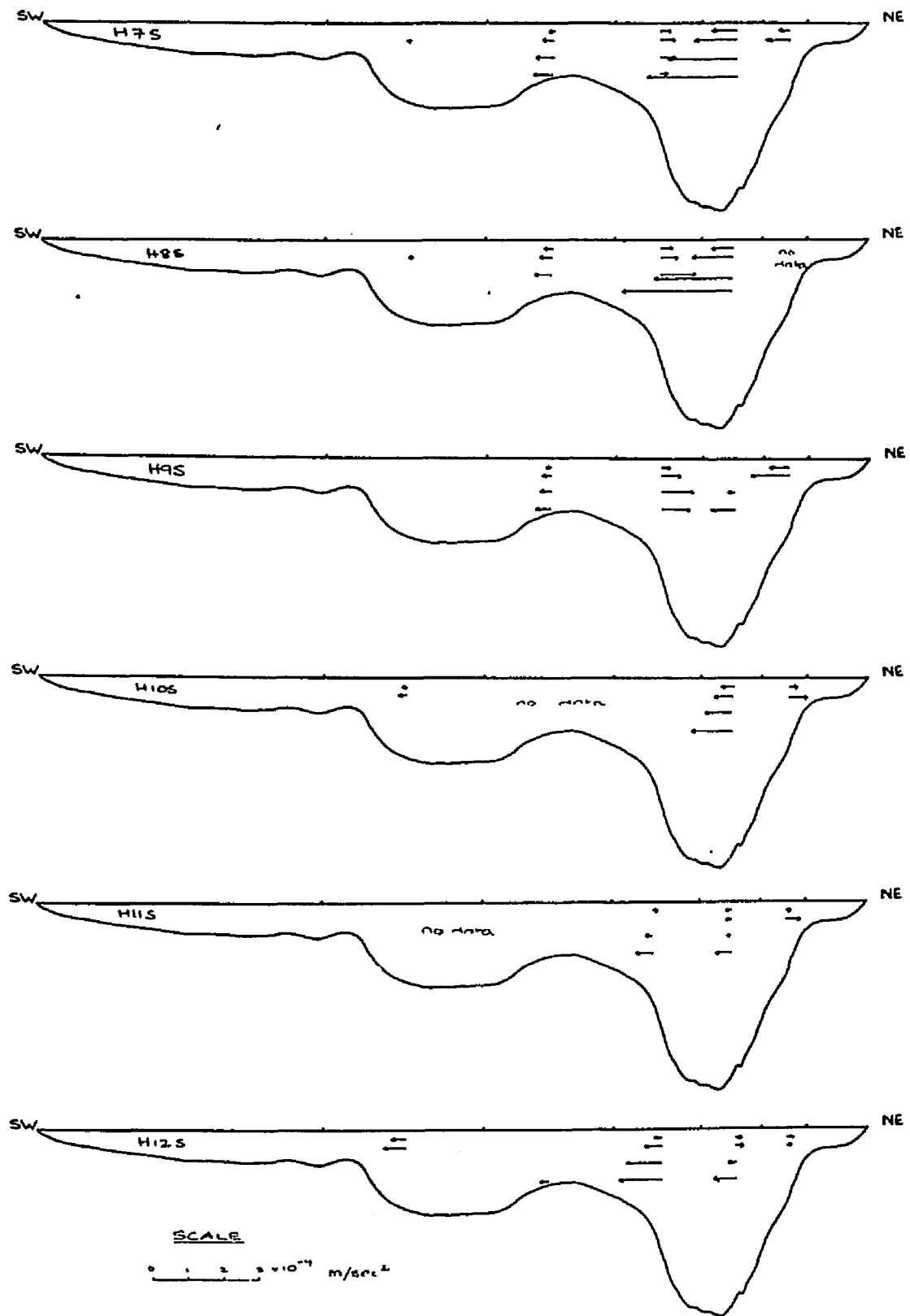


FIG. 3.10b Horizontal pressure gradients at Spring tides.

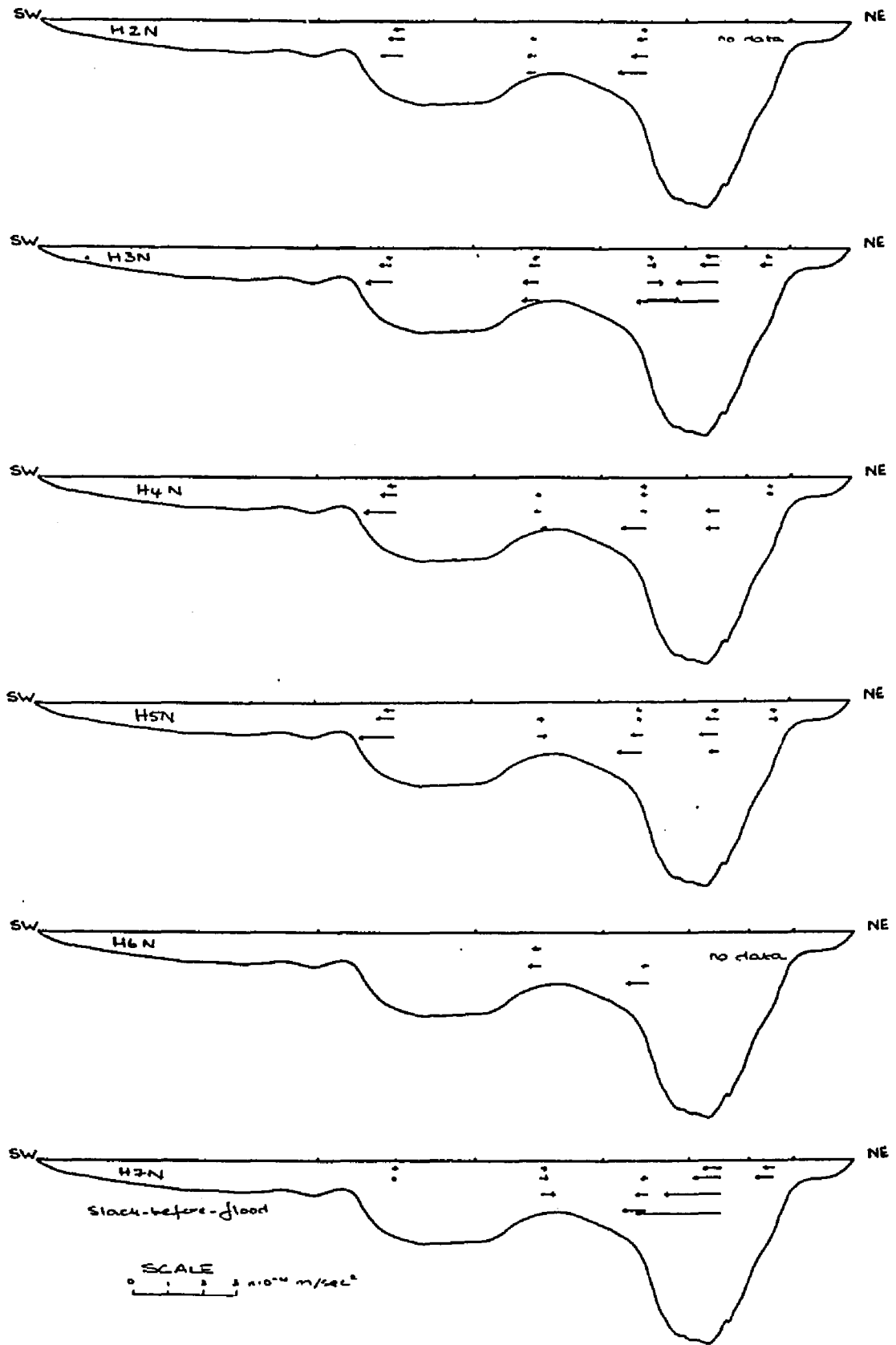


FIG. 3.11 Horizontal pressure gradients at Neap tides.

For this section of the York River, Ruzecki and Evans (1986) found values for the longitudinal pressure gradient varying between 18 Pa/km and 29 Pa/km at a depth of 3.0m below the surface. The numbers calculated here are in general an order of magnitude greater, although there is considerable variation within the tidal cycle and under different tidal range conditions. As can be seen by a comparison of Figs.3.9, 3.10 and 3.11, the pressure gradients at mean tides are generally greater than at spring or neap tides, and for each tidal range condition, the greatest horizontal pressure gradients are found at, or near, the times of slack water. This is in accordance with the previously discussed density distributions. Conversely the times of maximum current are the times of minimal lateral density gradients and hence minimal horizontal pressure gradients.

During mean tides the largest horizontal pressure gradients are found over the main channel and/or at the inner edge of the northeast shoal. At H1 (Fig.3.9a) there are significant pressure gradients at the inner edge of the southwest shoal also. The largest pressure gradients during the spring tide conditions are located over the main channel, especially during the early flood cycle (see H7,H8, Fig.3.10b). Similarly during neap tides when the largest pressure gradients occur at slack-before-flood (see Fig.3.11) and over the main channel.

3. LATERAL CIRCULATION

The lateral momentum equation can be formulated, using a right-handed coordinate system with x positive up-estuary, in the following way:

$$\frac{dv}{dt} = -\rho^{-1} \frac{\partial p}{\partial y} + fu - N_z \frac{\partial^2 v}{\partial z^2} - C \quad (3.5)$$

where C is the centripetal acceleration. Assuming that this acceleration is negligible for the section of the York River under consideration, and that for relatively small increments of time steady-state conditions pertain, this equation is reduced to:

$$0 = -\rho^{-1} \frac{\partial p}{\partial y} + fu - N_z \frac{\partial^2 v}{\partial z^2} \quad (3.6)$$

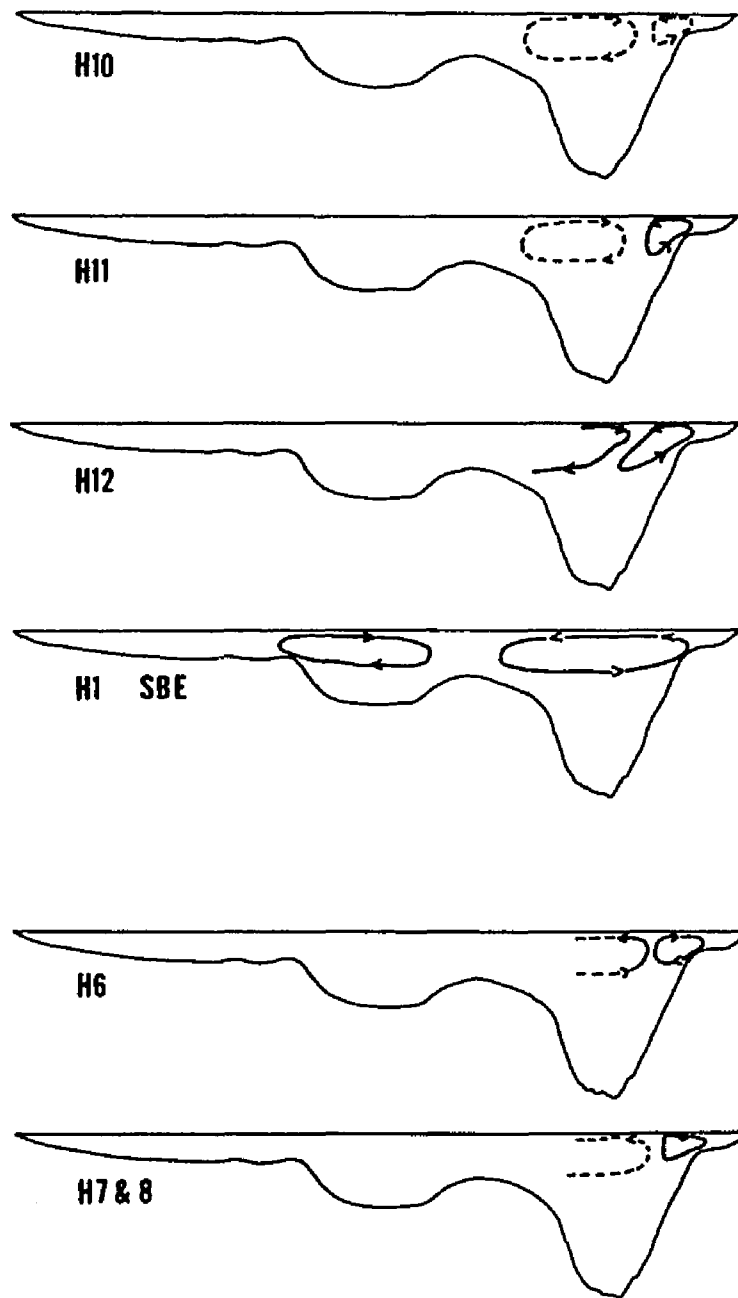
Under tidally-averaged conditions the Coriolis acceleration and pressure gradient terms are of similar magnitude (approx. 10^{-5} m/sec²) and likely to dominate the lateral dynamic balance. On a more localized spatial scale however, the pressure gradient varies significantly, and may at times be of sufficient magnitude to drive lateral circulations. Such circulations, if they occur, would be transitory and exist only over a portion of the width of the estuary.

In a completely homogenous water mass any horizontal pressure gradient is caused by a surface slope. Under stratified conditions the density distribution contributes, the value of this baroclinic term usually increasing with depth such that the barotropic contribution is

gradually compensated. This principal is the generally accepted explanation for non-tidal longitudinal estuarine circulation (Prych,1970, Officer,1977). The longitudinal surface slope acting in a down-estuary direction drives the upper layer flow, whilst the longitudinal salinity gradient acting in the up-estuary direction drives the lower layer flow. Thus the upper layer flow is primarily barotropic, the lower layer primarily baroclinic.

This same approach can be applied to lateral circulation. Considering only mean tide conditions in the first instance, and using H1 (slack-before-ebb) as an example: returning to Fig.3.9a, the horizontal pressure gradients at this time between stations 4 and 3, stations 3 and 2, and stations 2 and 1 are directed to the right-hand side of the estuary, their magnitude increasing with depth. Between stations 5 and 6 they are directed in the opposite direction, towards the south-western bank. A flow will be induced in the direction of these pressure gradients. This flow will be directed bankwards on both sides of the estuary. If we assume, from the density distribution, that there will be a corresponding set-up of the free surface over the shoal areas, the surface slope will drive a return flow towards the centre of the estuary. Thus a cellular circulation pattern can be inferred which is largely baroclinic within the water column and barotropic near the surface. This is illustrated in the section labelled H1 in Fig.3.12.

Utilizing the same reasoning lateral circulation patterns can be drawn for all the times when there are significant horizontal pressure gradients. For mean tides these have been compiled in sequence in



mean tides

FIG.3.12

Patterns of lateral circulation
at Mean tides.

Fig.3.12, centred around slack-before-ebb (H1, Fig.3.12) and slack-before-flood (H7, Fig.3.12). At the times of maximum current, both flood and ebb, when the estuary is most nearly laterally homogenous and resulting pressure gradients minimal, such lateral circulations would be essentially absent. At other times however they may be significant. As can be seen from Fig.3.12 the last 3 hours of the flood cycle generate a zone of surface convergence toward the right-hand side of the channel. The strength of the flows on either side of the convergence may be unequal creating what is sometimes termed a 'one-sided convergence'. By Hour 1 this convergence has moved nearer the centre of the estuary. Around the time of slack-before-flood a zone of surface divergence forms over the channel.

Similar reasoning was invoked by Simpson and Nunes (1985) in their discussion of the axial convergence fronts they had noted in several small and well-mixed estuaries. In that instance the differential longitudinal advection across the estuary brought more dense water into the centre of the estuary during the flood tide. The resulting pressure gradients are directed outwards from the centre within the water column, and inward toward the centre at the surface, forming the observed axial convergence. The density difference between the centre and the sides of the estuary was observed to be approximately 1 sigma-t. These authors did not attempt to calculate the magnitude of the horizontal pressure gradients, but instead solved the lateral momentum equation for v , the expected lateral velocity, which was subsequently verified by direct measurements (Simpson and Turrell, 1985). Observations show good

agreement with predictions suggesting that even small density differences can generate lateral circulations.

In the same way, circulation patterns have been drawn from the distribution of pressure gradients at spring and neap tides. The alternating zone of convergence and divergence over the main channel noted previously can also be seen at spring tides (Fig.3.13). Conditions during neap tides (Fig.3.14) appear to be anomalous to these general trends.

Experiments conducted by Sumer and Fischer (1977) in a flume showed similar transverse circulations. Their flume, which was trapezoidal in cross-section, had one side shallower and more gently sloping than the other. Using stratified and oscillating flow they found that during the ebb tide there was a transverse circulation from this side toward the deeper channel at the surface, with a return flow at depth, and vice versa during flood tide. The circulation pattern in the York River is more complex but a definite reversal in flow directions can be seen through the tidal cycle. It should be remembered that these circulations are very minor compared to the predominate longitudinal tidal flows. They may however be of sufficient strength to generate convergences and assist in cross-estuary exchange of water masses.

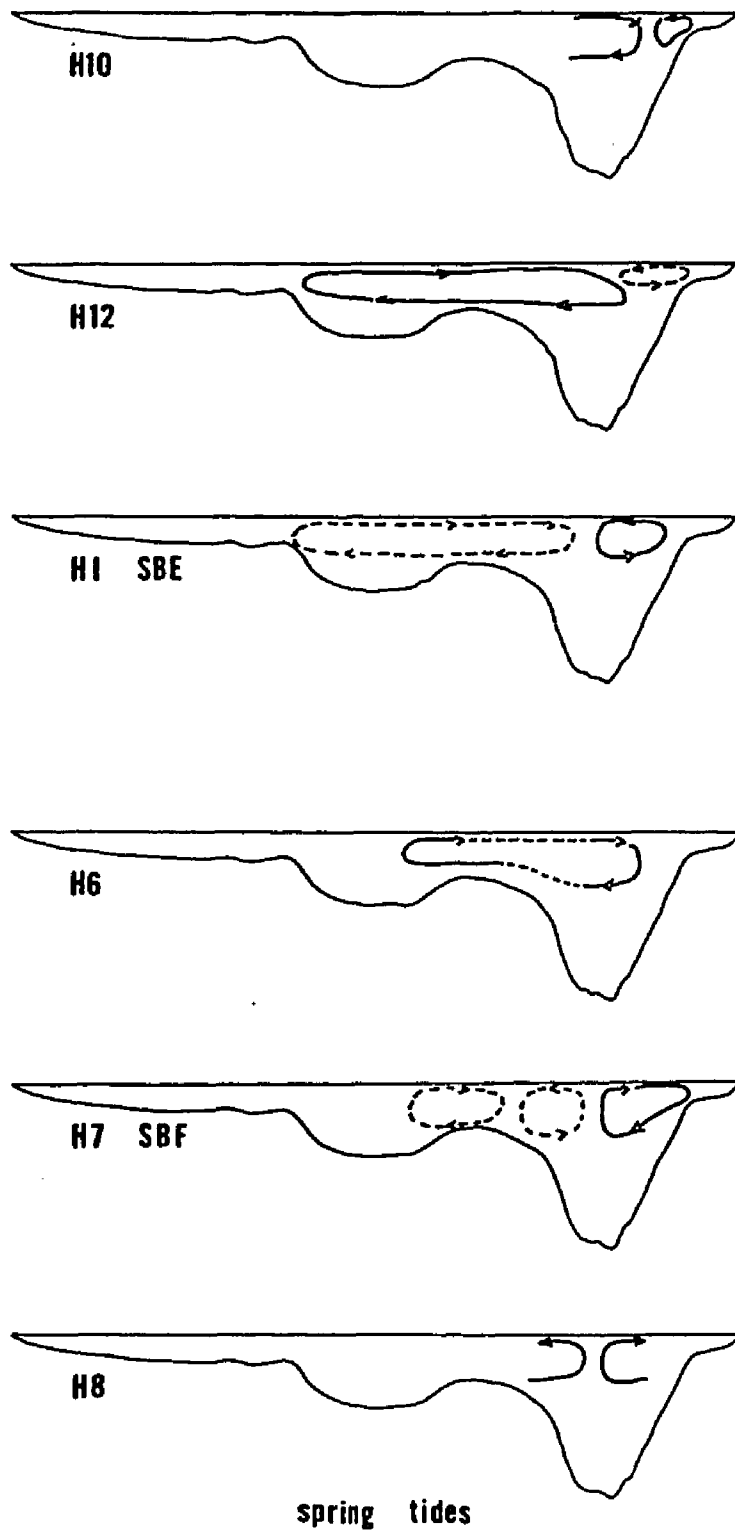


FIG. 3.13

Patterns of lateral circulation at Spring tides.

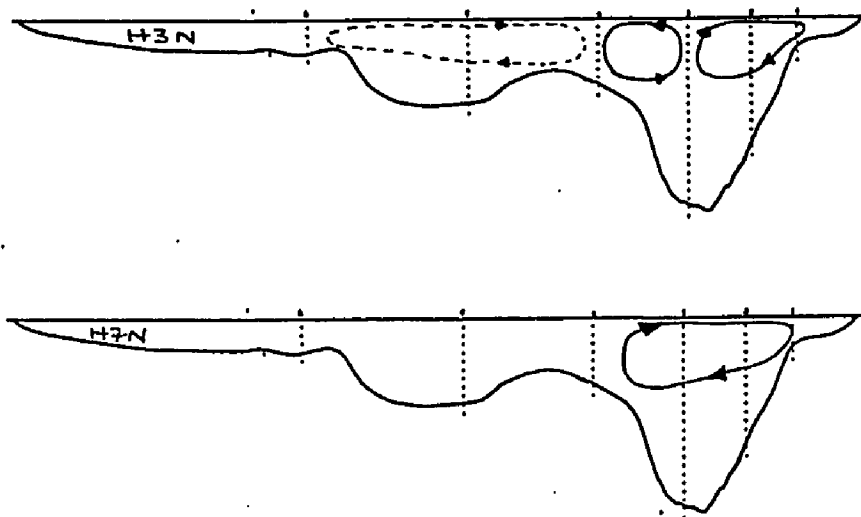


FIG.3.14 Patterns of lateral circulation at Neap tides

IV. CURRENTS

1. EXPERIMENTAL METHODS AND GENERAL RESULTS

The magnitude and direction of the currents in the study area were measured using General Oceanics winged current meters, self-contained inclinometer type meters, deployed at 3 locations across the estuary from 15 April to 21 May 1985. The station locations and water depths are listed in Table IV.1 below and their position relative to the bathymetry and CTD sampling stations is shown in Fig.4.1. At the two shoal stations the current meters were suspended from an arm which protruded at right-angles to a long pole set upright in the bed. In the channel a regular taut-wire mooring was used. All the current meters were set at a sampling rate of 4 observations (1.32 sec apart)/sample, 4 samples/hour.

TABLE IV.1

STN	LAT/LONG	WATER DEPTH (at MLW)	METER #	METER DEPTH (below MLW)	MOORING
CM1	37 22.03 76 37.89	2.8 m	54	1.5 m	pole
CM2	37 21.95 76 21.95	10.8 m	52 56	4.0 m 7.9 m	buoy
CM3	37 21.58 76 38.75	2.8 m	53	1.5 m	pole

STUDY TRANSECT

(LOOKING UP - ESTUARY)

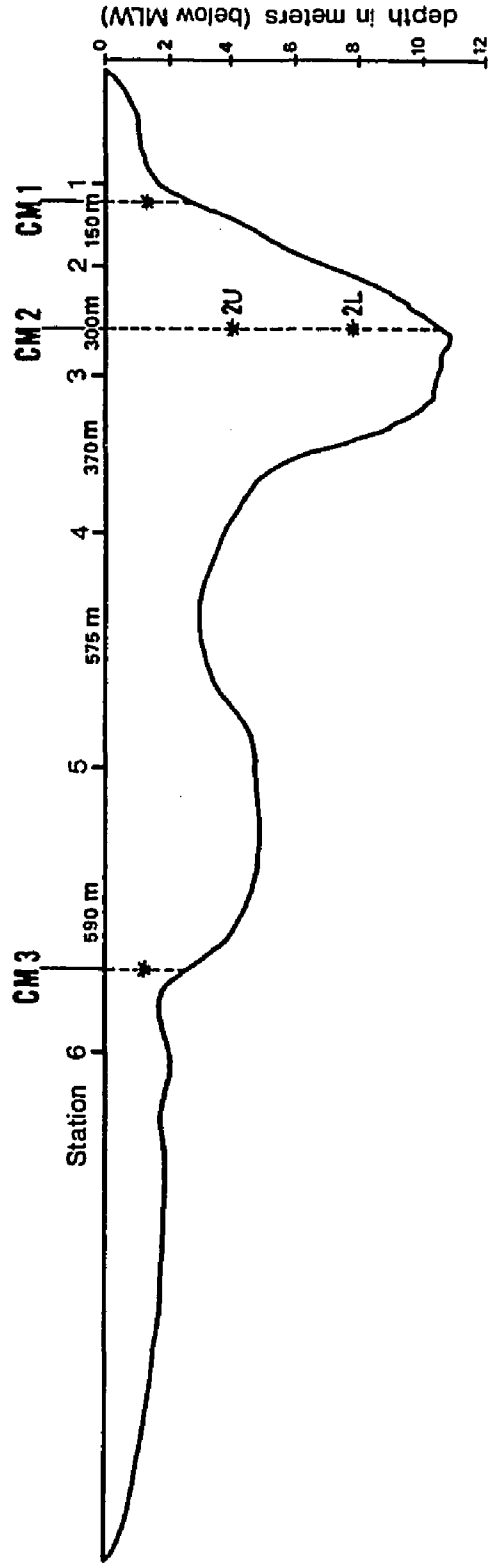


FIG. 4.1 Location of the current meter stations across the study transect.

The current meters were not checked or cleaned during deployment, hence upon retrieval several of the meters were found to be considerably fouled. A post-deployment flume test was conducted to estimate the effect such growth may have had on the recorded current speed. The results showed that the fouled meters recorded higher current speeds, but the difference was less than 5% and thus no attempt was made to include this effect in subsequent processing.

The data recovery was almost 100% on three out of the four current meters deployed: the current meter at station CM3 was apparently hung up on the mooring during the first 12 days of deployment.

The general features of the raw current meter records can be seen from the time series 'stick-plots' illustrated in Fig.4.2. All exhibit a flood/ebb direction of NW/SE in accordance with the alignment of the estuary in this area. The largest magnitude currents occurred, not surprisingly, in the channel with those at 4m (CM2U) being greater, and more directionally variable, than those at 8m (CM2L). At stations CM1 and CM3 the magnitudes were much less. Despite being located at the inner edge of a relatively broad shoal, the record from station CM3 shows minimal wind or wave induced scatter. By comparison the current meter record from station CM1, on the north-east shoal, shows a marked asymmetry in the magnitude of the flood and ebb tide, the ebb tide is particularly variable in both magnitude and direction.

Further illustration of the directional variability, most prevalent at stations CM2U and CM1, can be seen in the scatter plots shown in

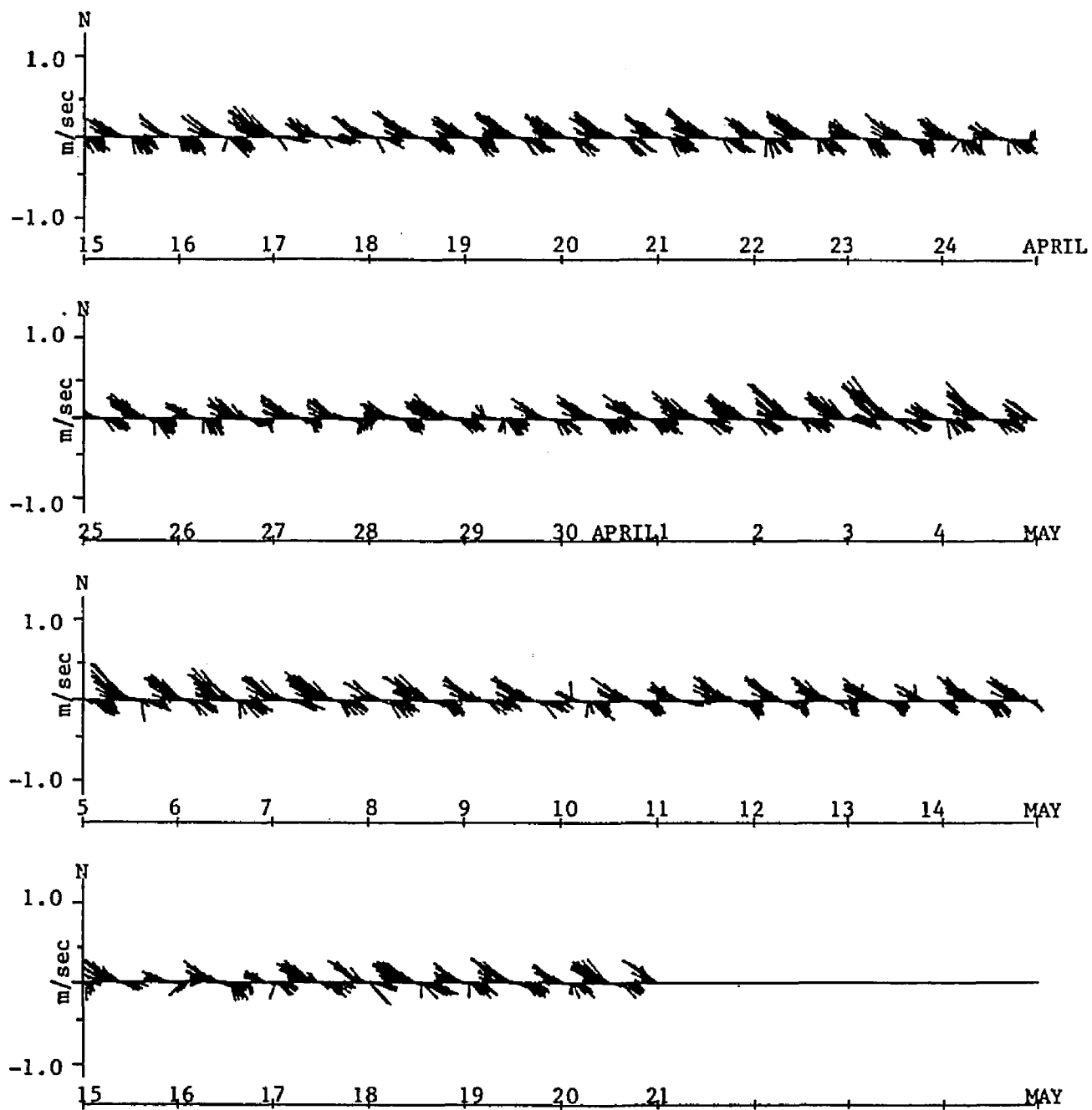


FIG.4.2a. TIME SERIES OF OBSERVED CURRENTS AT STATION CMI,
APRIL/MAY 1985.

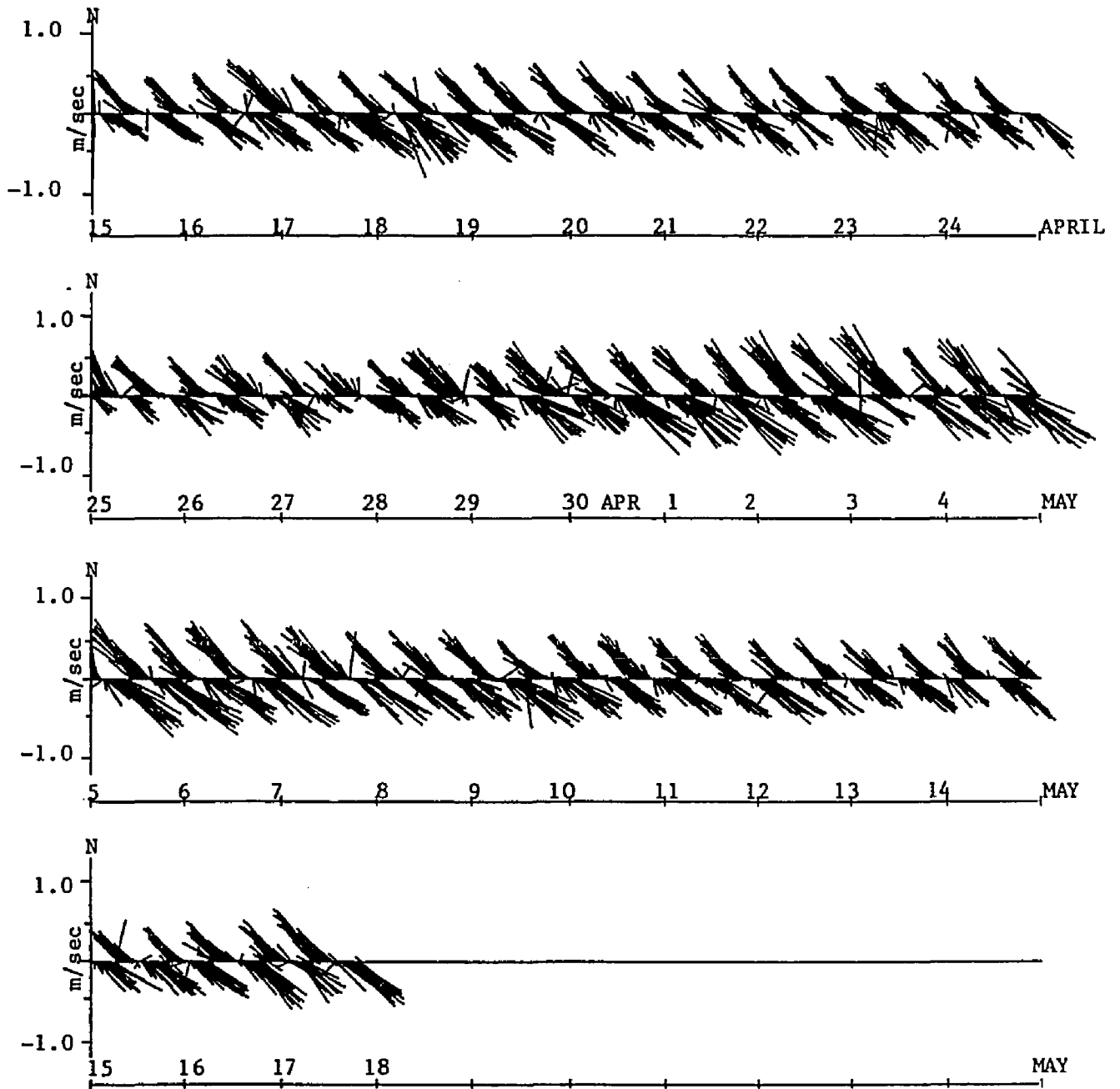


FIG.4.2b. TIME SERIES OF OBSERVED CURRENTS AT STATION CM2U,
APRIL/MAY 1985.

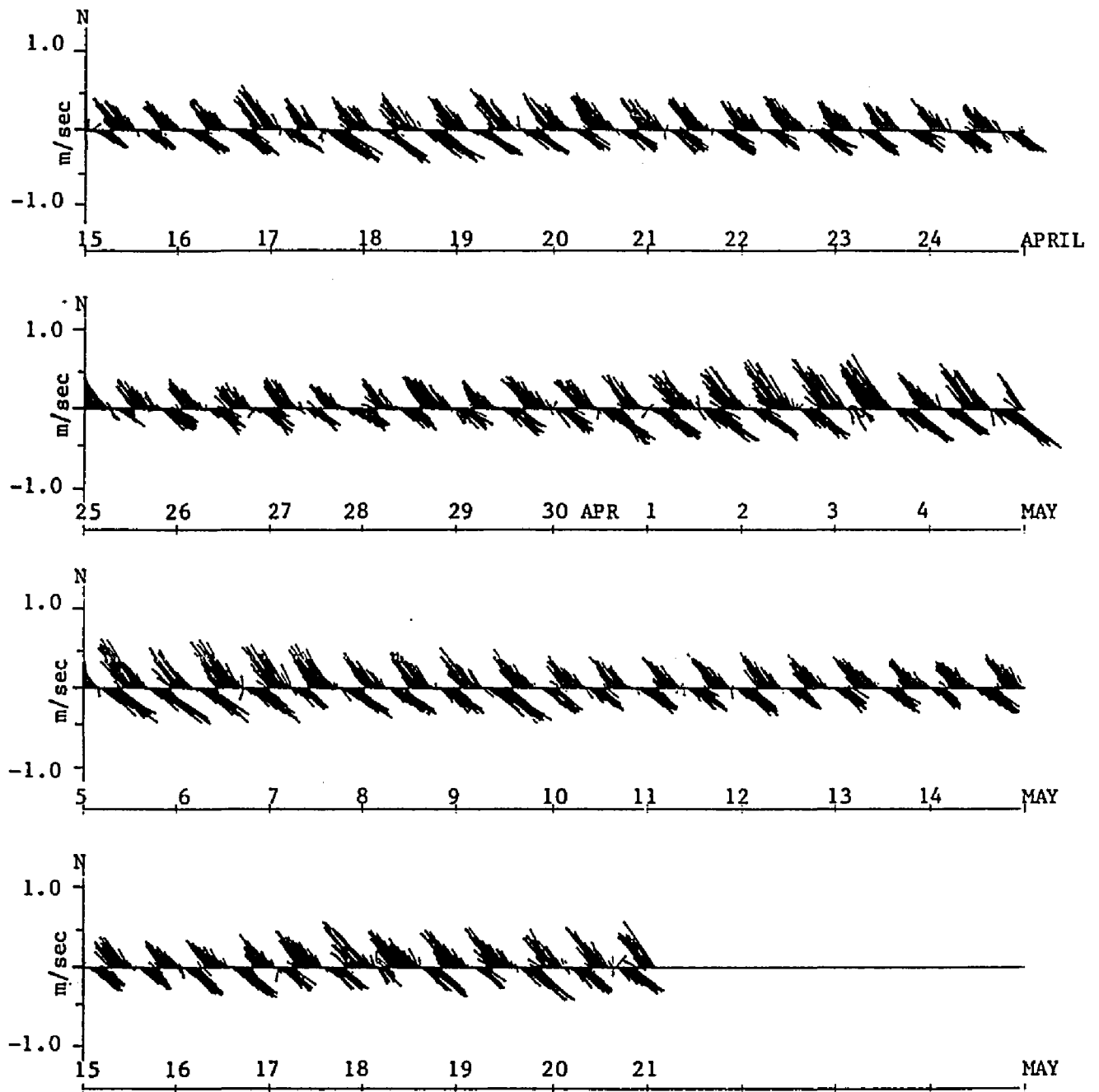


FIG.4.2c. TIME SERIES OF OBSERVED CURRENTS AT STATION CM2L,
APRIL/MAY 1985.

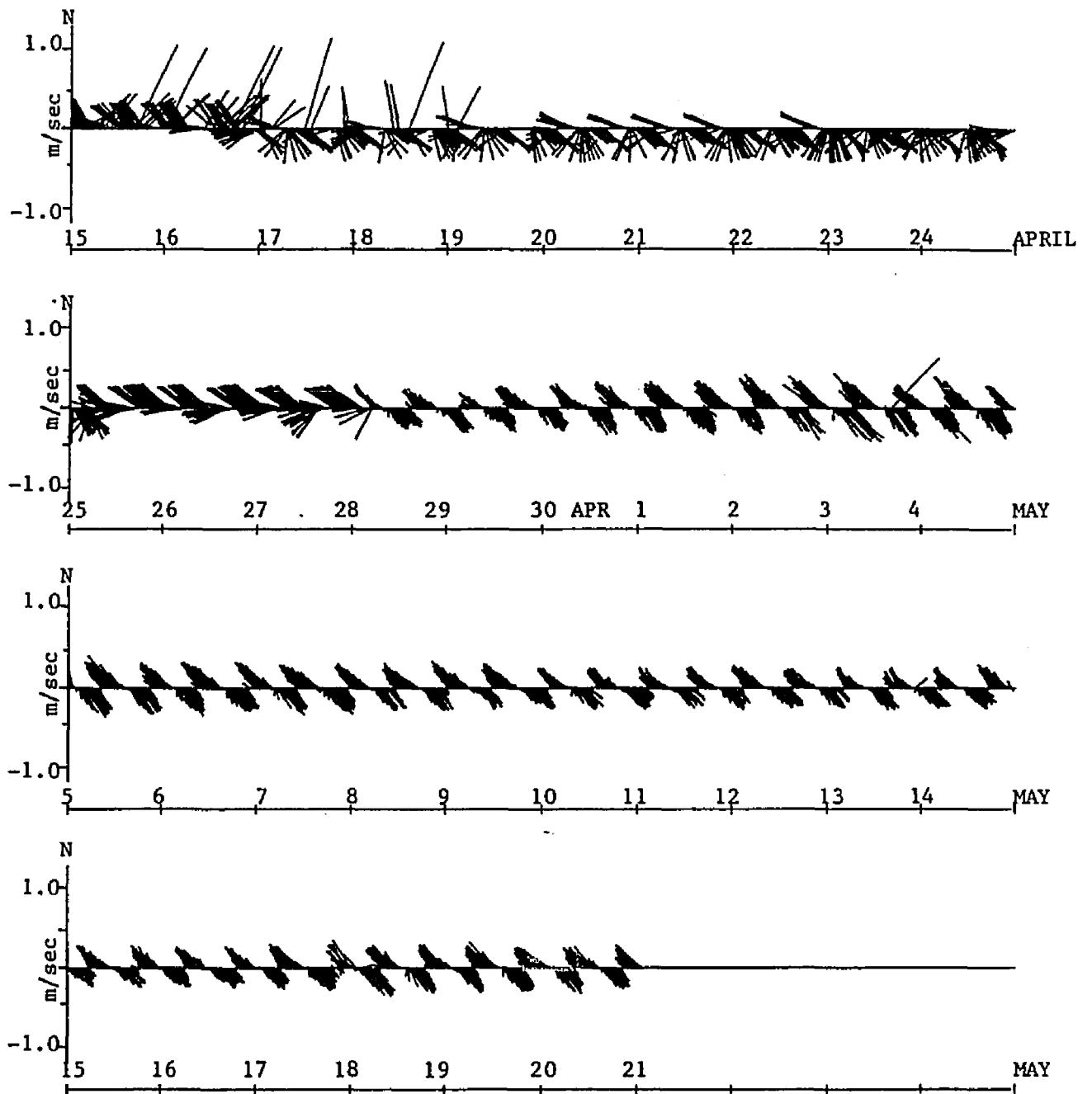


FIG. 4.2d. TIME SERIES OF OBSERVED CURRENTS AT STATION CM3,
APRIL/MAY 1985.

Fig.4.3. In addition, these plots show the extent of departure from exact anti-parallelism between flood and ebb directions, the difference being greatest in the channel and least at station CM3. At station CM2U the flood current shows a change in orientation with strength, becoming more northerly at higher speeds. The ebb current shows no such time history and has a maximum velocity greater than the flood current. The opposite occurs at station CM2L where the flood current is slightly greater than the ebb current. The record from station CM1 shows significant scatter at low speeds in both the flood and ebb directions, and a maximum flood current which is almost 1.5 times that of the ebb current. At station CM3 the strength of the flood and ebb currents is equal, their directions very close to anti-parallel and scatter minimal.

The principal axis for these records is defined as the direction in which the flow variance is maximized and is calculated using the following equation (Boicourt, 1982):

$$\beta = \frac{1}{2} \arctan \frac{2 \sum_{i=1}^N u'_i v'_i}{\left(\sum_{i=1}^N u'^2_i - \sum_{i=1}^N v'^2_i \right)}$$

where u' and v' are the north and east velocity components. Due to the marked non-parallelism in flood and ebb directions, a separate flood and ebb principal axis was calculated for each record. The dividing line between the flood and ebb portions of the record was obtained from examination of the scatter diagrams in Fig.4.3. Using this method the following directions were obtained.

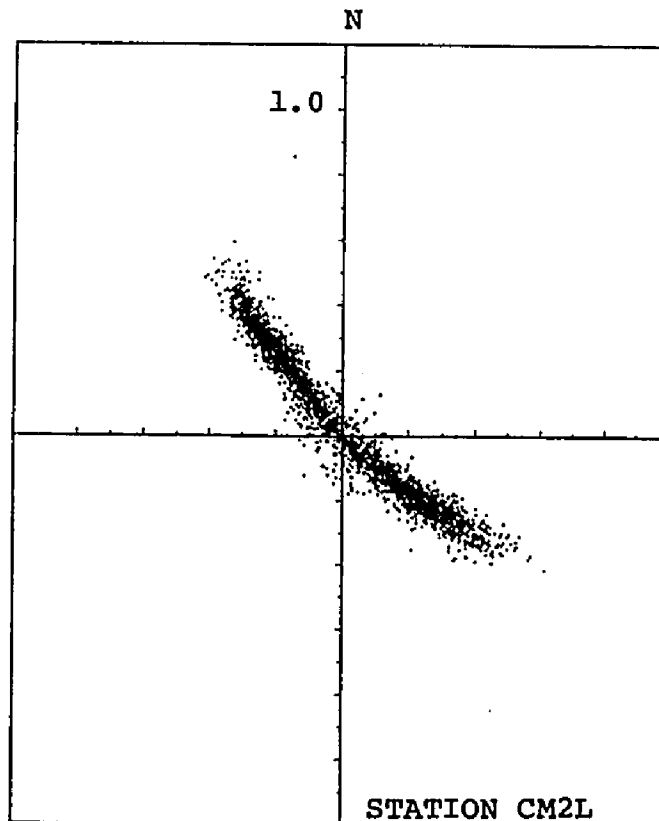
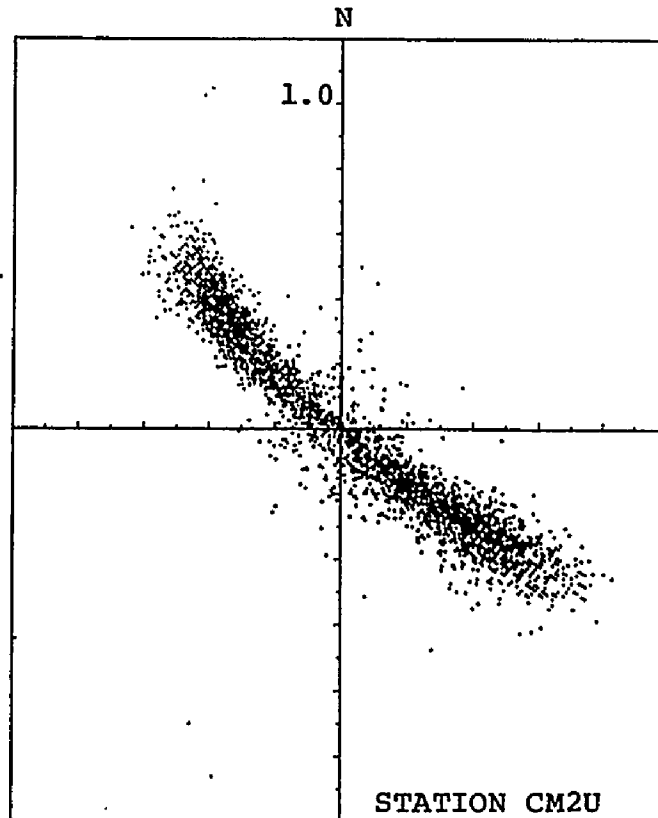


FIG.4.3a Scatterplots of observed currents, April/
May 1985.

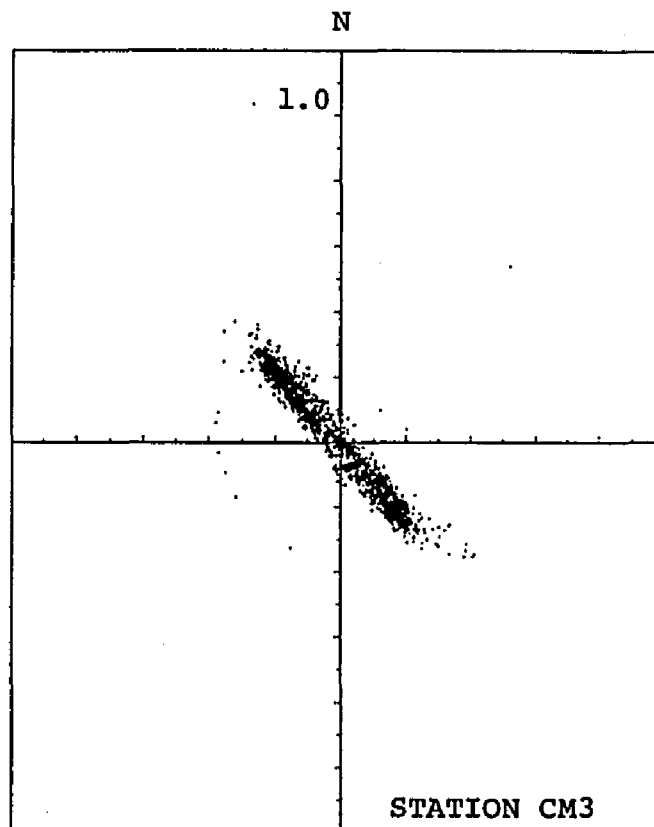
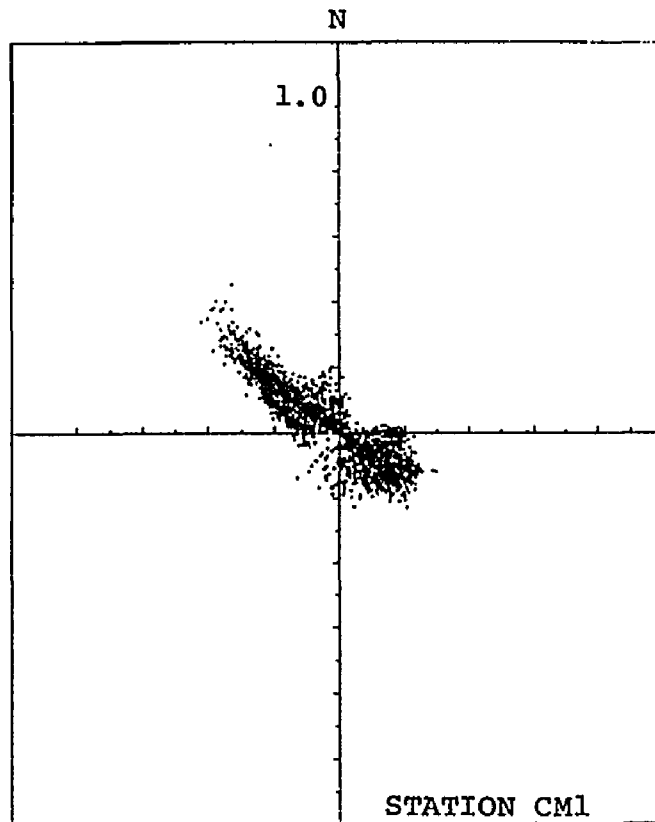


FIG.4.3b

Scatterplots of observed currents, April/
May 1985.

TABLE IV.2

STATION	FLOOD	EBB	DEPARTURE FROM ANTI-PARALLELISM
CM1	309.72	132.19	2.47
CM2 U	314.78	127.19	7.59
CM2 L	322.35	128.83	13.52
CM3	311.57	133.71	2.14

The alignment of the main channel in this section of the estuary is almost straight and orientated $321^{\circ}/141^{\circ}$. The relationship between these principal axes and the bathymetry is shown in Fig.4.4.

Additional information on current velocities was obtained from drogue tracking experiments conducted in a 2 mile reach of the York River surrounding the study transect. Using up to 4 drogues at one time, the drogues were tracked through portions of several tidal cycles, with the aim of establishing the near surface Lagrangian currents at particular phases of the tide. The drogues used were neutrally buoyant current drifters (Davis et al., 1982), illustrated in Fig.4.5. The dates, times and locations of the experiments are listed in Table IV.3 below.

TABLE VI.3

DATE	TIDAL RANGE (m)	TIME (EST)	# OF DROGUES USED	TIDAL PHASE	LOCATION
4 Apr	1.1	0842-1139	2	max flood/SBE	channel
7 Apr	1.1	0910-1414	3	max flood/SBE	chn1/NEshoal
13Apr	0.7	0627-1042	4	ebb	chn1/SWshoal
14Apr	0.7	0614-0856	4	max flood/SBE	chn1/NEshoal
18Apr	0.8	0808-1103	3	max flood/SBE	chn1/SWshoal
19Apr	0.7	0752-1335	3	max flood/SBE	chn1/SWshoal
23Apr	0.6	0932-1414	4	flood	chn1/NEshoal

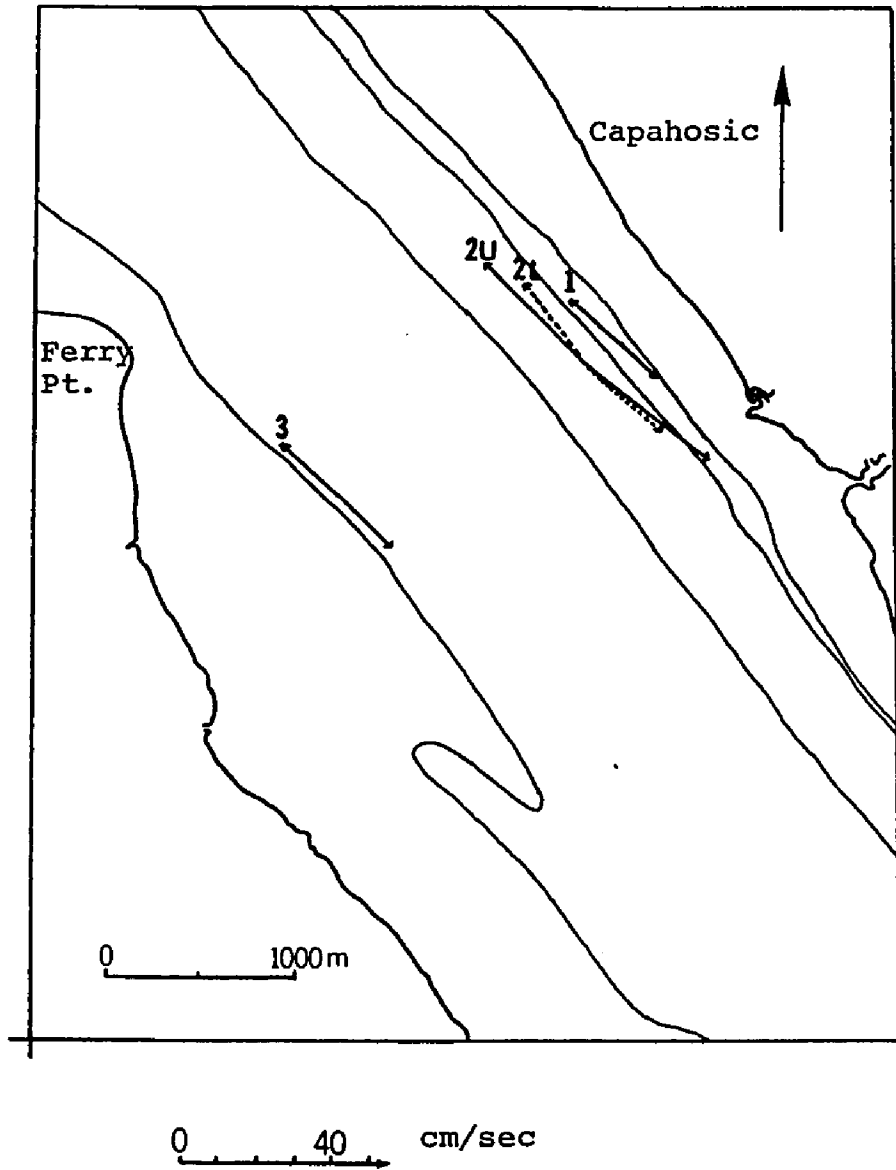


FIG.4.4 Orientation of principal axes and magnitude of mean currents, April/May 1985

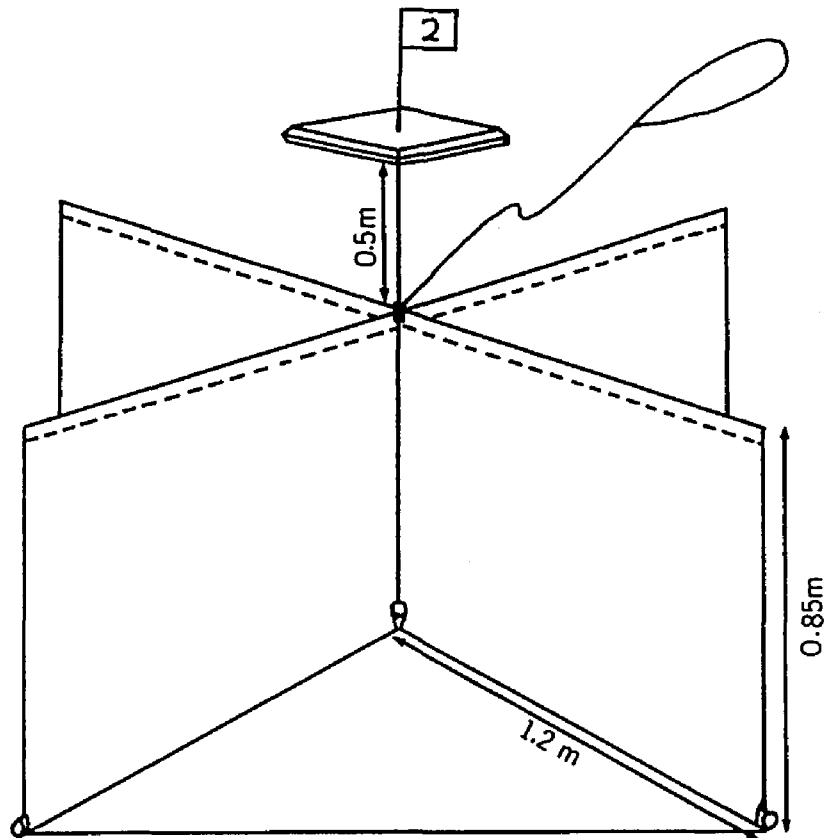


FIG.4.5 Schematic diagram of neutrally-buoyant drogue.

Construction: sails made of 15oz ripstop nylon; upper arms contain 1.14m lengths of capped PVC (1") pipe banded by two 7.5cm sections of foam pipe insulation; lower arms held rigid by 3.5cm diameter aluminum pipe;; surface float of polystyrene foam.

The drogues were positioned using Loran C. Whilst the absolute accuracy of Loran C is not optimal for such a study, it was felt that the relative accuracy of repeated fixes was sufficient to track the movement of the drogues. The location of each drogue was determined every 10-20 minutes. Water depth and wind speed, using a hand-held anemometer, were also recorded. A Loran fix was taken at a known position, Pages Rock Light, every day to determine the offset to be applied to that day's latitude and longitude readings.

The drogues could be easily deployed and retrieved over the side of the 24' garvey used throughout the study. The drogues were released at positions along a straight line across the estuary. The times of initial release were within five minutes of each other. Only one boat was used which limited the number of drogues which could be monitored. Thus the experiments were conducted in the channel and on only one of the adjacent shoals on a given day. Drogues which travelled beyond the defined section of the river were picked up and re-deployed. The experiments were conducted under a range of tidal conditions and only when the wind was less than 10 kts.

Fig.4.6 illustrates the tracklines and positions of the drogues at 30 minute intervals for selected days. The results of these experiments clearly demonstrate the large difference in velocity between the shoal and channel waters. This is especially apparent on April 7 (Fig.4.6b), April 18 (Fig.4.6c) and April 23 (Fig.4.6e). On April 4 (Fig.6.4a) a distinct foam line formed down the channel between the two drogues just prior to slack-before-ebb. The direction of travel of the drogues after

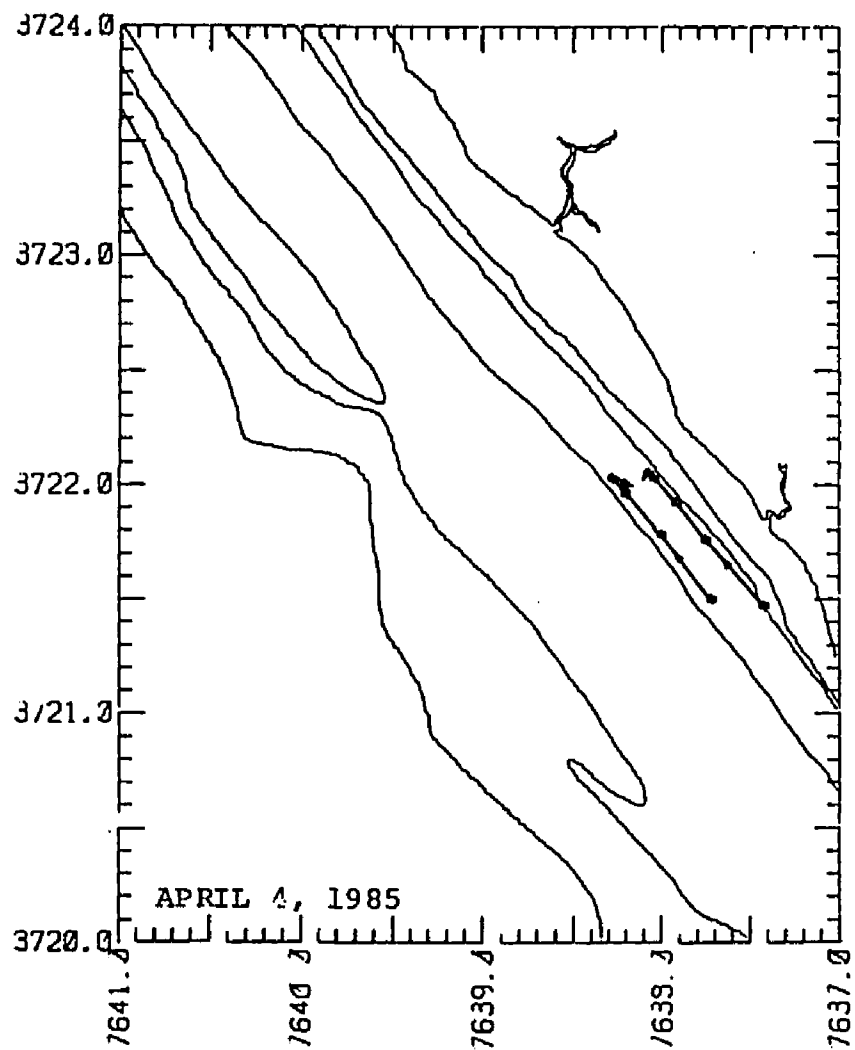


FIG.4.6a

DROGUE TRACKS, APRIL 4, 1985
(Dots on lines represent 30-
minute intervals)

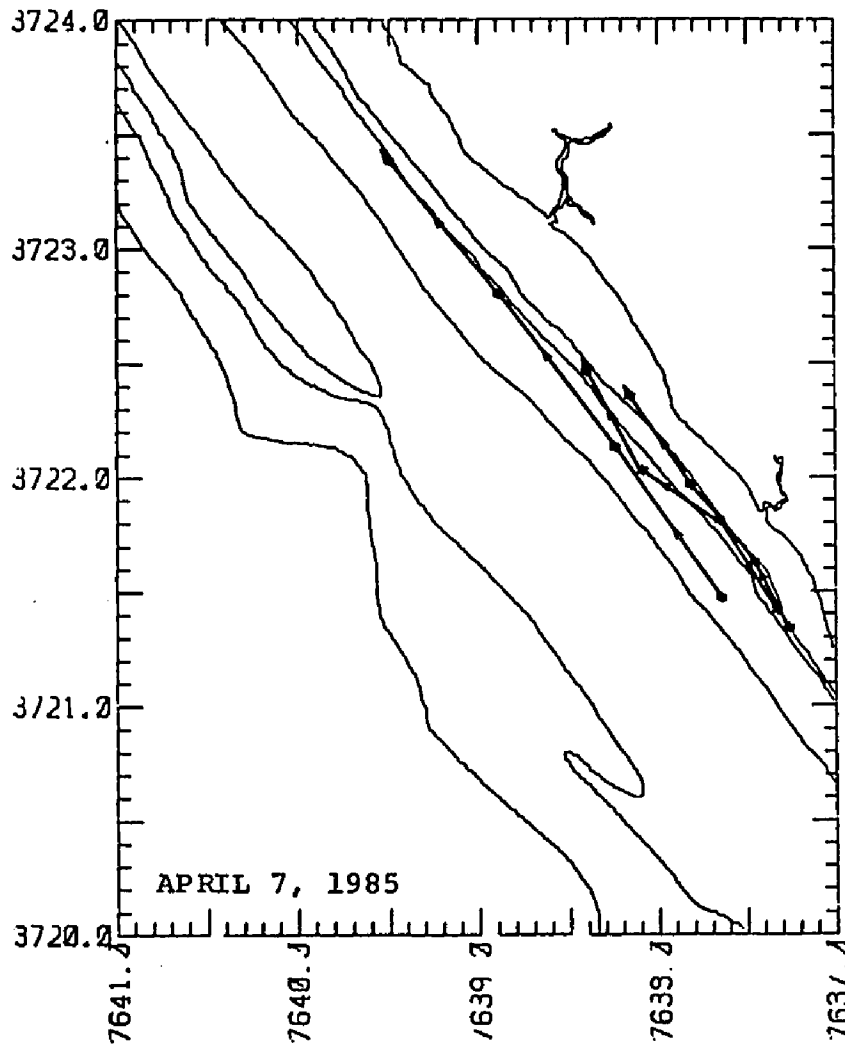


FIG. 4.6b

DROGUE TRACKS, APRIL 7, 1985
(Dots on lines represent 30-minute intervals)

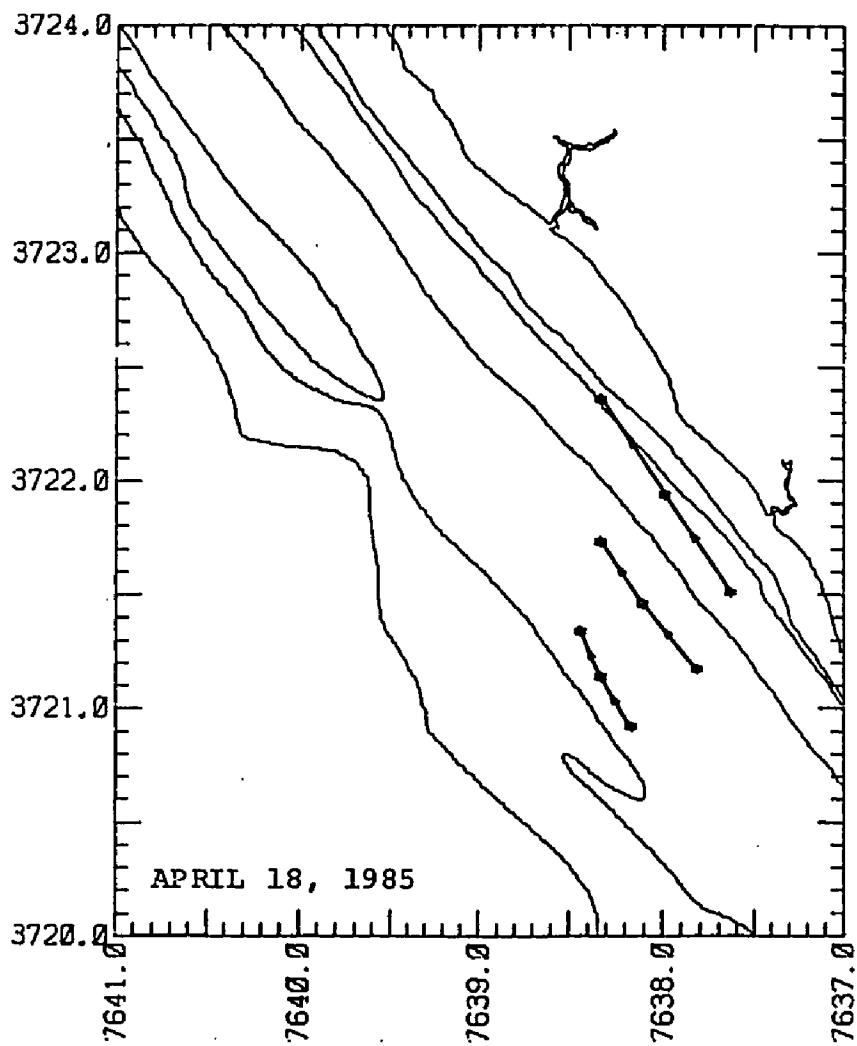


FIG. 4.6c

DROGUE TRACKS, APRIL 18, 1985.
(Dots on lines represent 30-minute intervals)

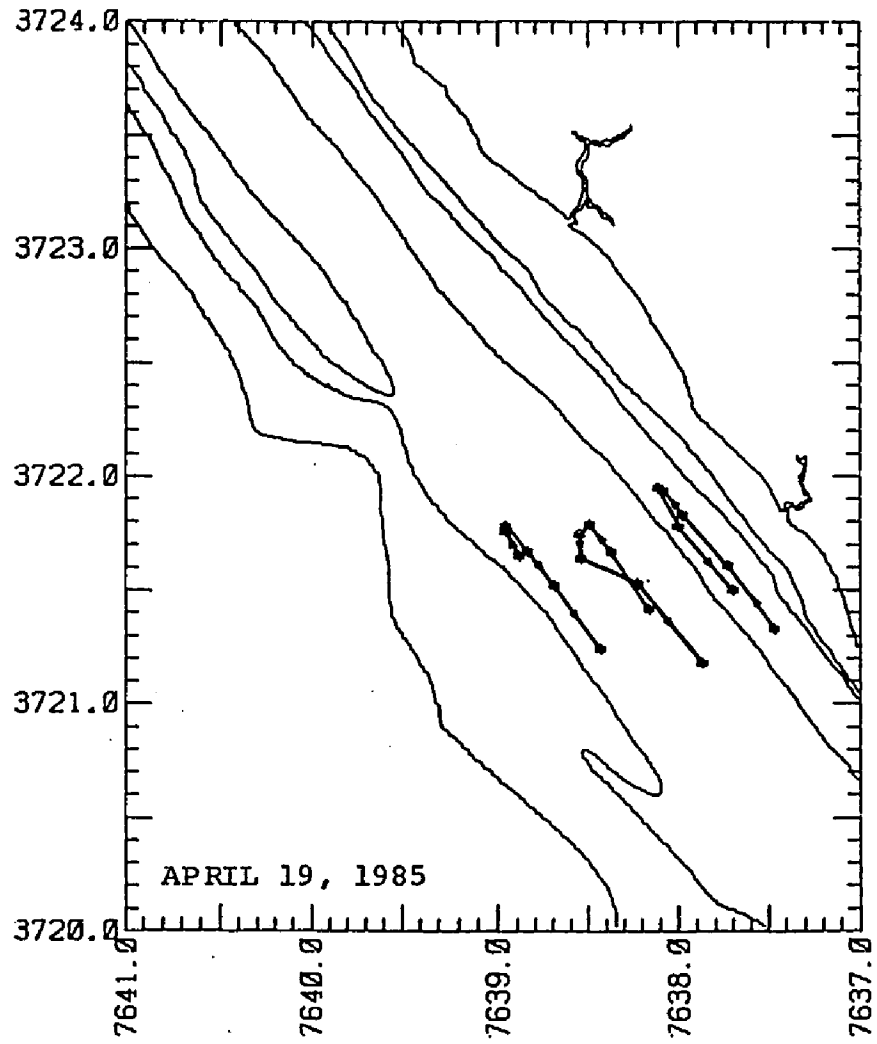


FIG. 4.6d

DROGUE TRACKS, APRIL 19, 1985
(Dots on lines represent 30-minute intervals)

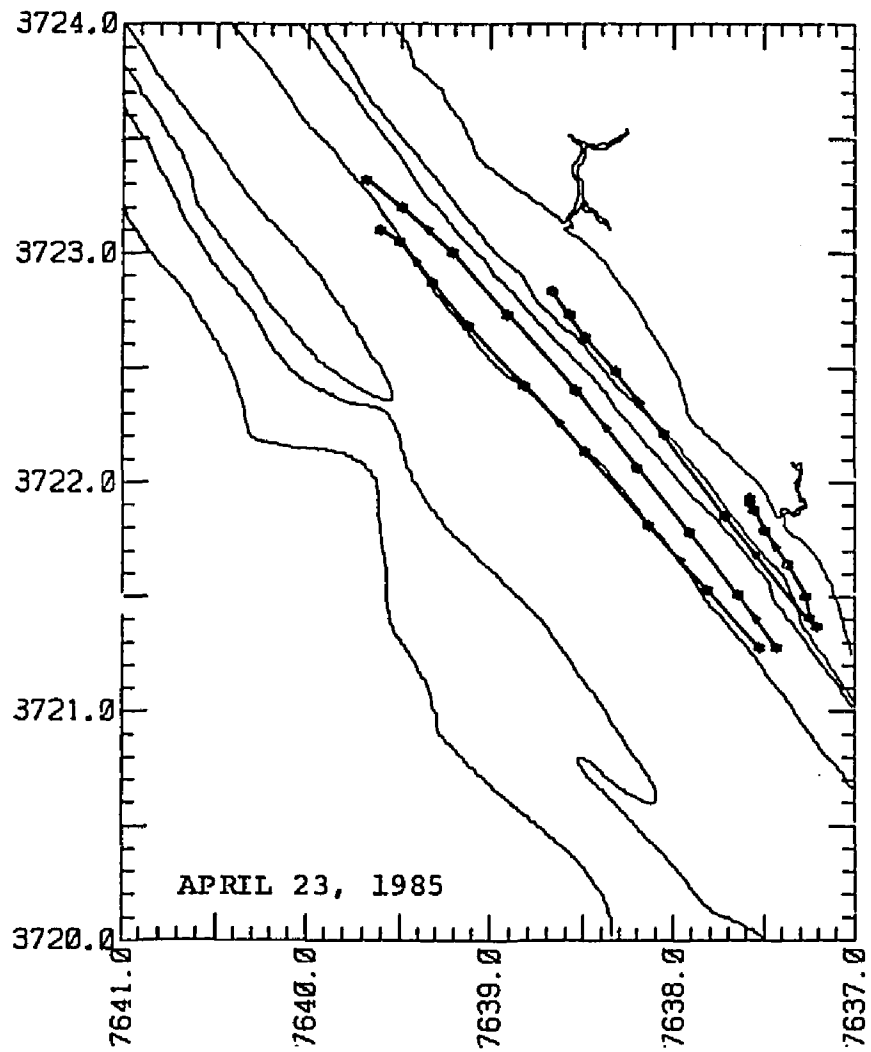


FIG. 4.6 e

DROGUE TRACKS, APRIL 23, 1985
(Dots on lines represent 30-minute intervals)

turning with the tide exhibits some convergence. The tracklines obtained on April 19 (Fig.4.6d) are interesting because, on this occasion at least, the drogue in the channel and that midway between channel and shoal both turned westward with the change in tide, whilst that on the shoal turned eastward, indicating an area of convergence at the inner edge of the shoal. No surface feature such as a foam line was observed at this time however. The drogue experiments served as a clear illustration of the velocity shear and possible lateral flows characteristic of this section of the York River.

2. TIDAL ANALYSIS

The tidal component of the observed currents was determined using the least squares method of harmonic analysis. This procedure requires 29 day-long records and yields quantitative estimates of the amplitudes of 25 tidal constituents, 10 of which are calculated directly, and the remainder inferred using formulae of Schureman (Boon and Kiley, 1978).

The requirements for a 29 day record prevented the data from station CM3 being analysed in this way. After smoothing and interpolating the raw current record to obtain hourly values, the HAMELS.29 procedure (Boon and Kiley, 1978) was run on the the other three current meter records for a 29 day period starting at midnight on the 16 April, 1985. The north and east velocity components were analysed separately and then recombined to obtain the amplitude

estimates. Only 8 of the constituents were found to be significant. They are listed in Table IV.4 along with their magnitudes.

TABLE IV.4

CONSTITUENT	PERIOD (solar hours)	AMPLITUDE (m/sec)		
		CM2 U	CM2L	CM1
O1	25.82	0.044	0.036	0.023
K1	23.94	0.044	0.028	0.023
N2	12.66	0.186	0.106	0.048
M2	12.42	0.566	0.391	0.239
S2	12.00	0.088	0.073	0.047
K2	11.97	0.024	0.020	0.013
M4	6.21	0.048	0.051	0.038
M6	4.14	0.013	0.014	0.011

In general the results show the expected dominance of the semi-diurnal tidal constituents, particularly the M2 whose magnitude is approximately 5 times that of the N2 and S2 constituents. The O1 and K1 are the dominant diurnal constituents and are of nearly equal magnitude. The magnitude of the other harmonics varies between locations. Of particular interest is the non-linearity indicated by the increase in the relative magnitude of the shallow water tides, the M4 and M6 harmonics, both nearer the bed and in the shallow water at station CM1.

In a study of non-linear tidal propagation in a shallow tidal inlet Aubrey and Speer (1985) found that the amplitude of the height of the M4 tide showed a steady increase with distance into the estuary. The rate of growth differed between channels - the greatest being a change in the M4/M2 ratio from .01 to .27 in a distance of 2km. The existence of harmonics was seen in velocity records also. The phase relationship between the M4 and M2 tides will cause an asymmetry in the duration and

magnitude of the the flood and ebb portions of the tidal cycle. In Nauset Inlet, Aubrey and Speer (1985) found that the M2 and M4 were in phase giving a velocity signal characterized by more intense flood than ebb currents. The effect was more pronounced further within the estuary where the tide is more non-linear. This study examined most closely the variation in the tidal height longitudinally along the estuary. Lateral and vertical variations in the tide were not considered.

The current meter records from the York River show similar non-linearities whose magnitude varied vertically and laterally. The ratios of the amplitude (of the velocity) of the M4 and M2, and M6 and M2, tidal constituents for the different current meter records are as follows:

	CM2L	CM2U	CM1
M4/M2 ratio:	.130	.085	.159
M6/M2 ratio:	.036	.023	.046

There is an almost 100% increase in both the M4/M2 and M6/M2 ratios between the channel and adjacent shoal. The magnitude of the M4 and M6 harmonics, the so-called shallow water tides, are expected to increase in the shallower upper reaches of any estuary. It is not surprising therefore to find that they increase in the shoal areas to the sides of the estuary. How characteristic these magnitudes are of similar coastal plain estuaries is not known because of the paucity of our knowledge of this aspect of lateral variability in such estuaries.

The non-tidal residual currents, calculated as a mean over the measurement period, gave results somewhat contrary to the expected pattern of such estuarine flows. Their magnitudes and direction are plotted in Fig.4.7. Although small, the magnitudes obtained here are similar to the observations of Kiley (1980) for this reach of the York River. The directions show a strong lateral component surprising in such a straight section of the estuary. The reason for this is not clear. The residual at station CM1 on the north-east shoal is directed north-west along the axis of the estuary. This direction is opposite to the proposal of Fischer (1976) who suggested that the non-tidal residual currents would be directed down-estuary in the shallows.

3. LATERAL VARIABILITY IN CURRENT MAGNITUDE AND PHASE

Coastal plain estuaries are characterized by having one or more major deep channels bordered by extensive shallow shoal areas. Almost 50% of the width of the York River at the location of the study transect is less than 2 meters deep. It would be expected that the currents in such shallow reaches would be strongly affected by bottom friction. This would lead to a reduction in current magnitude, and possibly a change in phase of the tidal currents across the estuary in such a way that all phases of the tide should occur first on the shoals (Proudman, 1953).

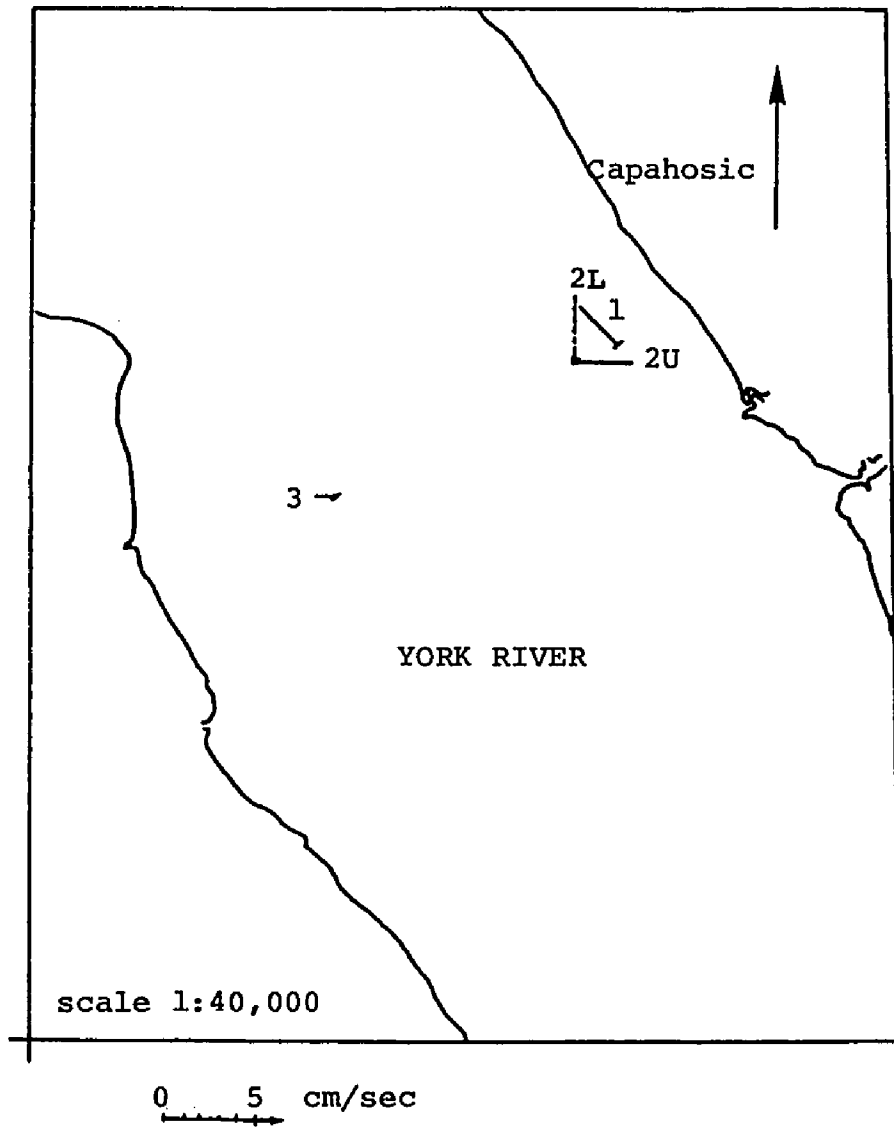


FIG.4.7 Direction and magnitude of non-tidal residual currents during the measurement period, April/May 1985.

(i) LATERAL PHASE DIFFERENCE

The phase variability across the study transect was determined using cross-spectral analysis between pairs of current meter records. For the purposes of this analysis, values of 'along channel' velocity were calculated from the observed record of speed and direction, the channel orientation being taken as $321^{\circ}/141^{\circ}$. The magnitude of these values may vary slightly from the 'along-principal-axis' values but the periodicities should be the same and such a technique allows comparison between different records.

Plots of the power spectrum for each of the time series obtained from the shoal stations, plus that of the upper channel, are illustrated in Fig.4.8. The greatest peak in spectral energy in all three series occurs at a frequency of 0.087 cph, a frequency closely equivalent to the semi-diurnal tidal frequency. More minor peaks occur at a diurnal frequency (0.040 cph) and, for stations CM1 and CM2 U, at a quarter-diurnal frequency (0.165 cph). The record from station CM3 on the south-west shoal is notably different having an energy peak at 0.243 cph (period of 4.12 hours) which is almost as great as the diurnal, and negligible energy at the quarter-diurnal frequency.

Cross-spectral analysis between the record obtained at station CM2 U and each of station CM1 and CM3, on the shoals, revealed the phase differences listed in Table IV.5 below. The coherence at each of these frequencies is significant at the 99% confidence level (Thompson, 1979). A positive sign for the phase difference, and corresponding time lag,

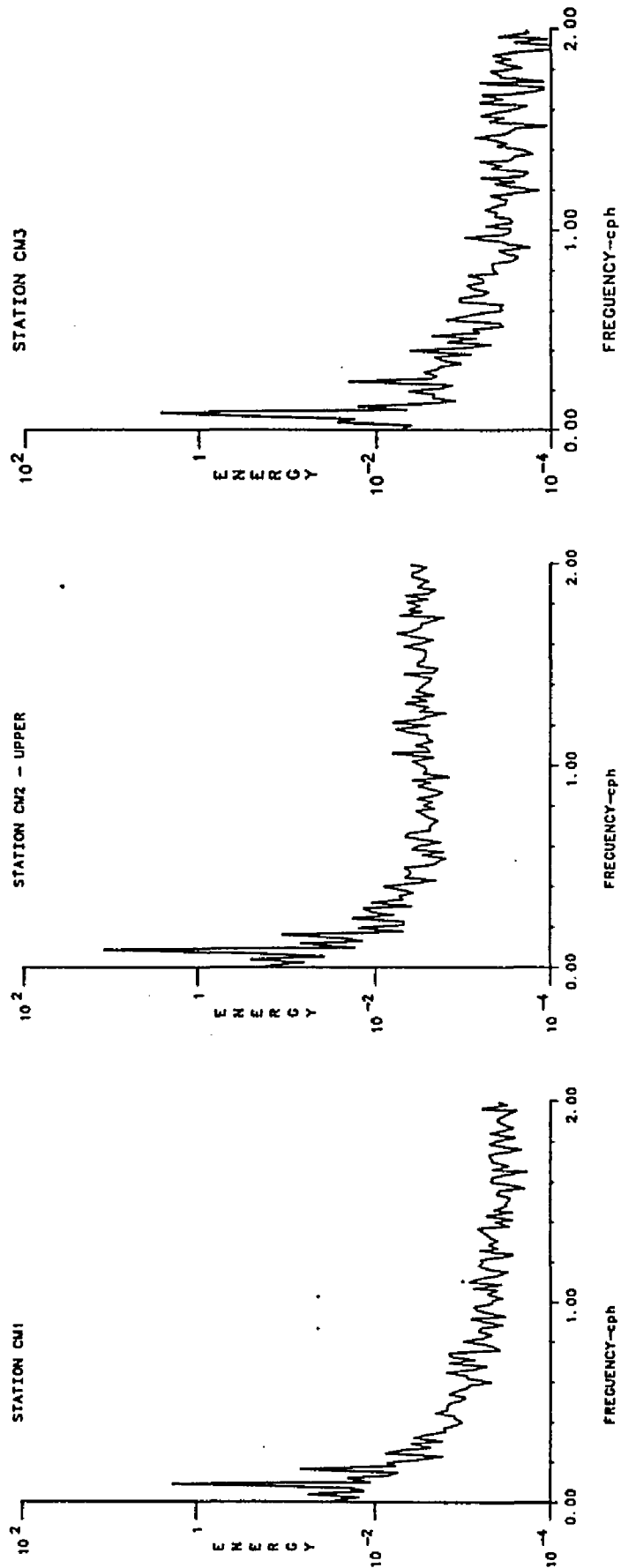


FIG.4.8 Power spectra of currents at stations CM1, CM2U and CM3, April/May 1985

means that the shoal station (CM1 or CM3) leads the channel station, CM2 U.

TABLE IV.5

	FREQUENCY (cph)	PERIOD (hours)	PHASE (degrees)	TIME DIFFERENCE (hours mins)	
CM2 U/CM1:	0.040	25.00	-40	2	48
	0.087	11.50	-7	0	14
	0.165	6.06	-143	2	24
CM2 U/CM3:	0.040	25.00	-31	2	09
	0.087	11.50	-1	0	02
	0.243	4.12	10	0	07

Considering that the phase difference between each pair of current meter records can be represented by the phase difference at the dominant frequency (0.087 cph), it can be concluded that there is no more than 14 minutes difference between the phase of the currents in the channel and those on the shoal. Moreover these results indicate that, if anything, the currents in the channel lead those on the shoal. The sampling times of the original data records, in the instance of stations CM2 U and CM1, are 3 minutes apart which may introduce an artificial phase difference. However this would have a magnitude of only two degrees. The essential result remains: this analysis shows there to be negligible phase difference between the currents on the shoals and those in the main channel.

Qualitative field observations, the results of drogue experiments, and the theoretical arguments of Proudman (1953) had led to an a priori assumption that the shoals led the channel by a time difference of as much as one hour.

The easiest phase of the tide to observe, and thus use as a guide to phase differences, is that of zero current, or slack water. The drogue experiments were conducted on both the north-east and south-west shoals but only around times of slack-before-ebb. On the north-east shoal on the 7 April drogue #4 located in 6 feet of water reached SBE approximately 7 minutes before drogue #3 in 20 feet of water, and 36 minutes before drogue #1 in the main channel. A similar gradation in times of slack water between the north-east bank and channel was seen on the 14 April on that day drogue #5 (6ft) led drogue #3 (20ft) by 16 minutes and drogue #1 in the channel by 62 minutes. On the 23 April the time difference between shoal and channel was 52 minutes, again with the shoal leading. An experiment on the south-western side of the estuary on 19 April gave similar results, the shoal leading the main channel by 44 minutes.

An understanding of these apparently conflicting results can be obtained if we look at a time series plot of the smoothed along-channel values of velocity at the three stations under consideration, the channel-upper and the shoals. Such a time series is plotted in Fig.4.9. What is immediately apparent is the difference in form of the current oscillation at all three stations. That of station CM2U most nearly approximates a sinusoidal curve, but those on the shoals reflect the greater influence of higher frequency tidal harmonics. The phase relationship between station CM3 and station CM2U (Fig.4.9b) shows greatest consistency. The duration of the flood cycle at station CM3 is greater than at station CM2U. As a result the flood generally starts earlier and ends later on the south-west shoal giving an apparent phase

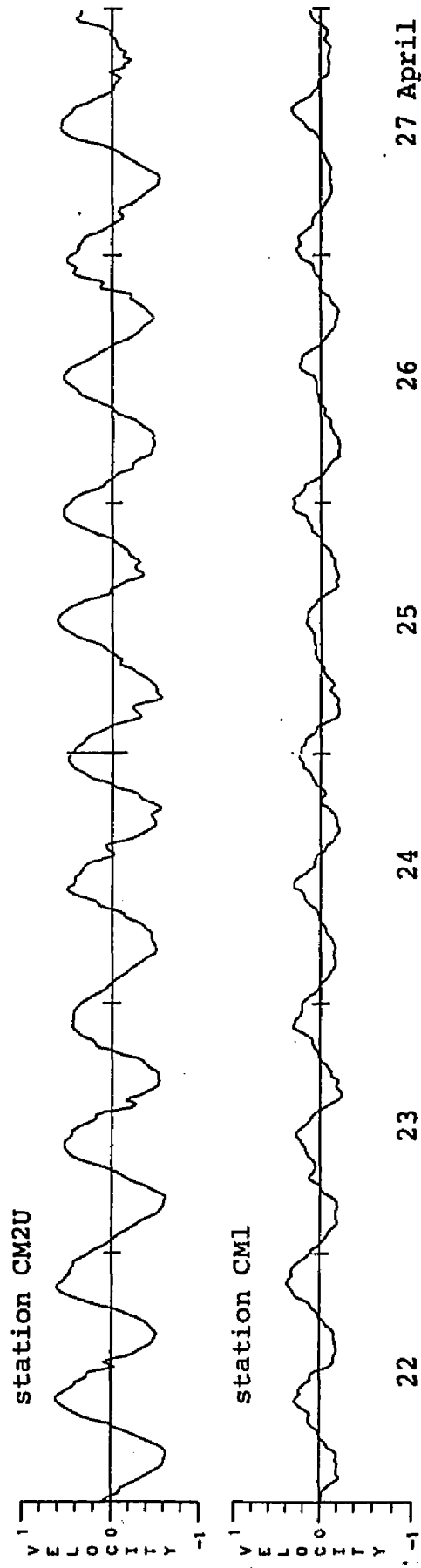


FIG. 4.9a Time series of 'along-channel' current velocities for station CM1 and station CM2U. (Velocities in m/sec, flood currents are positive)

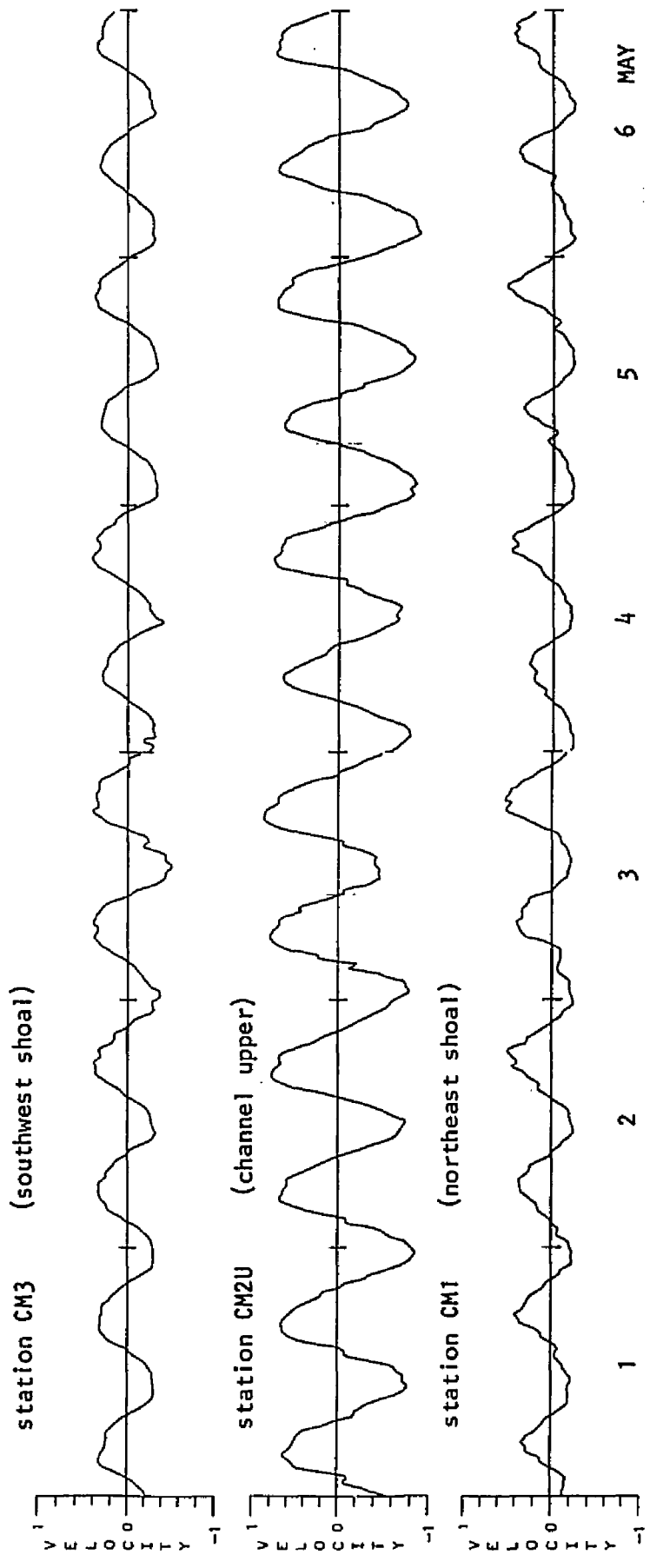


FIG. 4.9b TIME SERIES OF 'ALONG-CHANNEL' CURRENT VELOCITIES (in m/sec) FOR STATIONS CM1, CM2U and CM3. (Flood currents are positive)

difference, if only the times of slack water are considered. The results of the April 19 drogoue study are however inconsistent with this trend. The phase relationship between station CM1 and station CM2U is more complex. It appears to change through the month as a comparison of Fig.4.9a and b reveals. Around the 22-25 April, for example, both slack-before-ebb and slack-before-flood occur first at station CM1. Later in the measurement period, around the 3rd and 4th of May the opposite occurs. This variability may indicate the presence of a longer period tidal constituent modifying the flow characteristics on the north-east shoal. More likely it is due to the distinct irregularity of the current record at station CM1. The average duration of the flood cycle at this station is again greater than the ebb (see Table IV.6), but the standard deviations are greater than at station CM3. It appears that the resultant currents at station CM1 on any given day may be strongly affected by wind events or bank-induced turbulence.

The average duration of the flood and ebb portions of the along channel velocity for the period of 22 April to 9 May was calculated to be:

	<u>FLOOD</u>		<u>EBB</u>	
	mean	s.d	mean	s.d
Station 2U	6:00	.55	6:18	.78
Station 3	6:18	.45	6:00	.38
Station 1	6:30	.74	5:54	.76

Thus, in summary, it would seem that the currents at these three stations are not fundamentally out of phase by more than 14 minutes but that duration asymmetries in the flood and ebb portions of the tidal

cycle, due to the role of the harmonic tidal constituents in the shallower stations, generate much of the observed 'phase-lags'.

(ii) VELOCITY SHEAR

An estimate of the velocity shear across the York River in the vicinity of the study transect can be obtained from moorings of the General Oceanic current meters, and from the drogue tracking experiments. All of these data sources reveal a consistent, and at times considerable, velocity difference between the surface waters of the main channel and the waters over the bordering shoals.

The maximum observed flood currents at station CM2U were approximately 0.85 m/sec whilst those at station CM1 were 0.50 m/sec and at station CM3, 0.45m/sec. This indicates a reduction in flood velocities between the channel and shoals of up to 47%. The change is even greater during the ebb cycle with maximum ebb velocities at stations CM1, CM2U and CM3 of 0.25, 0.90 and 0.50 m/sec - a 72% attenuation between the channel and the north-east shoal. The depth changes from approximately 10 meters in the channel to 3 meters in the vicinity of stations CM1 and CM3. According to Mannings equation, which states that velocity is proportional to depth to the two-thirds power (Henderson, 1966), a 55% reduction in velocity would be expected. The values observed in the York River are of this order of magnitude with the exception of the ebb currents at station CM1. Thus the change in velocity across this estuary may be primarily due to the change in depth.

Calculating the velocity difference between the values of along-channel velocity at Station 2U, in the channel, and Stations 1 and 3 on the shoals reveals an oscillatory difference essentially in phase with the channel velocity. A representative 10 day segment of this record, starting at spring (3 May) and ending at neap tides (12 May) is illustrated in Fig.4.10. As we have already seen there is only a small phase difference in the tidal currents across the estuary. This means that the flow velocities will approach zero at a similar time everywhere across the section, and thus the velocity difference will also be minimal at this time. Maximum velocity differences occur at times of maximum current. Considering these velocity differences as lateral shear results in very small values for the shear between stations CM2U and CM3, due to the asymmetrical positioning of the channel in this reach of the estuary.

Using data from the General Oceanics current meter moorings gives only an average value for the shear between the channel and the shoal stations. The spatial variability of this shear on a smaller scale is evident from drogue and surface current meter data. By way of example, consider the drogue speed illustrated in Fig.4.11. The times selected are all at or near the time of maximum current. Large differences in current speed can be seen between the shoals and immediately adjacent deeper water. The greatest shear appears to be located in the water depths of 2 to 4 meters, and thus the shear is not evenly distributed between the main channel and shoal.

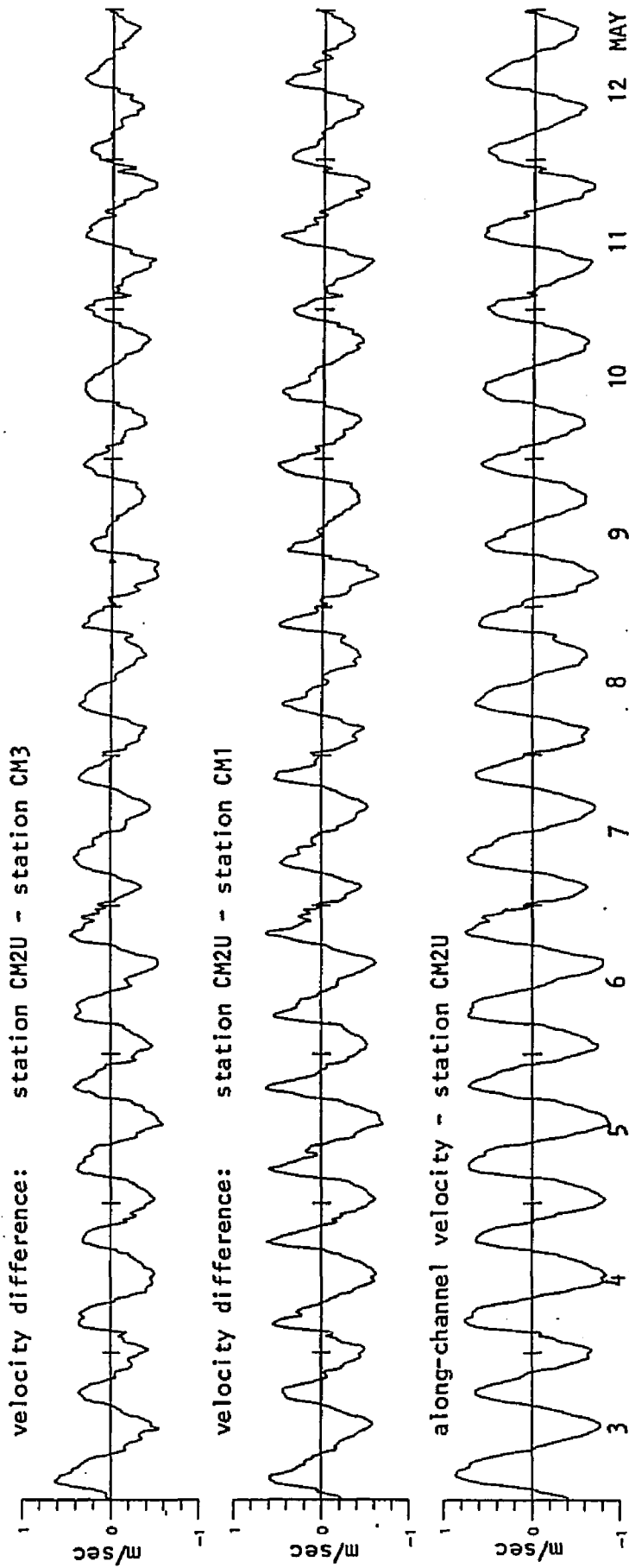


FIG. 4.10 TIME SERIES OF VELOCITY DIFFERENCE BETWEEN THE CHANNEL AND SHOALS
(Flood currents positive)

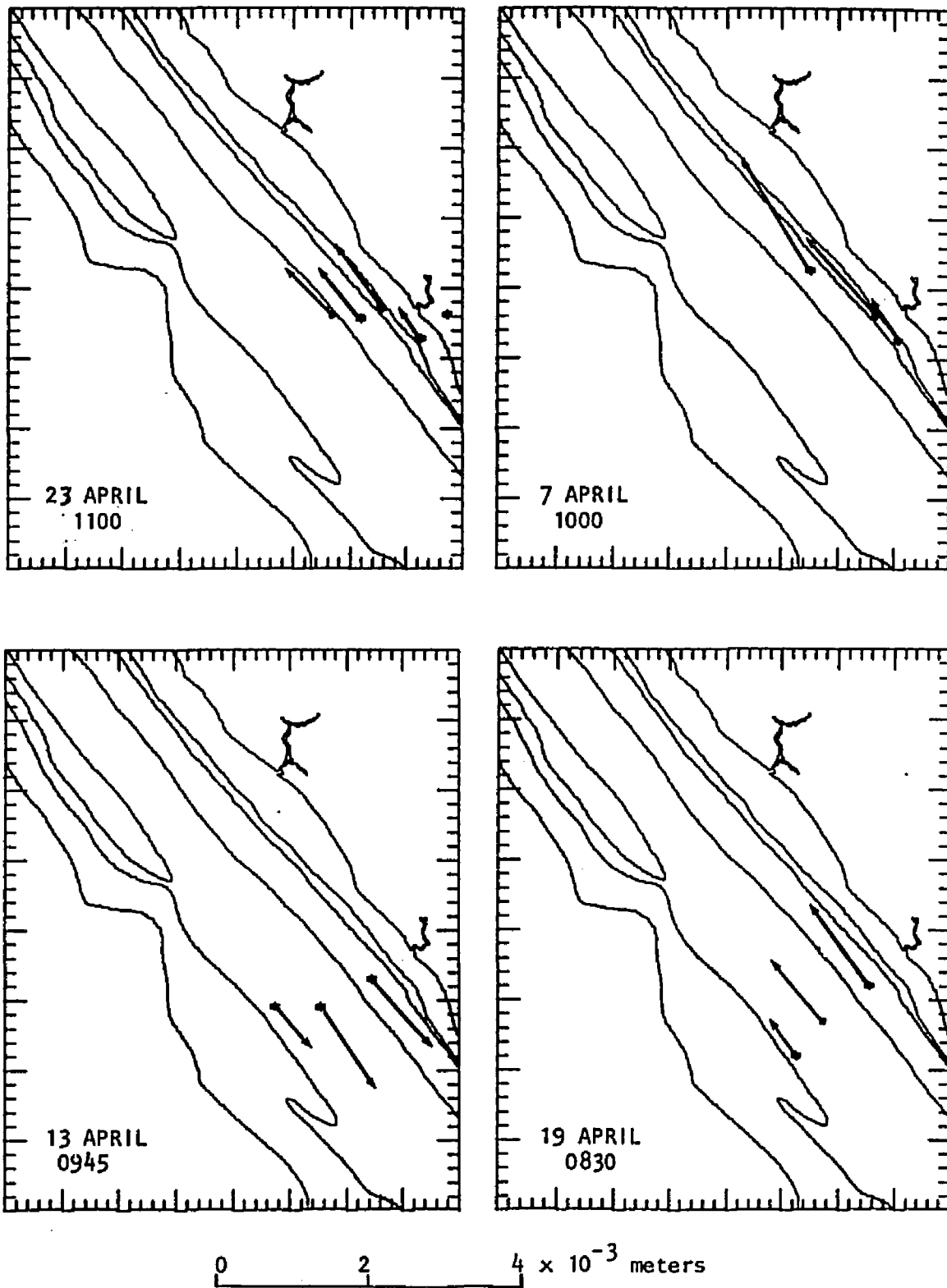


FIG.4.11 Velocity shear across the estuary as indicated by drogue speeds.

Further evidence of this is revealed by data collected using 'surface current meters' - an instrument developed by D. Johnson of NORDA to measure the speeds and directions of currents in the very near-surface layer. The nature of these instruments makes them susceptible to erroneous readings when there are significant surface waves. Under calm conditions however they are considered to give reliable estimates of current speeds and directions. On the 18th and 19th of April 1985, 4 of these instruments were moored at locations across the south-western side of the estuary. The magnitude of velocity shear calculated between adjacent pairs of current meters was observed to be locally maximum where the water depth was 2-3m.

The existence of a localized region of high velocity shear at the inner edge of each of the shoals suggests that the water masses in the upper layer can be divided into two regimes - 'channel' and 'shoal'. Those on the shoal are strongly affected by bottom friction and are likely to be not only more turbulent and vertically well-mixed, but also more turbid. This idea was first proposed by Welch (1979) who suggested that coastal plain estuaries can be regarded as having what was termed an 'inviscid core', where frictional effects play a secondary role, surrounded by boundary layers in which friction and buoyancy forces are important. Analogies can also be made with studies of the inner continental shelf where a 'coastal boundary layer' has been noted by some researchers.

V. FRONTS IN THE YORK RIVER

Fronts are readily observable features of the York River estuary. They can be seen in all parts of the estuary, are generally axially aligned and may be several miles in length. They are recurring features but are not persistent, existing for periods of time varying between 10 minutes and 2 or 3 hours at any given location. Thus their time scale is distinctly intra-tidal.

They are usually distinguished as a line of foam, and possibly a change in surface roughness, about 10m wide. At times however no foam line is seen, only a surface 'slick' zone. It is uncertain whether these features represent frontal zones with weaker convergent circulations, or whether the amount of foam produced is dependent on the chemistry of the surface layer. This varies seasonally, the level of organic compounds, for example, is at a maximum in the spring during times of strong algal blooms.

Aerial photography was used as a method of locating fronts, their positions in relation to the bathymetry and their movement with time. Large distances can be covered in a short time allowing a relatively syoptic picture to be obtained, and the complete pattern of slicks can be seen more clearly from the air than from the sea surface. Although strictly observational, comparison of the resulting aerial photographs

with bathymetric charts allows determination of the relation, if any, of such features to the bathymetry. Such photography was done on 4 different occasions: April 1, 1983, November 8, 1984, and on May 5 and May 19, 1985. The camera used throughout was a Hasselblad 500EL, with a 50mm, 1:4 Zeiss lens, mounted vertically in the bottom of the aircraft, a de Havilland Beaver. To cover the entire width of the York River in one frame, given the focal length and frame size of the camera, would have required an altitude of 14,000 feet. Due to loss of clarity and resolution when photographing from this height it was decided to fly at a lower altitude and cover the required ground distance by flying to the northwest along one bank and returning southeastward along the other. The necessary altitude was thus reduced to 9,500 or 10,500 feet. Only the portion of the York River up-estuary from Gloucester Point was included in these surveys.

On the 1st April, 1983, 2 flights were done - the first between 1247 and 1315 EST, the second between 1525 and 1600 EST. The time of predicted slack-before-ebb at the study site on that day was 1438 EST. The resulting photographs are illustrated in Fig.5.1. Distinct foam lines can be seen at many places along the estuary. Spatially they are most frequently located to the outer edge of the deeper channel regions. The relatively short time for genesis and decay of these features is illustrated by the changes apparent in the 2.5 hours between these two flights. For instance, on flight #1 a very distinct foam line can be seen just up-estuary of Ferry Point which has disappeared by flight #2. At other places, for example in the vicinity of Terrapin Point, it is uncertain whether the same frontal system is moving laterally across the

FIG.5.1 Photo mosaic of pictures taken
 during an aerial survey of the
 York River on April 1st, 1983.
 Flying height - 10,500 feet.
 White foam lines marking fronts
 can be clearly seen.

- a) 1247 - 1315 EST
- b) 1525 - 1600 EST

YORK RIVER AERIAL SURVEY

APRIL 1, 1983

1247 - 1315 EST



Capahosic

West Point

Gloucester Point

Capahosic

YORK RIVER AERIAL SURVEY

APRIL 1, 1983
1525 - 1600 EST



estuary, or whether the features seen are in fact different frontal systems. The fronts seen in the vicinity of Gloucester Point show a great deal of apparent movement and curvature.

A sequence of six flights was completed on the 8th November, 1984, all at 10,500 feet. The foam lines seen on that day were not as distinct or as numerous. On the 5 and 19 May, 1985, the sequence of flights formed a time series covering the entire tidal cycle. The aircraft altitude in this instance was 9,500 feet. Examination of the resulting photographs once again revealed the temporal and spatial variability of these features. Looking at the section of the York River between Clay Bank and Ferry Point, distinct fronts, marked by foam lines, were seen on three different occasions: flight #4 (Hour 11/12), flight #6 (Hour 2) and flight #7 (Hour 3/4). Their positions are plotted in Fig.5.2. If these were the same frontal system, a lateral movement across the estuary is indicated. More likely however the front seen at H11/12 on the northeast side of the channel is a separate feature to those seen later during the ebb tide on the other side of the estuary.

The position of any fronts observed whilst collecting CTD or drogue data was also noted. Although to a large extent this information is qualitative it does show the most frequent times, and places, of occurrence of fronts in the vicinity of the study transect. With reference to Fig.5.3 it can be seen that most of the fronts noted during the lateral CTD transects (described in Chapter 3) occurred during the ebb tidal phase (H1-H6) and towards the sides of the estuary, between

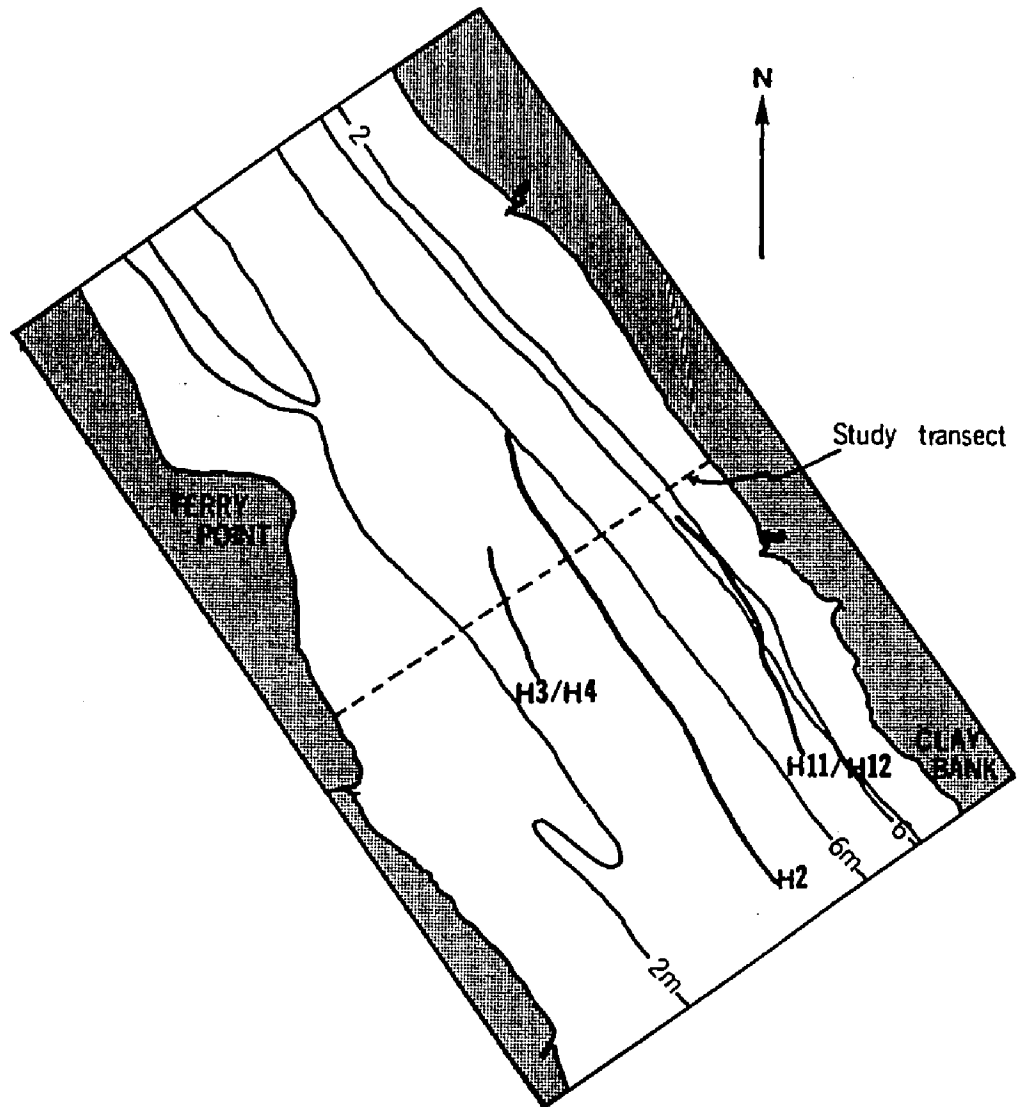


FIG.5.2 Location and times of fronts noted from aerial surveys on the 5th and 19th May, 1985.

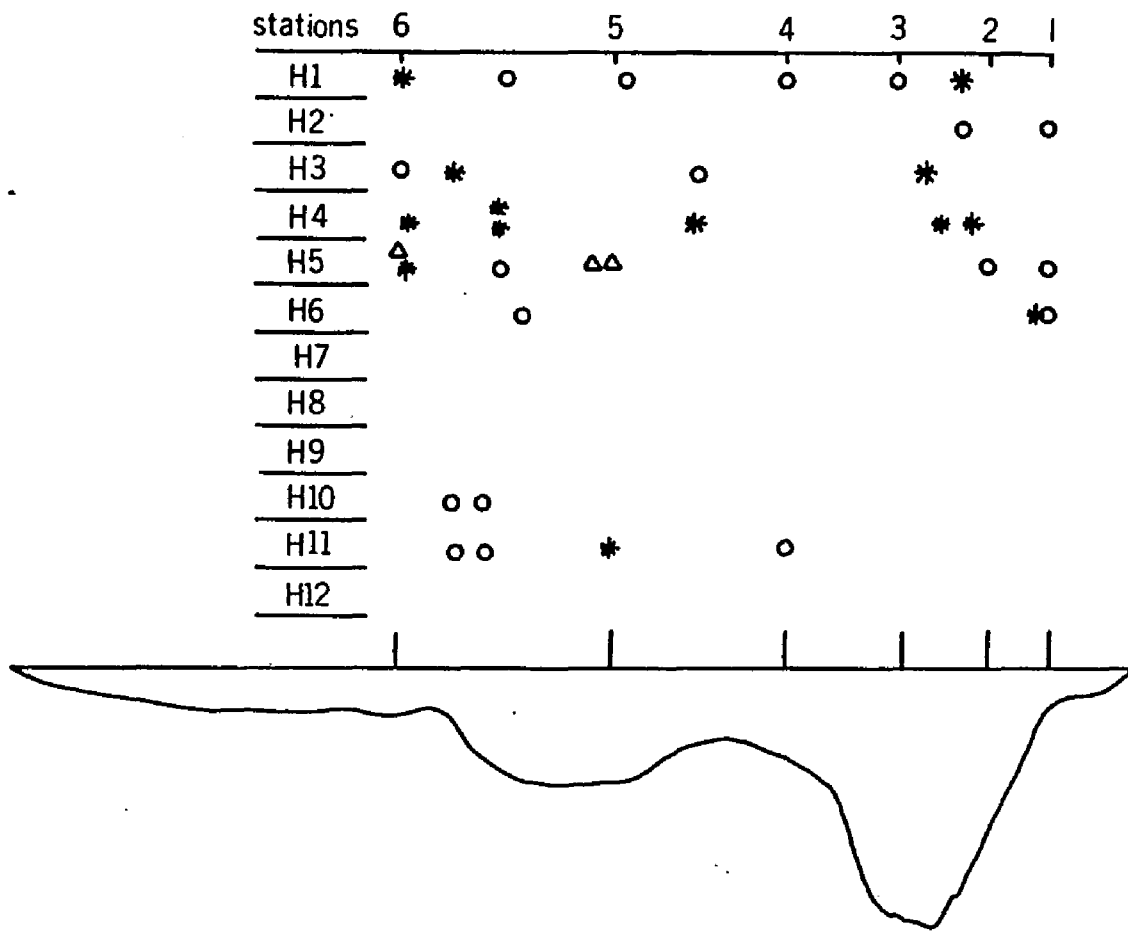


FIG.5.3 Fronts observed during CTD transects, May 1983 and May/June 1984.

- * - spring tides
- o - mean tides
- △ - neap tides

station 6 and halfway to station 5, and from midway between stations 3 and 2 to station 1. Positions of fronts, obtained from Loran-C, can be plotted for fronts observed on other field days. As an example, fronts observed during spring tidal conditions are illustrated in Fig.5.4. In plan view these features are clearly aligned with the direction of the main channel.

Unlike those observed at the boundaries of brackish plumes (eg. Garvine and Monk,1974), the local density difference across these frontal boundaries is very small. Use of a flow-through system (Ruzecki, 1981) to continuously measure the conductivity and temperature at a depth of 1 meter revealed very small gradients, and vertical CTD casts in the vicinity of these fronts showed little difference in the vertical density structure. Despite this, these fronts were observed to be active convergence zones, frequently drawing the boat into their location.

The observational evidence indicates therefore that fronts can be found in the York River, furthermore, those seen in the vicinity of the study area are most frequently aligned parallel to the axis of the estuary and occur during the latter part of the flood through to the middle of the ebb tidal cycle.

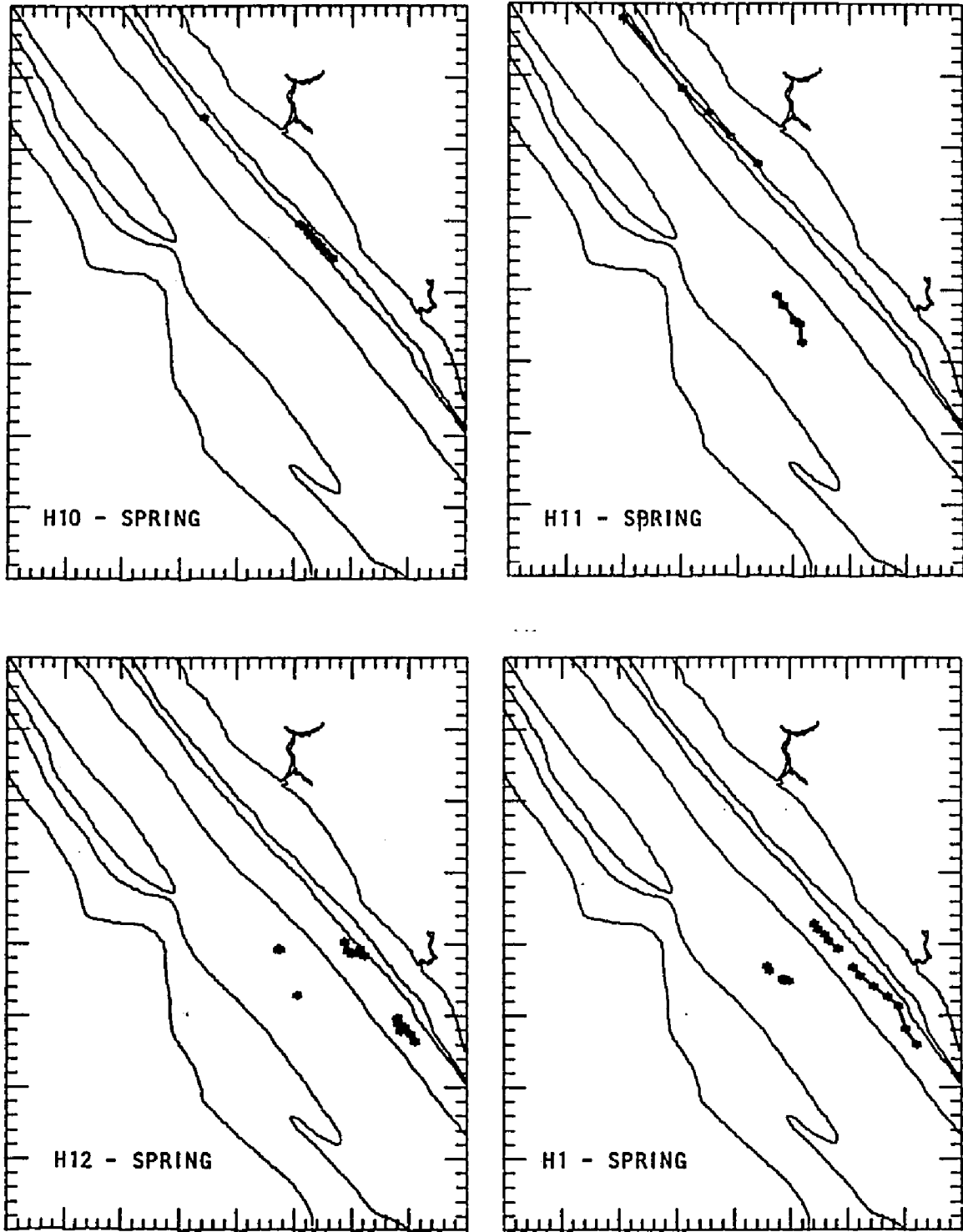


FIG.5.4 Locations of fronts observed during spring tides in the vicinity of the study transect.

VI. DISCUSSION

Observational evidence has shown that the lateral density distribution in the York River is not uniform: on the contrary it exhibits a distinct spatial and temporal variability. How can this be explained, and what are the implications for the formation of longitudinal fronts?

The density distribution within any estuary is a result of both advective and mixing processes. Differences in the magnitude of advection and the amount of turbulent mixing can be correlated with changes in depth. In the shallower areas bottom friction would act, not only to vertically mix the water column, but also to retard current speeds. Coastal plain estuaries have a cross-sectional bathymetry distinguished by extensive shoal areas bordering the main channel. Across such an estuary therefore, significant differences in the magnitude of these processes can be expected. Observations made in this study support this hypothesis. As was seen in Chapter 3, the water column over the shoals remains vertically homogenous throughout the tidal cycle, the inner edge of the shoal region acting as a boundary between well-mixed and partially-stratified regimes. Furthermore, in Chapter 4, a marked difference in the magnitude of the tidal currents over the shoal compared to those in the channel, was noted. Both

Eulerian and Lagrangian measurements indicated that the shear between the two areas was locally greatest near the inner edge of the shoal.

Combining this evidence allows the formulation of a conceptual model by which the density variability can be explained. Neglecting diffusive processes and assuming that the density distribution at any given place and time is due simply to advection in the longitudinal direction we can write:

$$\frac{\partial \rho(x, y, z, t)}{\partial t} = u(x, y, z, t) \frac{\partial \rho}{\partial x} \quad (6.1)$$

Taking $\partial \rho / \partial x$, the longitudinal density gradient, as a constant, L , and considering the depth-average density in a horizontal layer across the estuary within which the longitudinal velocity is assumed to be constant with respect to the x and z directions, gives:

$$\frac{\partial \rho(y, t)}{\partial t} = -u(y, t) L \quad (6.2)$$

The aim here is to evaluate the expected density difference between two locations across the estuary, specifically the channel and shoal, thus we can write:

$$\frac{\partial \Delta \rho(t)}{\partial t} = -L[u(y_a, t) - u(y_b, t)] \quad (6.3)$$

where $\Delta \rho = \rho(y_a) - \rho(y_b)$ and 'a' refers to the channel and 'b' to the shoal.

Thus, as described by equation (6.3), the density difference between the shoal and channel and its change with time, is considered to be simply the result of differential advection.

This expression can be evaluated by assuming a functional form for the longitudinal velocity, u . Taking

$$u_a = -A_a \sin(\omega t)$$

$$u_b = -A_b \sin(\omega t + \alpha)$$

and integrating with respect to time gives:

$$\Delta\rho(t) = \Delta\rho_0 + \frac{L}{\omega} \{A_b(\cos(\omega t + \alpha) - \cos\alpha) + A_a(1 - \cos(\omega t))\} \quad (6.4)$$

where $\Delta\rho_0 = \Delta\rho(t=0)$.

To separate the relative contributions of phase and amplitude difference, to the resulting density distribution, equation (6.4) was evaluated for two different cases:

(i) $\alpha = 0$, $(A_b - A_a)$ of varying magnitude

(ii) A_b and A_a both constant, and α of varying magnitude.

Throughout these calculations the following values were used:

$$\Delta\rho_0 = 0.24 \text{ kg/m}^3$$

$$L = -2.0 \times 10^{-4} \text{ kg/m}^4$$

$$\omega = 0.51 \text{ radians/hour or } 1.4 \times 10^{-4} \text{ radians/sec}$$

The value of $\Delta\rho_0$ was taken from the observational data of this study. The longitudinal density gradient was obtained from the York River Slack Water Survey data collected by VIMS. It represents a mean value, at a

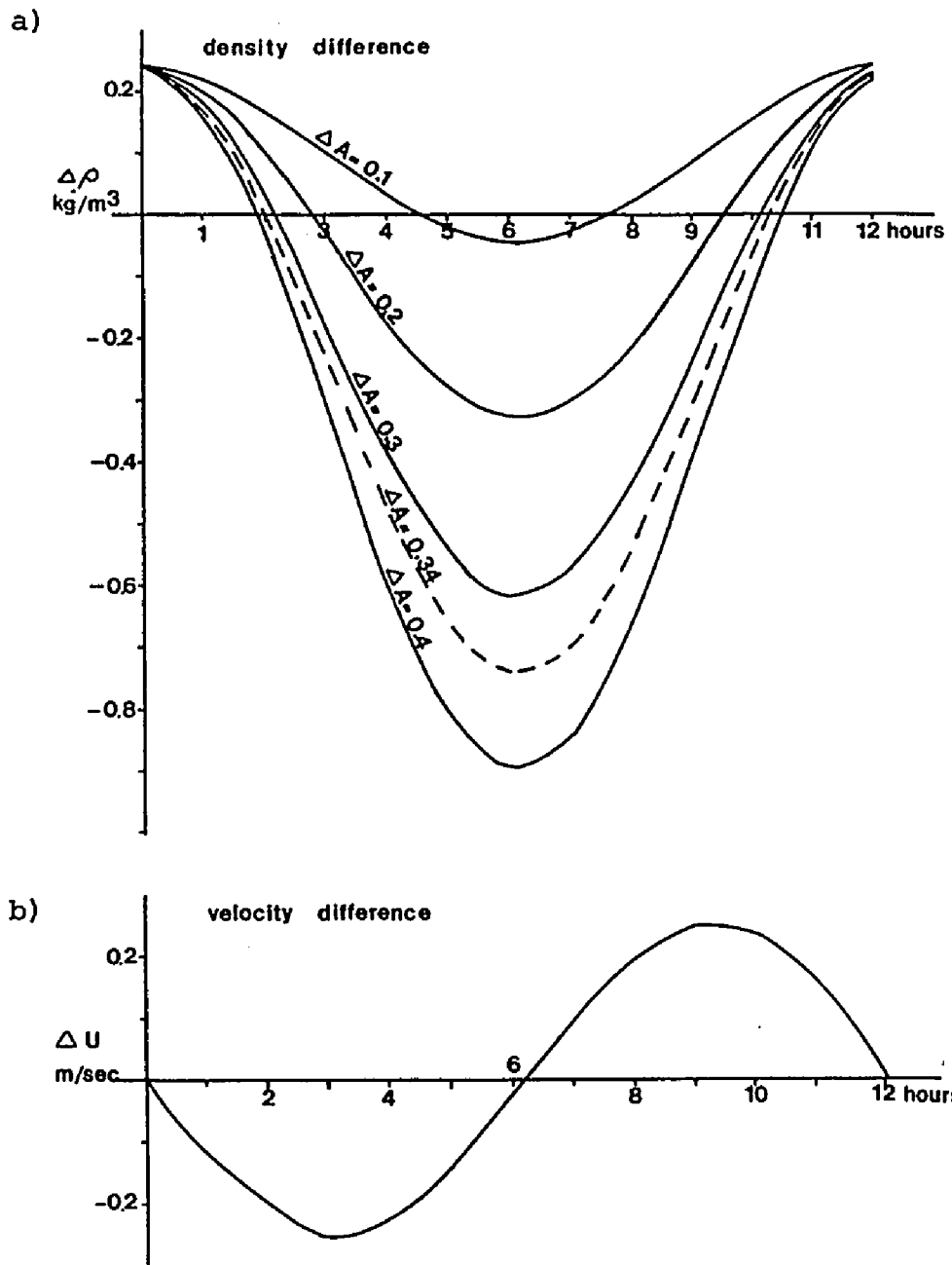


FIG.6.1a. Distribution of the density difference assuming zero phase and varying amplitude difference.

b. Variation in the velocity difference according to the model.

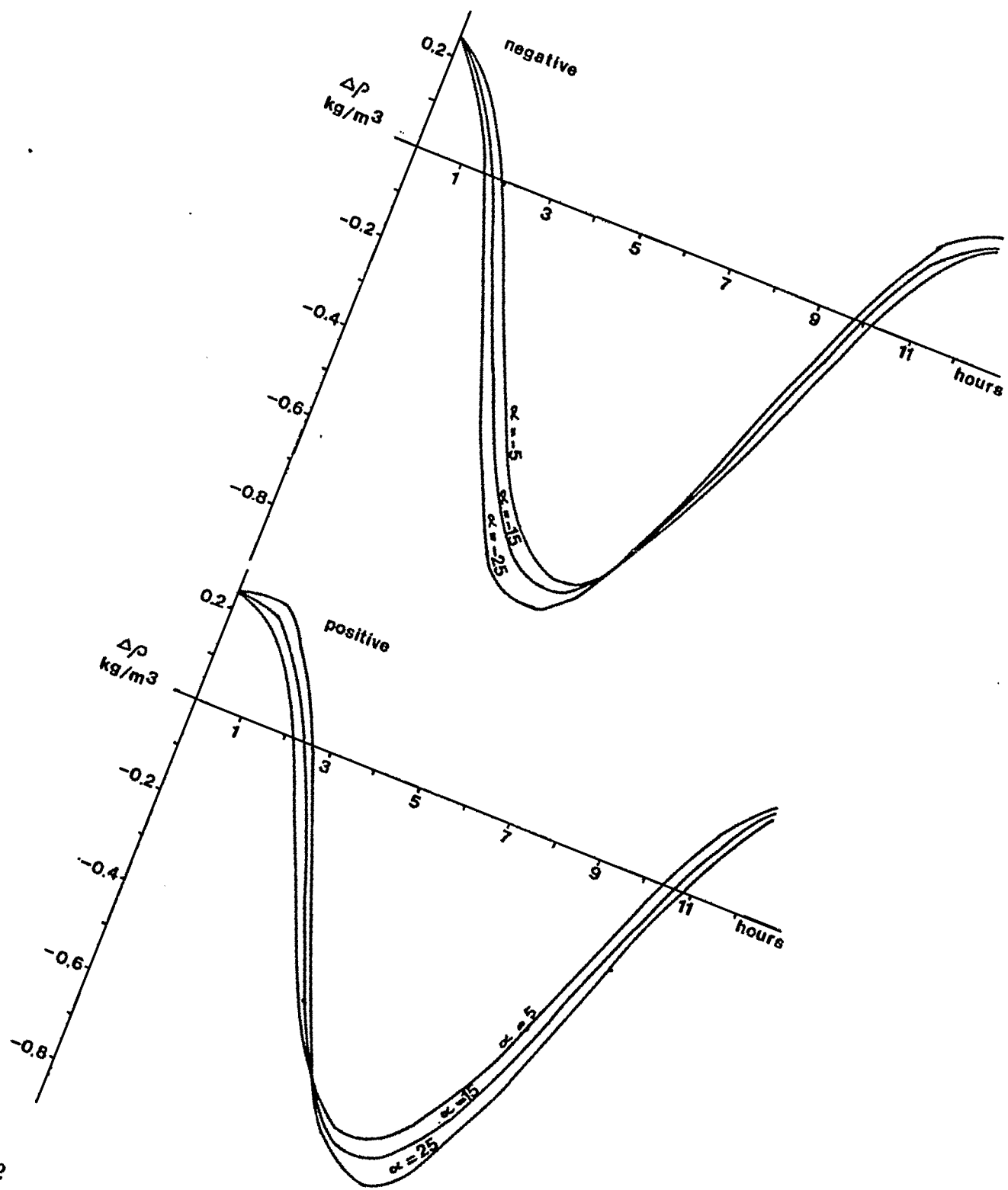


FIG.6.2

Density difference assuming an amplitude difference of 0.34m/sec and varying phase.

depth of 2m, for a 10km section of the York River centered on the study transect.

Taking $t=0$ as the time of slack-before-ebb, the variation of the density difference through a tide cycle under these different conditions is plotted in Figs.6.1 and 6.2. A plot of the velocity difference is included in Fig.6.1. A positive value of $\Delta\rho(t)$ indicates that the density in the channel is greater than that of the the shoal. If there is no phase difference between the channel and shoal, then the expression for $\Delta\rho(t)$ (equation 6.4) reduces to simple cosine function which gives, as illustrated in Fig.6.1, maximum values of density difference at times of minimum velocity and velocity shear. The larger the value of the amplitude difference, the more extreme the change in $\Delta\rho(t)$ through the tide cycle. The observed value of the amplitude difference of the M2 tidal components between the channel and the north-east shoal was 0.34 m/sec (refer TableIV.4,p92). This is plotted in Fig.6.1 as dashed line. A difference in the value of $\Delta\rho_0$, the initial density difference, will simply translate the curve up or down the $\Delta\rho(t)$ axis. It will not alter it's form.

Using the observed amplitude difference of 0.34 m/sec, but including a phase difference, gives curves for $\Delta\rho(t)$ which are not significantly different (see Fig.6.2). Even a phase difference of 25° which, for the M2 tidal component, represents a time difference of 52 minutes, only alters the expected maximum negative value of $\Delta\rho(t)$ by 0.06 kg/m^3 . The observed phase difference between channel and shoal was only -7° (refer Chapter 4). The times at which these maximum negative

values of $\Delta\rho(t)$ occur are offset compared to the 'no-phase' case - if the phase is positive they occur after, and if negative, before the time of slack-before-flood. It would seem however that the amplitude difference plays a far greater role in generating a density difference than any phase difference.

Observations of the density differences between the shoals and main channel in the York River display the same general trends as predicted by the model. The density differences were calculated by subtracting the depth average density at 1.0m at the shoals (Stations 1 and 6), from that of the main channel (Station 3). This was done for each tide hour, and for each of 'mean' and 'spring' tidal conditions. The results are plotted in Fig.6.3. Maximum positive and negative values of $\Delta\rho(t)$ do occur at, or near, the times of minimum current -SBE and SBF. However the form of the variation between these maxima shows a consistent anomaly during the ebb tidal cycle. Instead of steadily decreasing to a maximum negative value, the density difference drops rapidly to a local maximum, followed by an increase for several hours before decreasing sharply again. In other words, at slack-before-ebb the shoal is least dense, but within an hour this trend is reversed and the least dense water is found in the channel. This is so throughout the ebb cycle although the density difference is minimal at times of maximum current. With the exception of the density difference between the south-west shoal and the channel under mean tide conditions (curve B, Fig.6.3a), the range of observed variation is much greater than predicted. At spring tides this can probably be attributed to a greater magnitude in $(A_b - A_a)$. As shown in Fig.6.3b, the density difference between the south-west

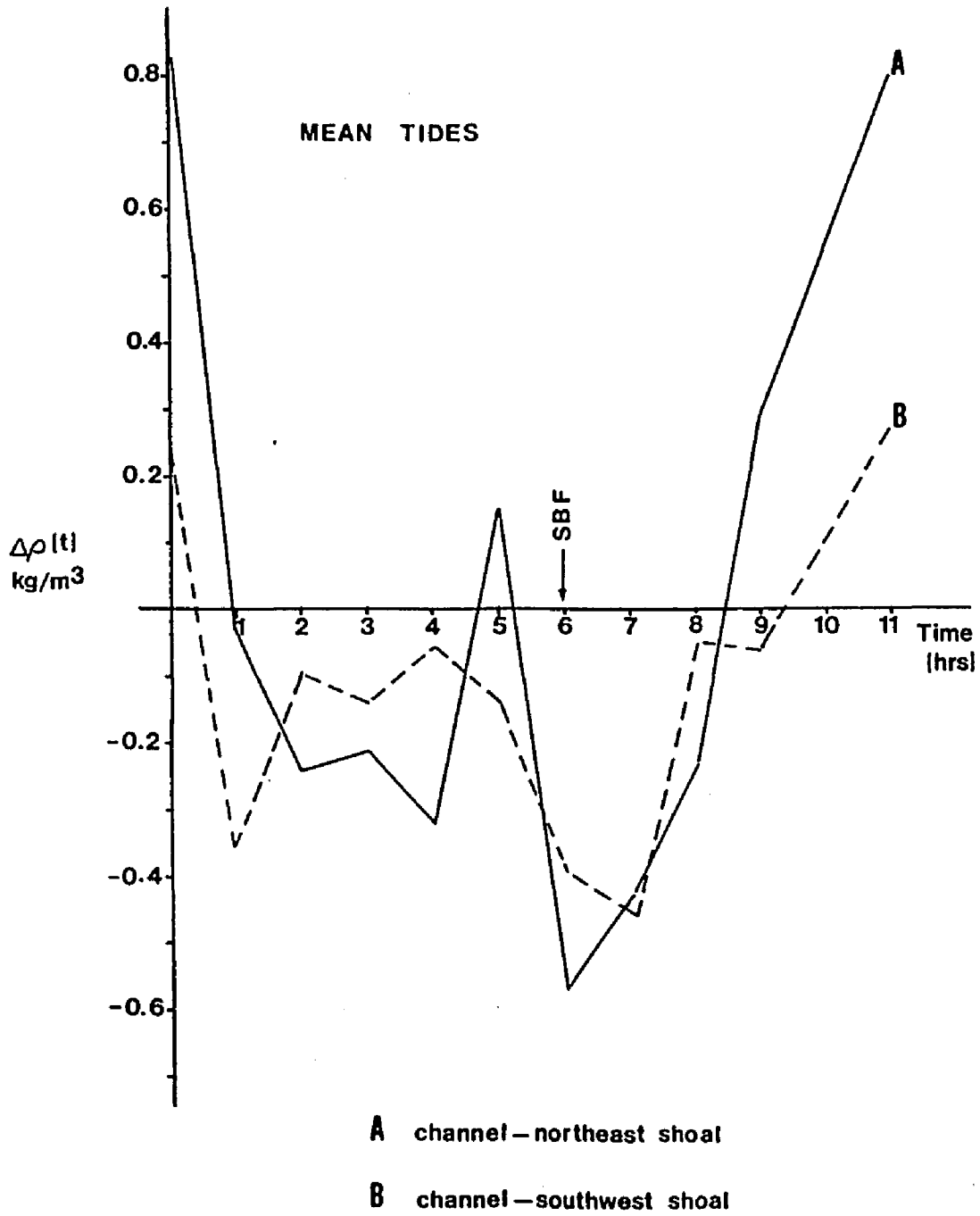


FIG. 6.3a

Density differences between the channel and shoals ans 'mean' tides.

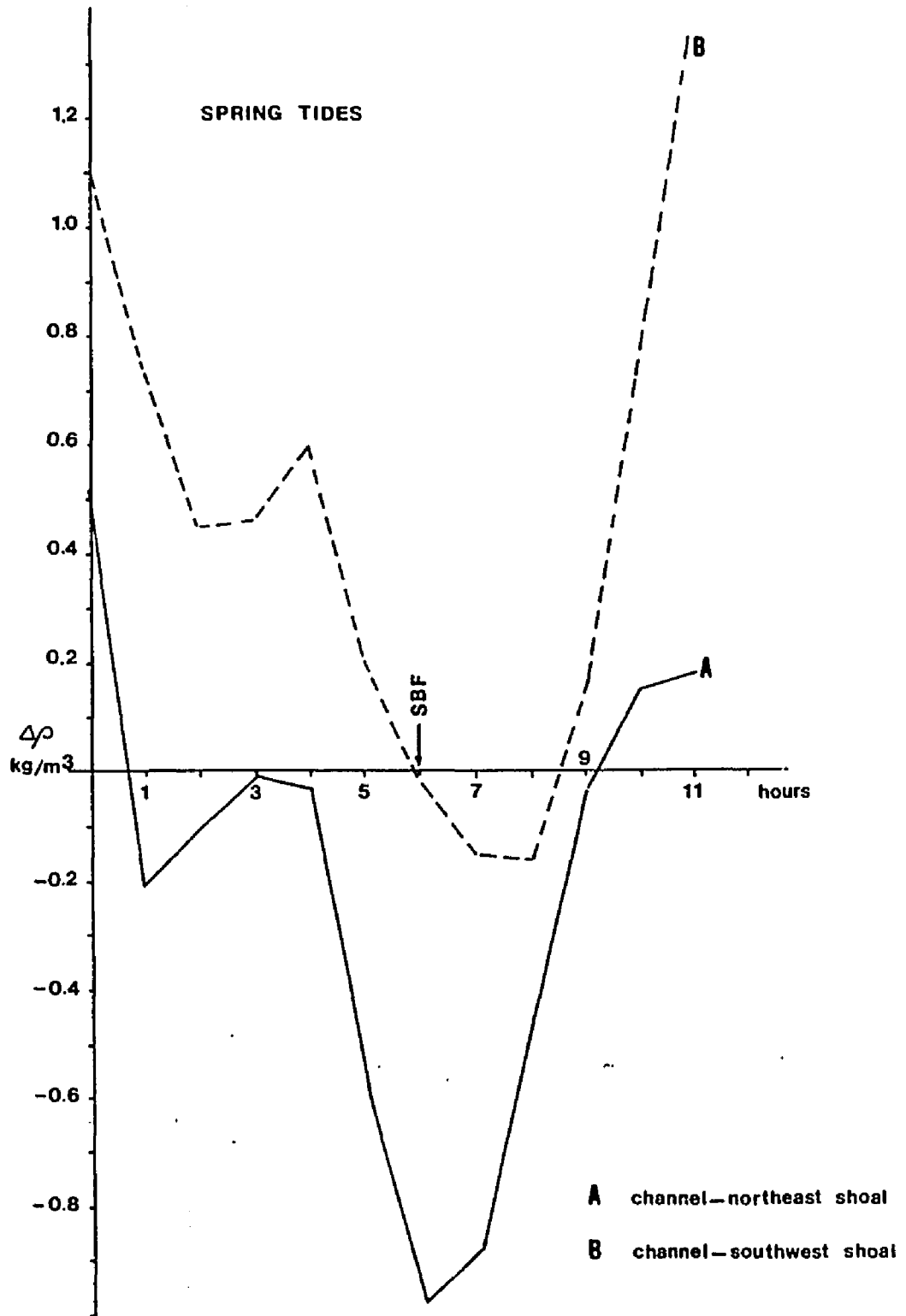


FIG.6.3b Density differences between the channel and shoals at 'spring' tides.

shoal and the channel at spring tides is greater than zero for all but two and a half hours of the tidal cycle. That is, the density over this shoal is almost always less than the channel under these conditions. This points to the influence of a Coriolis induced residual circulation which superimposes additional density differences on those expected from differential advection.

Differences between the observations and the conceptual model used here are to be expected because of the model's many simplifying assumptions. In addition to the possible influence of residual circulations, no account is taken of the possibility of lateral mixing between waters of channel and shoal, inequalities in the duration of flood and ebb cycles across the estuary or lateral differences in the longitudinal density gradient. As a first approximation however it would appear that the observed lateral density differences could be explained by simple differential advection.

If this is so, then distinct density differences between channels and shoals might be expected to occur throughout not only the York River, but other similar coastal plain estuaries. Such a lateral density structure might influence other aspects of estuarine dynamics, such as longitudinal dispersion, and allow the formation of longitudinal fronts.

By definition fronts represent the location of a discontinuity in the horizontal distribution of water mass properties on the scale of observation (Denman and Powell, 1984). This means therefore that two

differing water masses have to be brought into juxtaposition, or there has to be a strong local gradient in mixing processes which would change the characteristics of the water mass. In general when two such dissimilar fluids are adjacent, horizontal mixing will operate to reduce the gradients in water mass properties. In order to maintain a sharp gradient or boundary, advection of the water mass must overcome diffusion. Water masses in estuaries are usually primarily distinguished by their density characteristics and thus estuarine fronts of all kinds may be delineated by a density difference across the frontal boundary. This is very clearly so in river plume fronts where the buoyancy difference is generated by a constant flux of brackish river water. In some estuarine fronts, such as the axial convergence zones noted by Nunes and Simpson (1985), there may not be a marked density difference at the frontal boundary, merely a discontinuity in the velocity fields.

The observational evidence from the York River indicates that quite strong fronts can occur even though the localized change in density across the frontal boundary is small. Frequently these fronts occur at the times and locations of maximum lateral shear in the longitudinal velocity. Presumably therefore, the locally high value of velocity shear noted at the inner edge of the shoals augments the expected mean value of the density difference between channel and shoal to such an extent that discontinuities in the density field occur. Such conditions are favourable for the formation of fronts. Lateral pressure gradients could then drive the surface convergent circulations which are generally considered dynamically necessary to maintain a frontal boundary.

If fronts occur when the density difference is greatest, then fronts can be expected to occur at or near the times of minimum current. This is true for slack-before-ebb. However fronts are very rarely seen at the time of slack-before-flood - the time of maximum negative shear. Why is this so, when the absolute density difference may be just as great as at slack-before-ebb? The answer would seem to be that not only is a density shear necessary to produce fronts, but also a lateral horizontal density distribution such that the associated pressure gradients will generate convergent flows. The circulation inferred from these pressure gradient were illustrated in Chapter 3 and are repeated here in Fig.6.4. In general only the pressure gradients on the north-eastern side of the river were considered to be of sufficient strength to possibly generate circulations. These circulations are seen to be convergent near slack-before-ebb and divergent near slack-before-flood. This is in accordance with observations of fronts in this part of the York River, and suggests that the existance of convergent flows is not necessary merely for the maintainence of fronts, but also for their genesis.

As a further complication to this analysis of frontogenesis is the very frequent observation of fronts at the inner edge of the south-west shoal during the mid-part of the ebb tidal cycle (H3,H4,H5 - see Fig.5.3). At this time the difference between the depth average density for the upper 1.0m at stations 6 and 5 is very small, and horizontal pressure gradients between these stations are also very small. However this location marks the transition between a stratified and well mixed water column. This is clearly seen in the observations made at H3 on 7

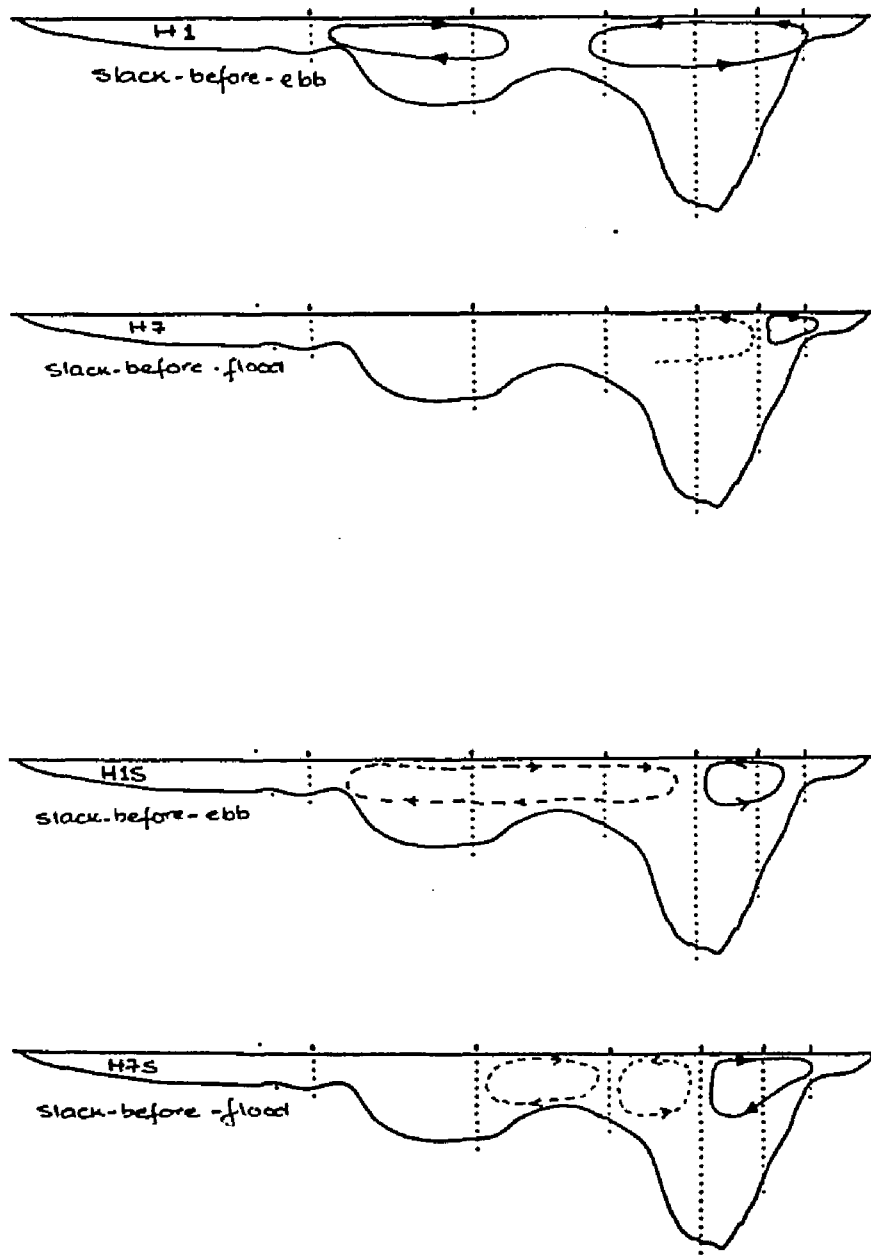


FIG.6.4 Circulations inferred from lateral pressure gradients.

June, 1984 (Fig.6.5). Fronts are commonly found at such a boundary in shallow shelf seas, and the longitudinal fronts in Delaware Bay described by Klemas and Polis (1977) were found to occur, at least in one instance, at a transition between stratified and mixed waters.

The general structure for such a front is depicted schematically in Fig.6.6a, the density in the well-mixed zone being intermediate between the upper and lower layers of the stratified zone. It has been observed in many shelf-sea situations that the surface front is much less pronounced than the bottom front (Van Heijst, 1986). Although the location of these tidal mixing fronts can be predicted using the energy criterion of Simpson and Hunter (1974), understanding of their frontogenesis and associated circulations is less well developed. Garrett and Loder (1981) found, semi-analytically, that the cross-frontal flow pattern has a two-cell structure as shown in Fig.6.6b. The circulation in the upper cell is expected to be weaker as the largest horizontal density differences occur in the deeper parts of the water column. Such a vertical variation in horizontal density differences was noted also at the inner edge of the south-west shoal. The dynamics used by Garrett and Loder (1981), however, incorporated rotation, and therefore their results are not directly applicable to estuaries. As with the fronts noted at other times and places during the tidal cycle, the maintenance of these fronts is very dependant on the surrounding vertical density structure. In estuarine environments changes in this structure may occur very rapidly, and therefore it is not surprising to

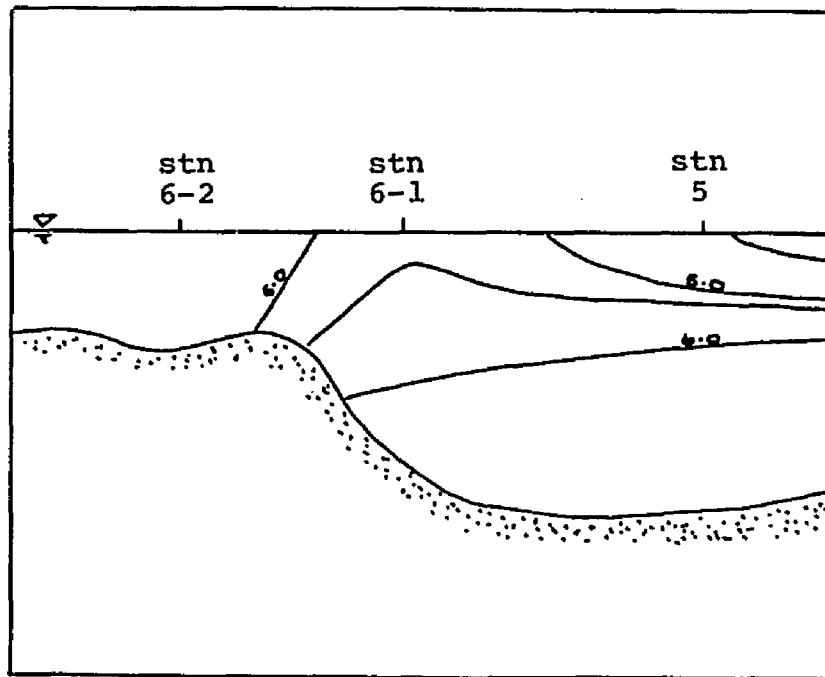
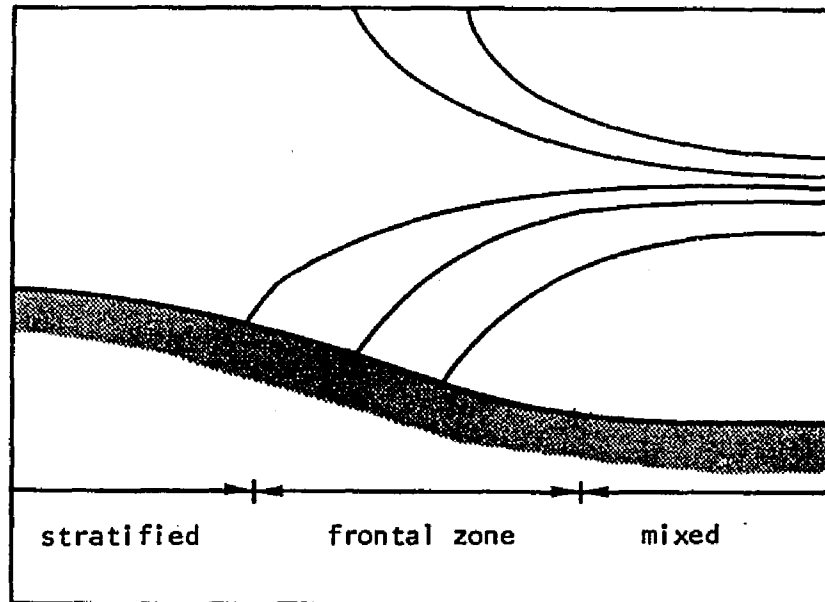


FIG.6.5 Isopycnals (0.5 sigma-t intervals) between the inner edge of the south west shoal and adjacent channel as measured on 7 June, 1984.

a)



b)

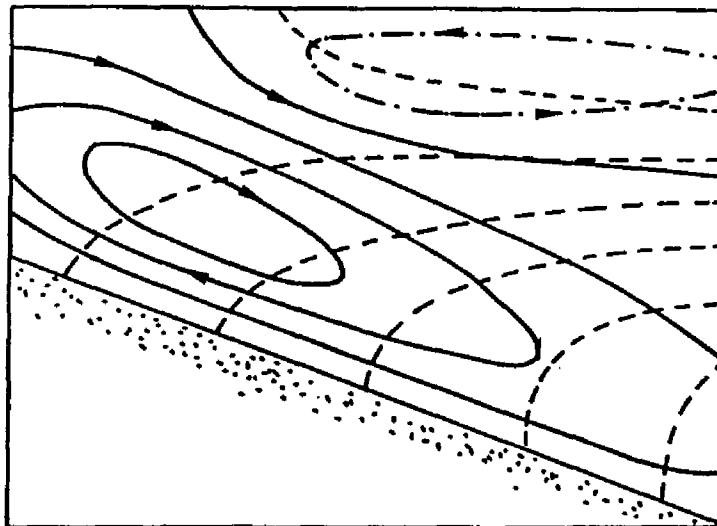


FIG.6.6 a) a schematic diagram of a tidal mixing front. (solid lines represent isopycnals)

b) streamlines of cross-frontal flow, dashed lines represent isopycnals. (from Garrett and Loder, 1981)

find that estuarine fronts have a relatively short time scale between genesis and decay.

The lateral circulations associated with horizontal pressure gradients, and at times fronts, will act to enhance cross-estuary mixing. Material which enters the estuary from the fringing marshes and small tidal creeks will be transferred from the shoals to the faster flowing waters of the channel during certain times of the tidal cycle. In this way the effective longitudinal dispersion of such material is greatly increased. The idea that shoals may act as temporary storage basins and thus influence longitudinal mixing was first proposed by Schijf and Schonfeld (1953). Similarities also exist in the coastal ocean where the nearshore zone may be characterized by high turbidity and lower salinity. The seaward boundary of this zone is often delineated by fronts. In a study off the Georgia coast, Blanton and Atkinson (1978) concluded that although the transfer of material alongshore is dominated by the mean alongshore flow, the transfer of material across the nearshore zone is due to the mean freshwater discharge, tidally-induced fluxes and fluxes due to gravitational circulation. Tidally-varying and density-driven lateral circulations are quite possibly characteristic of many estuaries, and measurement of their magnitudes an important topic for future estuarine research.

VII. SUMMARY AND CONCLUSIONS

The density distribution across the York River is characterized by distinct inhomogeneities, especially in the upper 2 meters of the water column. The pattern of variability is repetitive and closely correlated with the semi-diurnal tidal cycle and the water depth. In the shallower areas the water column remains vertically well-mixed at all times. The density differences are greatest at times of minimum currents. At slack-before-flood the least dense water is located in a shallow lens over the main channel. Towards the end of the flood cycle, and at slack-before-ebb, this is reversed with the least dense water situated over the shoals. These density differences result in horizontal pressure gradients which at times may be of sufficient strength to generate lateral circulations. Such circulation patterns would form zones of convergence or divergence across the estuary depending on the particular density distribution.

In the shoal areas bottom friction plays a major role, not only in providing sufficient turbulence to fully mix the water column, but also by reducing the longitudinal velocities. Lateral differences in the strength of the associated advection processes result. This difference, when acting upon a constant longitudinal density gradient, is of sufficient magnitude to generate the observed lateral density differences.

This lateral variability in density and velocity is not evenly distributed across the estuary. Zones of large velocity and density shear can be found, most notably at the inner edge of the shoals. At this location also, lateral differences in density, and/or vertical density structure, may generate estuarine fronts. The presence of these fronts, although transitory, may further enhance lateral flows.

In conclusion therefore, this study has shown that differential advection, and possibly mixing, between areas of 'shoal' and 'channel' in partially-mixed estuaries may create distinct density differences across the estuary. These density differences may then generate lateral circulations and estuarine fronts.

LITERATURE CITED

- Allen, C.M., J.H. Simpson and R.M. Carson, 1980, The structure and variability of shelf-sea fronts as observed by an CTD system, Oceanologica Acta, 3(1):59-68.
- Aubrey, D.G. and P.E. Speer, 1985, A study of non-linear tidal propagation in shallow inlet/estuarine systems, Part I: Observations, Estuarine, Coastal and Shelf Science, 21:185-205.
- Boicourt, W.C., 1982, The detection and analysis of the lateral circulation in the Potomac River estuary, Chesapeake Bay Institute Report.
- Boon, J.D. III and K.P. Kiley, 1978, Harmonic analysis and tidal prediction by the method of least squares, Virginia Institute of Marine Science, S.R.A.M.S.O.E. Report No. 186.
- Bowden, K.F. and S.H. Sharaf-el-Din, 1966, Circulation and river discharge in the Mersey Estuary, Geophysical Journal of the Royal Astrophysical Society, 10:383-399.
- Bowman, M.J., 1978, Spreading and mixing of the Hudson River effluent into the New York Bight. In: Hydrodynamics of Estuaries and Fjords, ed. Nihoul.
- Brooks, T.J., 1983, York River slack water data report - temperature, salinity and dissolved oxygen 1971-1980, VIMS Data Report #19.
- Brubaker, J.M., 1982, Observations of the small-scale structure of a coastal front. Dept. of Civil Engineering, Centre for Water Research, Report # ED-82-016, Univ. of Western Australia.
- Cannon, G.A., 1969, Observations of motion at intermediate and large scales in a coastal plain estuary, Chesapeake Bay Institute Technical Report #52.
- Cheng, R.T. and J.W. Gartner, 1985, Harmonic analysis of tides and tidal currents in south San Francisco Bay, California, Estuarine, Coastal and Shelf Science, 21:57-74.
- Cromwell, T. and J.L. Reid, 1956, A study of oceanic fronts, Tellus, 8(1):94-101.
- Davis, R.E., J.E. Dufour, G.J. Parks and M.R. Perkins, 1982, Two inexpensive current-following drifters, Scripps Institute of Oceanography Reference No. 82-28.

- Denman, K.L., and T.M. Powell, 1984, Effects of physical processes on planktonic ecosystems in the coastal ocean, Oceanography, Marine Biological Annual Review, 22:125-168.
- Doyle, B.E. and R.E. Wilson, 1978, Lateral dynamic balance in the Sandy Hook to Rockaway Point transect, Estuarine, Coastal Marine Science, 6:165-174.
- Dyer, K.R., 1973, Estuaries: A Physical Introduction, John Wiley and Sons, London.
- Dyer, K.R., 1974, The salt balance in stratified estuaries, Estuarine, Coastal and Marine Science, 2:273-281.
- Dyer, K.R., 1977, Lateral circulation effects in estuaries. In: Estuaries, Geophysics and the Environment, National Academy of Sciences, Washington, DC.
- Dyer, K.R., 1982, Mixing caused by lateral internal seiching within a partially mixed estuary, Estuarine, Coastal and Shelf Science, 15:443-457.
- Fearnhead, P.G., 1975, On the formation of fronts by tidal mixing around the British Isles, Deep Sea Research, 22:311-321.
- Fischer, H.B., 1972, Mass transport mechanisms in partially stratified estuaries, Journal of Fluid Mechanics, 53(4):671-687.
- Fischer, H.B., 1976, Mixing and dispersion in estuaries, Annual Review of Fluid Mechanics, 8:107-133.
- Fischer, H.B., E.J. List, R.C.Y. Koh, J. Imberger, N.H. Brooks, 1979, Mixing in Inland and Coastal Waters, Academic Press, New York.
- Garrett, C.J.R. and J.W. Loder, 1981, Dynamical aspects of shallow sea fronts, Philosophical Transactions of the Royal Society of London, A302:563-581.
- Garvine, R.W., 1974a, Physical features of the Connecticut River outflow during high discharge, Journal of Geophysical Research, 79(6):831-846.
- Garvine, R.W., 1974b, Dynamics of small-scale oceanic fronts, Journal of Physical Oceanography, 4:557-569.
- Garvine, R.W., 1977, Observations of the motion field of the Connecticut River plume, Journal of Geophysical Research, 82(3):441-454.
- Garvine, R.W., 1979a, An integral hydrodynamic model of upper ocean frontal dynamics: Part I. Development and analysis, Journal of Physical Oceanography, 9:1-18.

- Garvine, R.W., 1979b, An integral model of upper ocean frontal dynamics: Part II. Physical characteristics and comparison with observations, Journal of Physical Oceanography, 9:19-35.
- Garvine, R.W., 1980, The circulation dynamics and thermodynamics of upper ocean density fronts, Journal of Physical Oceanography, 10:2058-2081.
- Garvine, R.W., 1981, Frontal jump conditions for models of shallow, buoyant surface layer hydrodynamics, Tellus, 33:301-312.
- Garvine, R.W., 1982, A steady state model for buoyant surface plume hydrodynamics in coastal waters, Tellus, 34:293-306.
- Garvine, R.W., 1983, Stationary waves on oceanic density fronts, Deep Sea Research, 30(3A):245-266.
- Garvine, R.W., 1984, Radial spreading of buoyant surface plumes in coastal waters, Journal of Geophysical Research, 89(C2):1989-1996.
- Garvine, R.W. and J.D. Monk, 1974, Frontal structure of a river plume, Journal of Geophysical Research, 79:2251-2259.
- Godfrey, J.S. and J. Parslow, 1975, Description and preliminary theory of circulation in Port Hacking estuary, CSIRO Division of Fisheries and Oceanography Report No. 67, Cronulla, Australia.
- Haas, L.W., 1977, The effect of the neap-spring tidal cycle on the vertical salinity structure of the James, York and Rappahannock Rivers, Virginia, U.S.A., Estuarine, Coastal and Marine Science, 5:485-496.
- Hansen, D.V., 1965, Currents and mixing in the Columbia River estuary, Proceedings of Joint Conference on Ocean Science and Ocean Engineering, 2:943-955.
- Henderson, M.F., 1966, Open Channel Flow, MacMillan, New York.
- Huzzey, L.M., 1982, The dynamics of a bathymetrically arrested estuarine front, Estuarine, Coastal and Shelf Science, 15:537-552.
- Hyer, P.V., A.Y. Kuo, C.S. Fang and W.J. Hargis, Jr., 1978, Hydrography and Hydrodynamics of Virginia Estuaries XVII: Mathematical ecosystem modeling study of the York River, Virginia Institute of Marine Science S.R.A.M.S.O. Report No. 205.
- Imberger, J., 1976, Dynamics of a longitudinally stratified estuary, Proceedings 15th International Conference on Coastal Engineering, 3108-3117.
- Ingram, R.G., 1976, Characteristics of a tide-induced estuarine front, Journal of Geophysical Research, 81:1951-1959.

- Ingram, R.G., 1981, Characteristics of the Great Whale River plume, Journal of Geophysical Research, 86:2017-2023.
- James, I.D., 1978, A note on the circulation induced by a shallow-sea front, Estuarine, Coastal and Shelf Science, 7:197-202.
- Kao, T.W., H-P. Pao and C. Park, 1978, Surface intrusions, fronts, and internal waves: a numerical study, Journal of Geophysical Research, 83:4641-4650.
- Kao, T.W., C. Park and H-P. Pao, 1977, Buoyant surface discharge and small-scale oceanic fronts: a numerical study, Journal of Geophysical Research, 82:1747-1752.
- Klemas, V. and D.F. Polis, 1977, A study of density fronts and their effect on coastal pollutants, Remote Sensing and Environment, 6:95-126.
- Murray, S., D. Conlon, A. Siripong and J. Satoro, 1975, Circulation and salinity distribution in the Rio Guayas estuary, Ecuador. In: Estuarine Research II:345-363, ed.L.E. Cronin, Academic Press, New York.
- Murray, S., and A. Siripong, 1978, Role of lateral gradients and longitudinal dispersion in the salt balance of a shallow, well-mixed estuary. In: Estuarine Transport Processes, pp 113-124, ed.B. Kjerfve, University of South Carolina Press.
- Nichols, M., M. Kelly, G. Thompson and L. Castiglione, 1972, Sequential photography for coastal oceanography, Virginia Institute of Marine Science, S.R.A.M.S.O.E. Report No. 95.
- Nichols, M., 1975, Southern Chesapeake Bay water color and circulation analysis, Virginia Institute of Marine Science, S.R.A.M.S.O.E. Report No. 96.
- Nof, D., 1979, Generation of fronts by mixing and mutual intrusion, Journal of Physical Oceanography, 9:298-310.
- Nunes, R.A. and J.H. Simpson, 1985, Axial convergence in a well mixed estuary, Estuarine, Coastal and Shelf Science, 20:673-649.
- O'Donnell, J. and R.W. Garvine, 1983, A time-dependant, two-layer frontal model of buoyant plume dynamics, Tellus, 35A:73-80.
- Officer, C.B., 1976, Physical Oceanography of Estuaries (and Associated Coastal Waters), John Wiley and Sons, New York.
- Pingree, R.D., 1978, Cyclonic eddies and cross-frontal mixing, Journal of Marine Biol. Assn. of U.K., 58:955-963.
- Pingree, R.D., G.R. Forster and G.K. Morrison, 1974, Turbulent convergent tidal fronts, Journal of Marine Biol. Assn. of U.K., 54:469-479.

- Pingree, R.D. and D.K. Griffiths, 1978, Tidal fronts on the shelf seas around the British Isles, Journal of Geophysical Research, **83(C9):4615-4622.**
- Pritchard, D.W., 1952, Salinity distribution and circulation in the Chesapeake Bay estuarine system, Journal of Marine Research, **11:106-123**
- Pritchard, D.W., 1954, A study of the salt balance in a coastal plain estuary, Journal of Marine Research, **13:133-144**
- Pritchard, D.W., 1956, The dynamic structure of a coastal plain estuary, Journal of Marine Research, **15:33-42**
- Proudman, J., 1953, Dynamical Oceanography, John Wiley and Sons, London.
- Prych, E.A., 1970, Effect of density differences on lateral mixing in open-channel flows, Keck Laboratory of Hydraulics and Water Resources, California Institute of Technology, Report No. KH-R-21.
- Ruzecki, E.P., 1981, Temporal and spatial variations in the Chesapeake Bay plume. In: Chesapeake Bay Plume Study, Superflux 1980, NASA Conference Publication 2188.
- Ruzecki, E.P. and D.A. Evans, 1986, Temporal and spatial sequencing of destratification in a coastal plain estuary. In: Tidal Mixing and Plankton Dynamics, M.J. Bowman et.al. (eds), Springer-Verlag, Berlin.
- Schijf, J.B. and J.C. Schonfeld, 1953, Theoretical considerations on the motion of salt and fresh water, International Assoc. Hydraulic Research, Proceedings of the Minnesota Hydraulics Convention, pp 321-333.
- Schumacher, J.D., T.H. Kinder, D.J. Pashinski and R.L. Chamell, 1979, A structural front over the continental shelf of the Eastern Bering Sea, Journal of Physical Oceanography, **9:79-87.**
- Simpson, J.H., 1971, Density structure and microstructure in the western Irish Sea, Deep Sea Research, **18:309-319.**
- Simpson, J.H., 1976, A boundary front in the summer regime of the Celtic Sea, Estuarine, Coastal and Marine Science, **4:71-81.**
- Simpson, J.H., C.M. Allen and N.C.G. Morris, 1978, Fronts on the continental shelf, Journal of Geophysical Research, **83(C9):4607-4613.**
- Simpson, J.H. and D. Bowers, 1979, Shelf sea fronts' adjustments revealed by satellite IR imagery, Nature, **280:648-651.**
- Simpson, J.H. and D. Bowers, 1981, Models of stratification and frontal movement in shelf seas, Deep Sea Research, **28(7):727-738.**

- Simpson, J.H., D.J. Edelsten, A. Edwards, N.C.G. Morris and P.B. Tett, 1979, The Islay front: physical structure and phytoplankton distribution, Estuarine, Coastal and Marine Science, 2:713-726.
- Simpson, J.H. and J.R. Hunter, 1974, Fronts in the Irish Sea, Nature, 250:404-406.
- Simpson, J.H. and R.A. Nunes, 1981, The tidal intrusion front: an estuarine convergence zone, Estuarine, Coastal and Shelf Science, 13:257-266.
- Simpson, J.H. and W.R. Turrell, 1985, Convergent fronts in the circulation of tidal estuaries, paper presented at 1985 International Estuarine Research Federation conference, New Hampshire.
- Smith, R., 1980, Buoyancy effects upon longitudinal dispersion in wide well-mixed estuaries, Philosophical Transactions of the Royal Society, London, A296:467-496.
- Stigebrandt, A., 1980, A note on the dynamics of small-scale fronts, Geophysics, Astrophysics and Fluid Dynamics, 16:225-238.
- Stommel, H., 1953, The role of density currents in estuaries, Proceedings of International Assoc. for Hydraulic Research, 305-312.
- Sumer, S.M. and H.B. Fischer, 1977, Transverse mixing in partially stratified flow, ASCE Journal of Hydraulics Division, HY6:587-600.
- Uncles, R.J., R.C.A. Elliot and S.A. Weston, 1984, Lateral distributions of water, salt and sediment transport in a partly mixed estuary, paper presented at: Coastal Zone Engineering Conference, Houston.
- U.S. Dept. of Commerce, 1983/4/5, Tidal Current Tables 1983 (1984)(1985): Atlantic Coast of North America, National Ocean Service, Rockville, Maryland.
- Van Heijst, G.J.F., 1985, A geostrophic adjustment model of a tidal mixing front, Journal of Physical Oceanography, 15:1182-1190.
- Wang, D-P., 1984, Mutual intrusion of a gravity current and density front formation, Journal of Physical Oceanography, 14:1191-1199.
- Welch, C.S., 1979, The evidence for an inviscid core in some coastal plain estuaries, paper presented at: International Symposium on the Effects of Nutrient Enrichment in Estuaries, Williamsburg.
- West, J.R. and J.S. Mangat, 1986, The determination and prediction of longitudinal dispersion coefficients in a narrow, shallow estuary, Estuarine, Coastal and Shelf Science, 22:161-181.
- Wolanski, E. and P. Collis, 1976, Aspects of the aquatic ecology of the Hawksbury River. I. Hydrodynamical processes, Australian Journal of Marine and Freshwater Research, 27(4):565-582.

Wright, L.D. and J.M. Coleman, 1971, Effluent expansion and interfacial mixing in the presence of a salt wedge, Mississippi River delta, Journal of Geophysical Research, 76(36):8649-8661.

VITA

LINDA MARY HUZZEY

Born in Mansfield Australia, 14 September 1954. Graduated from Wangaratta High School in 1970. Recieved B.Sc.(Honours), with a major in Geology/Geography, from the University of Melbourne, Australia in 1974. Recieved M.Sc. from the University of Sydney, Australia in 1982. Thesis topic: Circulation associated with topographically-arrested fronts, Port Hacking, New South Wales. Entered doctoral program at the College of William and Mary, School of Marine Science in 1981.